

# Multidisciplinary Investigation of the Gut-Brain Ecosystem in a Model of Alzheimer's Disease

Présentée le 28 février 2022

Faculté des sciences et techniques de l'ingénieur  
Laboratoire de biologie à l'échelle nanométrique  
Programme doctoral en biotechnologie et génie biologique

pour l'obtention du grade de Docteur ès Sciences

par

**Arielle Louise PLANCHETTE**

Acceptée sur proposition du jury

Prof. G. Fantner, président du jury  
Prof. A. Radenovic, Prof. A. J. Macpherson, directeurs de thèse  
Dr K. Endres, rapporteuse  
Prof. A. Bassi, rapporteur  
Prof. H. Lashuel, rapporteur









# Acknowledgements

The PhD is an experience of scientific and personal growth like, I believe, no other. There were many lessons learned throughout my PhD, most of which due to the entourage that guided and supported me along the way. For this growth, there are many I must thank.

First and foremost, my growth was inspired by the example set by my supervisors. My thesis director, Aleksandra Radenović, taught me the perseverance and attention to detail that was indispensable for my thesis. Beyond this, she gave me creative freedom to pursue scientific questioning that was 'off-script' but led to findings that increased our depth of understanding of the gut-brain axis. In addition, the welcome she and her other students gave me made my experience at EPFL rich in friendships and many an interesting discussion. For all of the support you have given me Aleksandra, I thank you. My second thesis director, Andrew Macpherson, opened his extremely experienced and technical laboratory to me. There I was surrounded by scientists that I felt were immense sources of knowledge and from whom I was able to learn all I know about the gut microbiome and ways to probe its effects on health. Within this setting, I must thank my collaborators, without whom I would have been lost on numerous occasions. Thank you to Mercedes Gomez de Agüero, Francesca Ronchi, Terry Müller, Monica Iachizzi and Andrina Rutsch. Your guidance and collaboration was indispensable for the success of this work. A strong pillar within this project, for whom I am extremely grateful, is Alessio Mylonas. For the scientific and personal support you provided me, especially the laughter during the long final years of the thesis, I thank you.

The story of my PhD, especially at the start, is woven with changes. I would like to thank Theo Lasser and his laboratory members for the scientific exposure and the friendships during my first couple of years as a PhD. I remember feeling incapable of conducting microscopy research, despite your encouragement and unique facilities, in my first year. I am now very proud of the two microscopy chapters included in this thesis, which were entirely inspired by working with the members of the Lasser group. In particular, I would like to thank David, Jérôme, Paul, Miguel, Vincent and Séverine. A few members of the AD-gut group who also transitioned between laboratories and whose friendship and memories I value are Jochem, Kristin and Adrien. I also direct a special thank you to the brilliant scientist that chose me to join this project and inspired me to believe that the gut does indeed manipulate our health, Taoufiq. As my research progressed within the EU Horizon 2020 collaborative project, I was able to forge relationships with scientists from all over Europe. This is an experience I particularly enjoyed

## Acknowledgements

---

and cherish now that this journey as come to an end. Beyond the collaborators I already mentioned from Bern, I must thank Cédric and Katrin for their expertise in metabolomics. In Lund, Frida, Olena, Stephen, Ling, Thao and Tannaz were essential in assessing gut microbiome composition. In Leuven, Raffaele was a pleasure to work with on performing the complex multivariate analyses needed to attempt at understanding our data.

It is undeniable that my experience of the PhD would be entirely different had I not been surrounded by open-minded, kind, funny friends and family. Some of those mentioned previously fall within this umbrella and I must thank some more who made the last five years as enjoyable as they have been. To all my day-in-day-out friends, whether you are in Lausanne, or in another country entirely, I am so grateful for your support throughout the years.

Finally, I would not be where I am without my family. Starting out with my grandparents, who fostered a scientific interest in me from a young age. My parents, who fostered that interest for all these years and made me understand that I could follow any path I wished. My brother, who was always there for a call to show me how adorable our Alizée was being (the family Siamese cat). To Charles, who was closest to me throughout the entire experience, who celebrated with me and lifted me up on the tougher days. All of you believed in me, which made me believe in myself.

*Lausanne, December 23, 2021*

# Abstract

The search for an understanding of the causal elements that lead to neurodegenerative diseases has motivated researchers for decades. Alzheimer's disease (AD) was first clinically described in 1906 by Alois Alzheimer, who observed the first patient's decline for four years and subsequently assessed morphological and biochemical alterations in the brain tissue. Today, it is the most prevalent form of dementia and affects approximately fifty million people worldwide, with only 5% of patients carrying causal genetic mutations. A significant research effort over the last fifty years has identified early-onset clinical biomarkers, developed novel imaging technologies to study AD in live patients, and yielded an understanding of the risk factors and genetic predispositions that can lead to Alzheimer's disease. The latter has led to the development of pre-clinical animal models of AD that further enable in-depth research with a capacity to manipulate genetics, lifestyle and treatment.

In recent years, studies of animal models as well as observations in humans have brought the gut microbiome to the forefront of AD research, as a significant contributor to the development of Alzheimer's disease. In fact, the gut microbiome is now understood to be a modulator of health and disease in numerous areas of physiology, including energy metabolism, immunity, endocrinology, and most relevant to this thesis, brain health and cognition. The gut microbiome is a complex environment composed of symbiotic bacteria, fungi and viruses (the microbiota) that produce a wide range of signalling molecules that are interpreted both by members of the microbiota and by the host (the microbiome). The host-gut interface is an ecosystem that consists of bi-directional signals and pressures applied by both constituents in order to maintain symbiotic homeostasis. Significant deleterious effects on health occur when homeostasis is lost, which may take place due to a variety of factors. These include host genetic factors and environmental factors, such as diet. Modulation of the gut microbiome has become a potentially viable therapeutic avenue for Alzheimer's disease, though it currently remains at the early stage of discovery.

The first part of this thesis aims to contribute to the field of microbiota modulation and its therapeutic outcomes in neurodegenerative diseases. I characterize the evolution of Alzheimer's disease in the 5xFAD mouse model under conventional rearing conditions, with a focus on the gut microbiome and on cognitive decline and brain biochemistry. In addition, I describe

## Abstract

---

for the first time the power of co-housing healthy and AD animals to significantly impact gut microbiota composition and hallmarks of AD in aged animals. This form of microbiota modulation is accompanied by strict gnotobiotic rearing conditions, whereby germ-free and low-complexity bacterial cocktails were implemented in the 5xFAD model. In this part of the study, I outline the effects microbiota modulation on hallmarks of AD and provide insights into the metabolite profile of the brain altered by the microbiota and AD.

The work in this thesis was equally motivated by the development of diagnostic tools using microscopy techniques. Biochemical assessments of disease status and progression provide information pertaining to "what" is interacting and "how much" this affects disease. With microscopy, we may gain the additional knowledge of "where" physiological constituents are and how they interact with the surrounding environment.

I describe a novel multi-modal microscopy pipeline that enables the observation of signals of interest in large volumes and at high resolution with a capacity to cross-reference regions of interest in both modalities. The pipeline, known as gutOPT, consists of a sample preparation workflow compatible with mesoscale optical projection tomography (OPT) of fluorescently-labelled targets and subsequent imaging of pre-selected regions of interest in high-resolution modalities, such as confocal microscopy. I outline an optimized OPT optical setup for imaging the mouse intestine and demonstrate its applicability for imaging components of the organized immune system of the gut known as gut-associated lymphoid tissues.

Key words: Alzheimer's disease, 5xFAD model, microbiota, microbiome, conventionally-raised, germ-free, gnotobiotic, bacterial cocktails, microscopy, optical projection tomography, gut-associated lymphoid tissues

## Résumé

La compréhension des éléments causaux qui conduisent aux maladies neurodégénératives motive les chercheurs depuis des décennies. La maladie d'Alzheimer (MA) fut décrite cliniquement pour la première fois en 1906 par Alois Alzheimer, qui a observé le déclin comportemental de la première patiente reconnue et qui a ensuite étudié les altérations morphologiques et biochimiques du tissu cérébral. Aujourd'hui, il s'agit de la forme de démence la plus répandue, touchant environ cinquante millions de personnes dans le monde, avec seulement 5 % de patients étant porteurs de mutations génétiques causales. Au cours des cinquante dernières années, d'importants efforts de recherche ont permis d'identifier des biomarqueurs cliniques précoces, de mettre au point de nouvelles technologies d'imagerie pour étudier la maladie d'Alzheimer chez des patients vivants et de mieux comprendre les facteurs de risque et les prédispositions génétiques qui peuvent conduire à son développement. Ce dernier point a conduit à la mise au point de modèles animaux précliniques qui permettent des recherches approfondies avec la possibilité de manipuler la génétique, le mode de vie et les traitements appliqués.

Ces dernières années, les études sur les modèles animaux et les observations chez l'homme ont mis le microbiome intestinal au premier plan en tant que facteur important au développement de cette maladie. Le microbiome intestinal est un modulateur de la santé dans de nombreux domaines physiologiques, notamment le métabolisme énergétique, l'immunité, l'endocrinologie et la santé du cerveau, dont la mémoire et la cognition. Le microbiome intestinal est un environnement complexe composé de bactéries, de champignons et de virus symbiotiques (le microbiote) qui produisent un large éventail de molécules de signalisation qui sont interprétées à la fois par les membres du microbiote et par l'hôte (le microbiome). L'interface hôte-intestin est un écosystème constitué de signaux bidirectionnels ayant pour but de maintenir l'homéostasie symbiotique. Des effets délétères importants sur la santé se produisent lorsque l'homéostasie est perdue, ce qui peut se produire en raison d'une variété de facteurs. Il s'agit notamment de facteurs génétiques de l'hôte et de facteurs environnementaux, tels que l'alimentation. Ainsi, la modulation du microbiome intestinal est devenue une avenue thérapeutique potentiellement viable pour la maladie d'Alzheimer, bien qu'elle reste actuellement au stade de la découverte.

La première partie de cette thèse vise à contribuer au domaine de la modulation du microbiote et de son potentiel thérapeutique dans les maladies neurodégénératives. Je caractérise l'évolution de la maladie d'Alzheimer dans le modèle de souris 5xFAD dans des conditions d'élevage conventionnelles, en mettant l'accent sur le microbiome intestinal, le déclin cognitif et la biochimie du cerveau. Je décris pour la première fois une modulation microbale par le biais de la cohabitation d'animaux sains et d'animaux atteints de la maladie d'Alzheimer. Je démontre l'impact significatif de cette cohabitation sur la composition du microbiote intestinal et sur les caractéristiques de la maladie d'Alzheimer chez les animaux âgés. Pour démontrer la viabilité de cocktails probiotique en tant que traitement potentiel de symptômes cognitifs, le même modèle (5xFAD) fut élevé sous des conditions sans-germes et gnotobiotiques. Je décris les résultats observés due à ce type de modulation du microbiote sur les caractéristiques de la maladie d'Alzheimer et je donne un aperçu du profil des métabolites du cerveau influencé par le microbiote et la maladie d'Alzheimer.

Les travaux de cette thèse ont également été motivés par le développement d'outils de diagnostic utilisant des techniques de microscopie. Les évaluations biochimiques de l'état des symptômes de la maladie d'Alzheimer fournissent des informations sur "ce" qui interagit et "dans quelle mesure" cela affecte la maladie. Grâce à la microscopie, nous pouvons acquérir des connaissances supplémentaires sur "l'endroit" où se trouvent les constituants physiologiques et sur la façon dont ils interagissent avec le milieu environnant.

Je présente une configuration de tomographie par projection optique (OPT) optimisée, permettant l'imagerie de l'intestin de souris et je démontre son applicabilité pour l'imagerie de structures organisées du système immunitaire intestinal. Je décris un nouveau pipeline de microscopie qui permet l'observation de signaux d'intérêt dans une modalité à grands volumes et une autre à haute résolution avec une capacité de référence croisée des régions d'intérêt dans les deux modalités. Le pipeline, connu sous le nom de gutOPT, consiste en une préparation d'échantillons d'intestins de souris compatible avec la tomographie par projection optique (OPT) à l'échelle millimétrique et l'imagerie ultérieure de régions d'intérêt présélectionnées dans des modalités à haute résolution, comme la microscopie confocale.

Mots clés : Maladie d'Alzheimer, modèle 5xFAD, microbiote, microbiome, sans-germe, gnotobiotique, cocktails microbiens, microscope, tomographie par projection optique

# Contents

<b>Acknowledgements</b>	<b>i</b>
<b>Abstract</b>	<b>iii</b>
<b>1 Introduction</b>	<b>1</b>
1.1 Alzheimer's Disease . . . . .	2
1.1.1 Human Alzheimer's Disease . . . . .	2
1.1.2 Animal Models of AD . . . . .	4
1.2 The Host-Gut Ecosystem . . . . .	5
1.2.1 Components of Ecosystems . . . . .	6
1.2.2 Immunity . . . . .	7
1.2.3 Energy Metabolism . . . . .	7
1.2.4 The Nervous System . . . . .	9
1.3 Evidence of Gut-Brain Dysregulation in Neurodegenerative Disorders and Therapeutic Targets . . . . .	10
1.3.1 Autism Spectrum Disorder . . . . .	11
1.3.2 Parkinson's disease . . . . .	11
1.3.3 Alzheimer's Disease . . . . .	12
1.4 Microscopy Tools to Study the Gut Ecosystem . . . . .	13
<b>2 Effect of Gut Microbiota Modulation in a Model of Alzheimer's Disease</b>	<b>17</b>
2.1 Introduction . . . . .	18
2.2 Methods . . . . .	19
2.2.1 Animal models . . . . .	19
2.2.2 16S sequencing of the gut microbiota . . . . .	19
2.2.3 Cognitive testing . . . . .	20
2.2.4 Amyloid- $\beta$ plaque quantification . . . . .	20
2.2.5 Metabolomic Analysis . . . . .	21
2.3 Results . . . . .	21
2.3.1 Gut microbiota composition is altered in the 5xFAD model . . . . .	21
2.3.2 Co-housing 5xFAD and control littermates alters microbiota composition and reduces severity of AD . . . . .	24
2.3.3 The metabolite profile is altered in the AD brain . . . . .	26
	vii

## Contents

---

2.3.4	Low-complexity gut microbiota compositions significantly influence hallmarks of AD . . . . .	28
2.4	Discussion . . . . .	31
2.4.1	AD affects gut microbiota composition in a conventional environment . . . . .	31
2.4.2	Evidence for the bi-directional gut microbiota modulation through co-housing . . . . .	32
2.4.3	Altered Brain Metabolite Profile Reveals Pathological Hallmarks of AD . . . . .	33
2.4.4	Low-complexity cocktails influence amyloid plaque burden and cognition . . . . .	34
2.5	Conclusion . . . . .	35
2.6	Supplementary Information (SI) . . . . .	37
<b>3</b>	<b>High resolution optical projection tomography platform for multispectral imaging of the mouse gut</b> . . . . .	<b>41</b>
3.1	Introduction . . . . .	42
3.2	Methods . . . . .	43
3.2.1	Sample Preparation Protocol . . . . .	43
3.2.2	Acquisition setup . . . . .	45
3.2.3	Image reconstruction algorithm . . . . .	46
3.3	Results . . . . .	48
3.3.1	Instrument resolution and optimization . . . . .	48
3.3.2	Mouse gut imaging . . . . .	49
3.4	Conclusion . . . . .	51
<b>4</b>	<b>Optical Imaging of the Small Intestine Across Scales</b> . . . . .	<b>53</b>
4.1	Introduction . . . . .	53
4.2	Methods . . . . .	55
4.2.1	Animal Handling . . . . .	55
4.2.2	Sample preparation . . . . .	55
4.2.3	Microscopy . . . . .	56
4.2.4	Image Processing . . . . .	56
4.2.5	Isolated Lymphoid Follicle Segmentation . . . . .	57
4.3	Results . . . . .	57
4.3.1	Sample preparation pipeline and the power of tissue autofluorescence . . . . .	57
4.3.2	Cell-type specific signal distribution throughout the gut volume . . . . .	60
4.3.3	gutOPT pipeline for multi-modal imaging and high resolution characterisation of the gut . . . . .	63
4.4	Discussion . . . . .	65
4.5	Supplementary Information . . . . .	68
4.5.1	Supplementary Figure 4.5 . . . . .	68
4.5.2	Supplementary Figure 4.6 . . . . .	69
<b>5</b>	<b>Conclusion and Outlook</b> . . . . .	<b>71</b>
5.1	Experimental Approach and Open Questions . . . . .	71



5.2 Perspectives On Microbiota Modulation in Alzheimer's Disease . . . . .	74
5.3 Value of the gutOPT Pipeline for Host-Gut Investigation . . . . .	75
<b>Bibliography</b>	<b>77</b>
<b>Curriculum Vitae</b>	<b>107</b>



# 1 Introduction

Neurodegenerative diseases are an increasingly prevalent health affliction that not only affect the patient but also their entourage. Its societal burden has grown as populations have aged, thus making our search for diagnostic and therapeutic tools a global public health priority. The etiology of neurodegenerative disease is complex and in some cases, such as Alzheimer's disease (AD), has yielded few concrete treatment options for patients. However, the recently understood involvement of the microbiome in modulating the development of neurodegeneration has opened a new and hopeful field of study in both pre-clinical and clinical research.

In this thesis I investigate gut microbiome alterations in the context of Alzheimer's disease using the 5xFAD mouse model. Multiple methods of gut microbiota modulation are implemented and their effects on hallmarks of AD are examined. With this research, I advance the field's understanding of the bi-directional dynamics of the gut-brain connection and how the gut microbiota may be manipulated in the hopes of providing treatment options for Alzheimer's disease.

Furthermore, I address the need for novel diagnostic tools by presenting a multi-modal three-dimensional microscopy pipeline with the capacity to concatenate high-volume mesoscale imaging of the gut with high-resolution confocal microscopy. With this method, termed gutOPT, I hope to provide a novel diagnostic pipeline for tissues in the centimetre range, originating from pre-clinical models or clinical biopsies.

This thesis is structured as follows:

**Chapter 1** will introduce the main topics covered by the research presented in this thesis. I will outline the hallmarks of Alzheimer's disease and introduce the 5xFAD animal model. I will describe the complex host-gut ecosystem whose capacity to modulate health and disease is becoming increasingly clear. Having gained an understanding of this ecosystem, its physiological connection to the brain will be explored, with an interest in how the gut microbiome has been reconsidered as a therapeutic axis in disease contexts. As will be discussed early on, diag-

nostic tools for the assessment of Alzheimer's disease severity and progression remain limited, especially for mesoscale observations. Hence, the power of microscopy to elucidate structural and functional parameters of the gut will be introduced. **Chapter 2** presents the research I performed on the link between the gut microbiota and Alzheimer's disease in conventionally-raised animals, as well as the effects I observed as a result of gut microbiota modulation. In **chapter 3**, the development of the optimized optical projection tomography setup for imaging mouse intestine is described, with a proof-of-concept two-channel measurement of the gut autofluorescent structure and stained vascular network along five centimetres of intestine. **Chapter 4** outlines the gutOPT sample preparation and multi-modal acquisition pipeline, with which large-volume and high-resolution cross-referenced observations of regions of interest can be acquired. To demonstrate the usefulness of this workflow, I present the first millimetre-long uninterrupted acquisition and reconstruction of gut-associated lymphoid tissues. I also illustrate the value of label-free OPT scans to characterize mucosal structures of the intestine by applying virtual unfolding and image processing of villi density. Finally, concluding remarks and perspectives are given in **chapter 5**.

## 1.1 Alzheimer's Disease

### 1.1.1 Human Alzheimer's Disease

Dementia is a syndrome most visibly characterised by a steady decline in cognitive function, including memory, that eventually leads to significant disability (1). The most common form of dementia is Alzheimer's disease (AD), representing up to 70% of the 50 million dementia cases worldwide. Diagnostic tools have evolved in recent years to improve diagnosis confidence prior to death, including for example live patient functional and structural brain imaging techniques. However, the very common co-occurrence of AD with other morbidities, such as vascular dementia or Lewy Body disease, makes diagnosis a very complex process (2). A full understanding of the etiology of AD continues to elude researchers, which has led to a very low success rate in therapy development and ultimately no cure existing today.

The hallmarks of Alzheimer's disease, summarised in figure 1.1, center around two proteinopathies characterised by the extracellular aggregation of amyloid- $\beta$  peptides into amyloid plaques and the intracellular accumulation of phosphorylated tau protein into neurofibrillary tangles. The combination of aggregated tangle-positive neurons surrounding amyloid plaques forms neuritic plaques (3) that contribute to the complexity of AD's proteinopathic presentation. Pathophysiological processes, such as angiopathy (4; 2), neuroinflammation (5) and cognitive decline (6; 7), arise due to these local cellular disturbances and lead to a generalised imbalance in brain physiology characteristic of Alzheimer's disease.

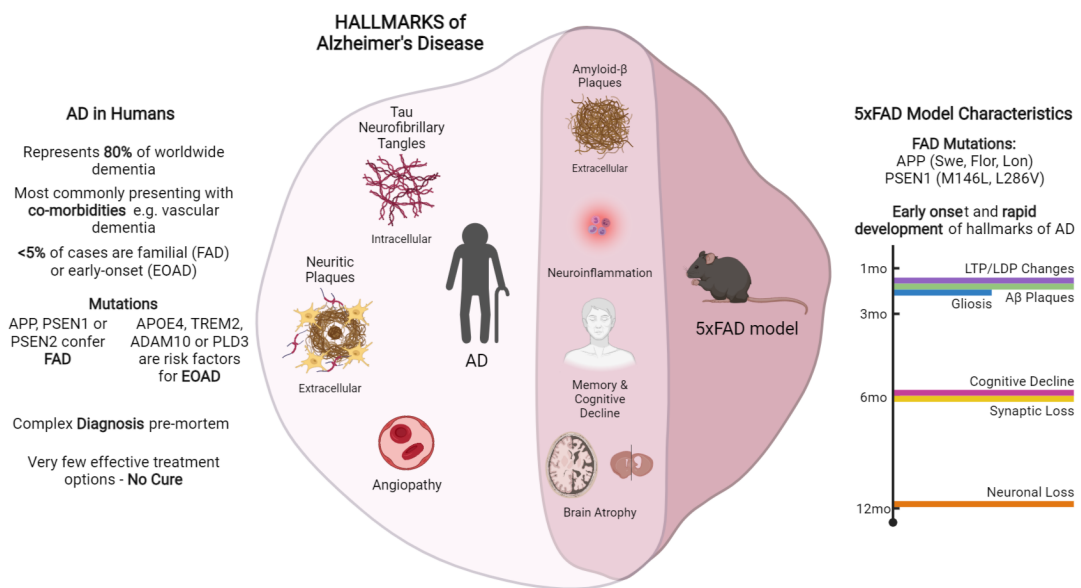


Figure 1.1 – *The Hallmarks of Alzheimer's disease in Humans and the 5xFAD mouse model*  
Pathophysiological hallmarks of AD are summarised in the center, with the overlapping region encompassing symptoms that are induced in the 5xFAD model. On the left is an overview of AD prevalence and etiological statistics in the human disease. On the right is a list of the familial AD mutations implemented to generate a model form of AD as well as a timeline of symptom development. *Abbreviations:* AD [Alzheimer's disease], FAD [familial Alzheimer's disease], EOAD [early-onset Alzheimer's disease], APP [amyloid precursor protein], PSEN1 [presenilin 1], PSEN2 [presenilin 2]

Sources: (8); World Health Organization Dementia (1); Alzforum Research Models 5xFAD (C57BL6) (9); Figure design is author's own, created using Biorender.

The majority of Alzheimer's disease cases are sporadic and have no associated genetic pre-dispositions (figure 1.1, left). On the other hand, less than 5% of cases are linked to genetic mutations that either confer familial AD (FAD, (10)) or are risk factors for early-onset AD (EOAD, (11)). Familial AD is caused by mutations in the genes that encode enzymes directly involved in the truncation of the trans-membrane amyloid precursor protein (APP), as shown in figure 1.1. Subsequent cleaving of the APP by  $\beta$ -secretase and  $\gamma$ -secretase leads to the production of 42 peptide-long amyloid- $\beta$  fragments capable of seeding the formation of plaques (12). Known familial AD mutations with loci within the amyloid precursor protein and the presenilin-1 sub-unit of  $\gamma$ -secretase (13; 14) increase the activity of this amyloidogenic pathway and lead to the over-production of pathogenic A $\beta$  fragments.

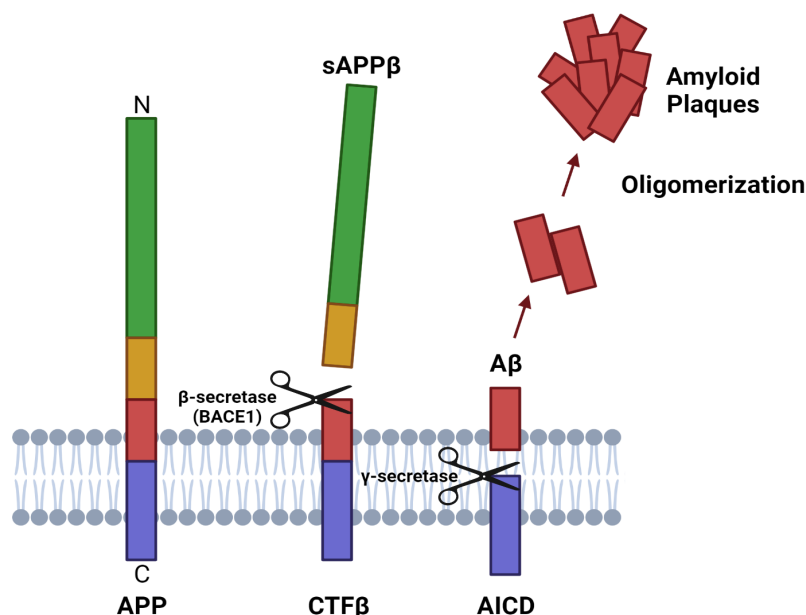


Figure 1.2 – *Amyloid-β formation through the truncation of the amyloid precursor protein*  
 The formation of amyloid-β fragments relies on the subsequent truncation of APP by β-secretase and γ-secretase. *Abbreviations:* APP [Amyloid precursor protein], sAPPβ [soluble APP-β], CTFβ [C-terminal fragment β], Aβ [amyloid β], AICD [APP intracellular domain]  
 Sources: Figure design is inspired by (15) , created using Biorender.

### 1.1.2 Animal Models of AD

The discovery of genetic mutations with significant associations to Alzheimer's disease (16; 17; 18) led to the creation of disease models in animals ranging from rodents (19) to insects (20) and nematodes (21). Several murine models of AD exist and vary in the landscape of implemented genetic mutations as well as their phenotypic presentation. In particular, the range of phenotypic hallmarks, such as amyloid plaques and neurofibrillary tangles, and the speed at which these develop can vary widely. The 3xTg model is an example where both amyloid and tau pathology develop, as well as gliosis and cognitive impairment (22). The cognitive decline occurs by four months, thus preceding amyloid plaque and tau build-up, but does not represent a learning deficiency otherwise more aligned with pathology observed in humans. Some widely used models, including the APPPS1 (23) and 5xFAD (24) models, rely solely on amyloid plaque formation to cause an AD phenotype. Phenotypic presentation is similar in these two models, with onset of amyloid plaques occurring within 6 weeks and cognitive impairment becoming detectable by the Morris water maze at approximately 7 months. Comparatively, the 5xFAD model presents a more complex cognitive phenotype with motor deficits and reduced anxiety (25) being recorded as well as spatial working memory impairments (26). For this reason, the 5xFAD model was selected for the studies presented in this thesis.

In the 5xFAD mouse model, five mutations are implemented to target neurons: three in APP (named Sweden, Florida and London after identified hot-spot regions for each mutation) and two in presenilin-1 (M146L and L286V after the localisation of the mutation within the PSEN1 gene) (13; 14). As a result of these mutations, the 5xFAD mouse is a robust model of amyloidosis-dependent Alzheimer's disease. The phenotypic hallmarks common to humans and the 5xFAD model, with a timeline of their presentation, are outlined in figure 1.2 (right). Cerebral structural deficits include early-onset deterioration of the myelin surrounding axons (27), region-specific axonopathy (28), amyloid angiopathy and microvascular inflammation (29) culminating to neuronal loss in cortical and subiculum regions (24). The subiculum, being a part of the hippocampal formation, plays a key role in mediating the interaction between the hippocampus and cortex (30), with evidence supporting that connectivity between these regions influences recollection at old age (31).

The presentation of inflammation in the 5xFAD model is central to its phenotype (32; 33; 34), with treatment methods targeting inflammation showing successful remediation of amyloid plaque deposition (34), neuronal loss (35) and cognitive impairment (36). This last hallmark is of particular diagnostic interest in pre-clinical research due to its deleterious significance in humans. In the 5xFAD model, spatial memory is significantly impacted from mid- to late-life (24; 37; 38; 25). Other forms of observed cognitive decline include increased anxiety (25), social avoidance and aggressivity (39), motor deficits (40) and auditory processing loss (41).

Despite similarities existing in the phenotypic presentation between animal models and the human disease, central hallmarks are often absent. In the 5xFAD, this includes tau phosphorylation and neurofibrillary tangle development. Preclinical models offer significant advantages for one's ability to robustly manipulate genetics and environment, and to study specific organs and behaviours as well as their response to treatment. However, they do not replicate the intricate complexities of the true disease found in patients. As a result, this context must be accounted for whilst making system-wide interpretations of scientific results.

## 1.2 The Host-Gut Ecosystem

The gut microbiome is composed of numerous elements that exist and interact with the host to create a symbiotic relationship when in equilibrium. The abundance of these elements and the system's interactive cues are largely impacted by the host's environment starting from birth and spanning one's lifetime (42). The singular nature of each individual's experiences and their inherently personal genetic makeup means that the gut microbiome is unique as well as exceptionally complex.

This fundamental uniqueness considered alongside the increasing commonality of Alzheimer's disease in today's society causes a question to arise. How can an entity characterized by such unique features be strongly associated with a disease affecting so many? We may begin to understand this concept when considering the host-gut microbiome interface as an ecosystem that amounts to more than the sum of its parts.

### 1.2.1 Components of Ecosystems

Ecosystems are defined as "a complex of living organisms, their physical environment and the interrelationships" within that environment (Encyclopedia Britannica). Living organisms are the biotic components of the ecosystem that interact with the physical environment through abiotic (non-living) components (figure 1.3). In figure 1.3 (A), a typical example of an ecosystem is shown. Resources such as the sun, temperature and molecules are abiotic contributors that are consumed and transformed by biotic elements, i.e. plants and animals.

We draw a parallel between this classical ecosystem to outline the elements and connections that make up the host and gut microbiome in figure 1.3 (B). Here, the abiotic constituents are raw dietary materials and host- and microbiota-derived metabolites, respectively acting as a source of complex fibers necessary for metabolism and as signalling molecules. The biotic components of the host-gut microbiome ecosystem originate from distinct spaces on either side of the gut lining. Examples of host-gut interactions include immune cells and host metabolites crossing into the lumen to facilitate physiological function and to ensure equilibrium and symbiosis with the biotic components of the gut microbiome are maintained.

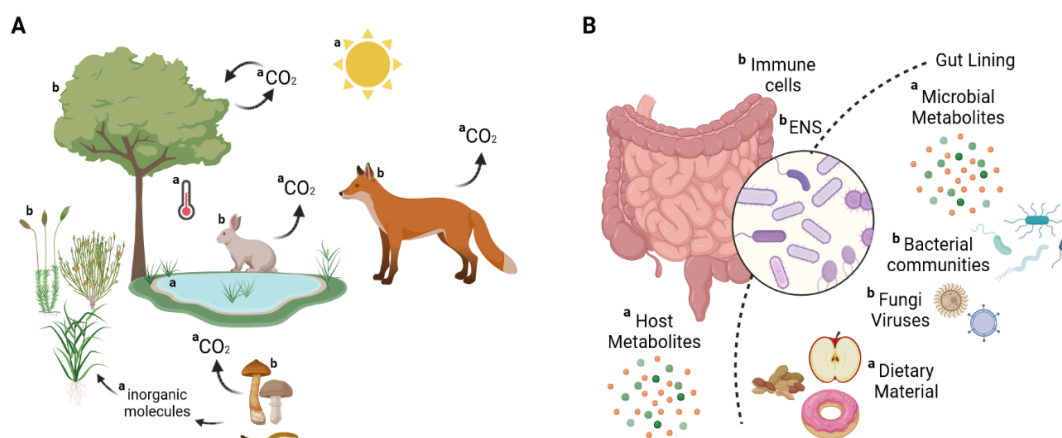


Figure 1.3 – *The Host-Gut Ecosystem Explained in Terms of a Traditional Ecosystem* Ecosystems are made up of abiotic (a) and biotic (b) components that circulate within webs to efficiently and sustainably use resources for life. The framework of a commonly described ecosystem, as displayed in **A**, can be applied to the host-gut microbiome ecosystem and simplify its understanding as in **B**.

Sources: **A** is modified from (43). **B** is author's own, inspired by **A**. Created using Biorender.

Early studies of the gut microbiota in health and disease contexts focused on the composition and relative abundance of the bacteria harboured in relevant regions of the gastro-intestinal (GI) tract. As this field has expanded, so too has our understanding that the ecosystem as a whole is crucial. Figure 1.4 provides an overview of the main communication axes that make up the host-gut ecosystem, these being immunity, energy metabolism and the connection to



the nervous system and will all be discussed henceforth.

### 1.2.2 Immunity

Host immune function at the gut lining is the physiological frontline maintaining homeostasis in the gut between host cells and the bacteria, fungi and other symbionts colonising the lumen. Cell type-specific modes of action range from pathogen detection by microfold (M) and dendritic cells, targeting and segregation of pathogens by secreted immunoglobulin A (sIgA) and their destruction and removal by recruited neutrophils (44; 45) (figure 1.4).

The gut microbiome contributes to the stimulation of host immune responses via the production of short-chain fatty acids (SCFA), that are able to activate inflammasomes through G-protein coupled receptors (GPCR) at the epithelial lining. This stimulation also leads to an increased production of mucus by goblet cells, improving the physical barrier between the gut lining and pathobionts, as well as the release of sIgA.

Antimicrobial peptides (AMP) are another means by which the host regulates gut microbiota population. Once released, their mechanism of action can range from suppression of cell division, inhibition of microbial metabolism or interruption of ATP synthesis (46). Interestingly, self-regulation of bacterial populations is also possible via the production of bacteria-derived AMPs known as bacteriocins (46).

As a whole, immunity is a principal effector of host-mediated modulation of gut function and gut microbiota population homeostasis. Furthermore, immune responses at the gut lining are heavily influenced by various other factors that fall into the energy metabolism and nervous system branches of this ecosystem. The effects of microbiota dysregulation on immune function has been observed at relatively distant sites, such as the brain. Microglia are the main immune cell type in the brain and have been found to depend on microbiota-derived short-chain fatty acid sensing for maturation and activity modulation (47). Microglial dysfunction is also observed in neurodegenerative diseases (48), such as Alzheimer's disease (34; 49), thus forming another axis by which gut microbiota modulates brain health.

### 1.2.3 Energy Metabolism

The bidirectional host-gut modulation of energy metabolism is grounded in the gut's main role of harvesting energy from ingested food. The main symbiotic axis linking the microbiome and the host is the capacity for microbes to metabolize complex carbohydrates through fermentation processes (50). This catalysis increases the accessibility of nutrients locked in dietary fiber and leads to the bi-product release of short-chain fatty acids.

As mentioned previously, SCFAs are powerful signalling molecules that in this context can be directly taken up as an energy source or induce paracrine signalling cascades through G protein-coupled receptor stimulation in white adipose tissue as well as epithelium-resident

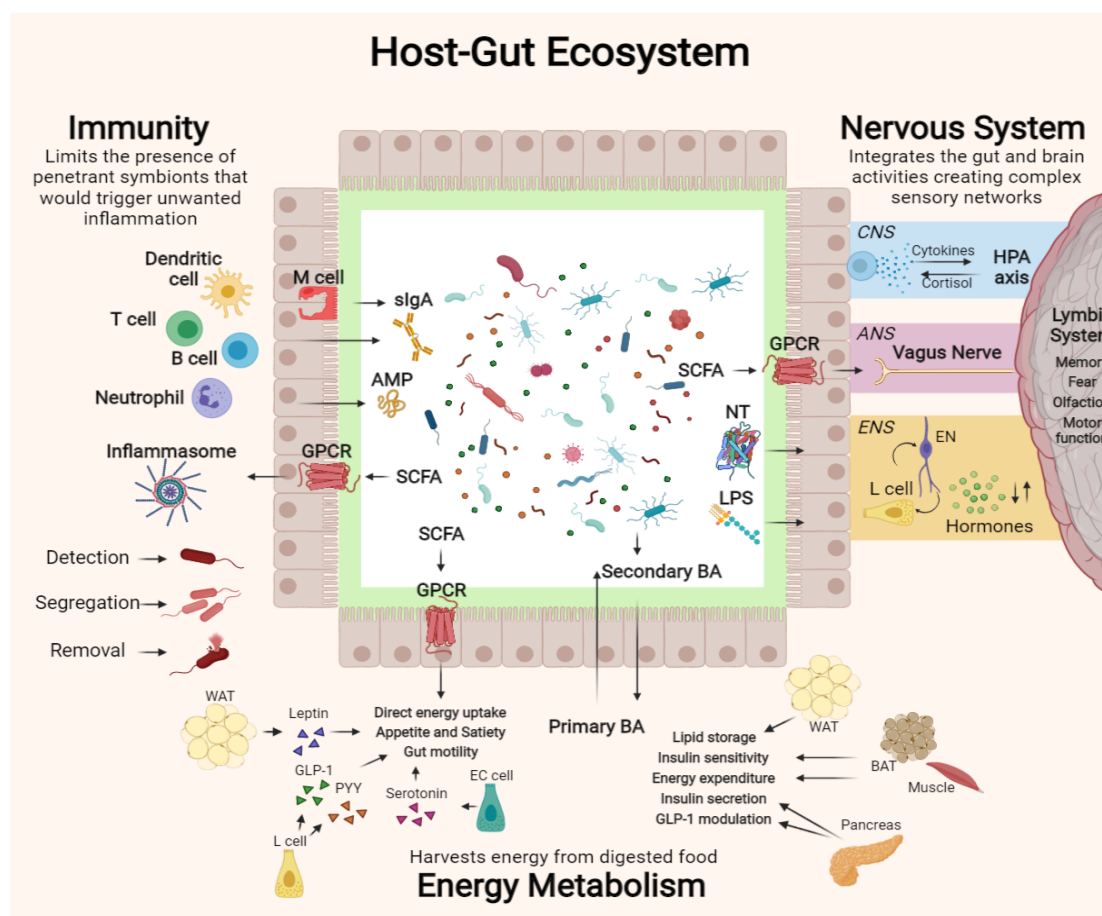


**Figure 1.4 – Principal Axes of the Host-Gut Ecosystem** The main physiological axes through which host-gut cross-talk occurs are immunity, energy metabolism and nervous system sensing. Each axis has a multitude of effects localised both in the gut and throughout the whole organism. The bidirectional nature of the interactions and their widespread influence has led to the gut microbiome being linked to the healthy development of organisms. As is shown in this figure, numerous physiological pathways are involved in maintaining host-gut homeostasis ranging from physical aspects of the gut (e.g. gut motility and permeability) to the efficient harvest of nutrients from diet. As will be made evident throughout the ensuing discussion, each branch is heavily interlinked thus highlighting the complexity of this ecosystem.

**Abbreviations:** M cell [microfold], sIgA [secreted immunoglobulin A], AMP [anti-microbial peptide], GPCR [G protein-coupled receptor], SCFA [short-chain fatty acid], WAT [white adipose tissue], GLP-1 [glucagon-like peptide 1], PYY [peptide tyrosine tyrosine], L cell [enteroendocrine], EC cell [enterochromaffin], BA [bile acid], BAT [brown adipose tissue], LPS [lipopolysaccharide], HPA [hypothalamus-pituitary-adrenal], ENS [enteric nervous system], NT [neurotransmitter].

enteroendocrine (L) and enterochromaffin (EC) cells (figure 1.4). These specialised tissues and cells produce hormones that directly influence aspects of gut health such as gut motility, and appetite and satiety. Leptin is one such hormone produced in adipose tissue that when secreted reduces lipid absorption, stimulates intestinal motility and has an important role in modulating inflammatory processes in the gut (51). Enteroendocrine cells produce a number of other hormones, such as PYY and GLP-1 which are capable of regulating satiety and food intake as well as gut transit time (52). Enterochromaffin cells, located within the gut epithelium, sense their environment and are triggered by molecules such as SCFAs to produce serotonin. Serotonin is best known as having neurotransmitter properties but in the gut acts in endocrine pathways to closely regulate motility (53). Gut motility and satiety are the main physiological processes modulated by the pathways described here. They are extremely important as they affect the intake of raw materials and the length of time the host and the gut are exposed to them, respectively.

Another important class of molecules that play a key role in the host-gut ecosystem are bile acids (BA). They originate from the catalysis of cholesterol in the liver and are delivered to the GI tract to facilitate lipid breakdown and absorption (54). Prior to delivery in the gut, bile acids are in their primary conformation and once there are transformed by members of the gut microbiota to secondary bile acids. These secondary bile acids can be detected in various tissues that harbour the appropriate receptors, as is summarised in figure 1.4. Via BA stimulation, lipid storage is influenced by white adipose tissue, whilst energy expenditure and insulin sensitivity are controlled both by brown adipose and muscle tissue. Additionally, secondary BA signalling triggers insulin secretion and GLP-1 modulation from the pancreas (54).

Evidently, all of the involved pathways significantly impact the host's metabolic system. Furthermore, this links gut microbiota function to several diseases such as obesity and diabetes, which are known risk factors for numerous co-morbidities including Alzheimer's disease (55). Thus, two major signalling molecules either produced or modified by members of the gut microbiota are able to directly influence host energy metabolism through wide-ranging pathway involvement. This highlights the importance of the raw materials that shape gut microbiota populations by providing an ideal environment for some over others.

### 1.2.4 The Nervous System

The nervous system branch of the host-gut ecosystem is composed of neural connections between the gut and the brain that involve the central nervous system (CNS), the autonomic nervous system (ANS) and the enteric nervous system (ENS).

Within the CNS, sensory networks transmit signals to the brain that largely lead to efferent neurons implementing physiological responses (56). One of the core CNS pathways between the gut and brain is the adrenal-pituitary-adrenal (HPA) axis, which mediates stress responses via step-wise signalling through each of the HPA constituents, leading to the eventual release of cortisol (57). Stressors, for example pro-inflammatory cytokines, will activate the HPA

axis in order to address the physiological needs in the gut. HPA adrenal cortisol release at these sites affects various intestinal effector cells including immune cells, epithelial cells, enteric neurons and enterochromaffin cells. As has been mentioned previously, these cell types are also under the influence of the gut microbiota, thus revealing one of the underlying mechanisms responsible for the bidirectional communication of the gut-brain connection.

The vagus nerve is the most prominent component of the autonomic nervous system involved in the gut-brain axis (GBA). It can be stimulated by various gut-derived ligands, including SCFAs, neurotransmitters and hormones secreted by enteroendocrine cells in response to microbiota-derived lipopolysaccharide (LPS) stimuli (58). Its efferent roles include the regulation of gut motor and secretory functions, more specifically gut permeability, whilst its afferent effects are closely linked to complex host behaviour due to its direct communication with the limbic system. By connecting to the limbic system, the vagus nerve enables the gut to influence fear and arousal responses in the amygdala, memory and spatial recognition in the hippocampus as well as olfactory and sensory motor functions in the limbic cortex (56). As will be discussed in further sections, the direct effect of the gut microbiota on cognitive health, including on memory, makes the gut microbiota a highly relevant area of research in neurodegenerative diseases.

The enteric nervous system constitutes a GI tract-spanning network of ganglia interconnected by nerve fibers (59), whose particular structure and function vary according to organ-specific niche development. In the small intestine, the ENS has extensively evolved to detect nutrients, modulate epithelial secretion of various molecules including bioactive peptides and hormones, influence intestinal barrier integrity and more (60). One of the prominent physiological functions fulfilled by the ENS is the coupling of exocrine secretion with microvascular circulation in response to neurotransmitters mostly originating from afferent neurons as well as epithelial cells (59; 60).

### **1.3 Evidence of Gut-Brain Dysregulation in Neurodegenerative Disorders and Therapeutic Targets**

The relevance of gut-brain homeostasis in the maintenance of health and the development of disease has become increasingly evident alongside our understanding of the host-gut ecosystem. Having provided an overview of the axes connecting the gut and the brain, we progress to examples of the organism-wide impairments that can arise when a dysregulated gut-brain axis contributes to disease. Autism spectrum disorder (ASD) is an important example of this, as studies of this syndrome's gut-brain characteristics were seminal in bringing the gut microbiome to the forefront of neurological disease research. The current status of the gut-brain link and associated therapeutic approaches for ASD, Parkinson's and Alzheimer's disease will be presented.

### 1.3. Evidence of Gut-Brain Dysregulation in Neurodegenerative Disorders and Therapeutic Targets

---

#### 1.3.1 Autism Spectrum Disorder

Autism spectrum disorder is characterized by stereotyped behaviour, communication deficits and a diminished capacity for social interaction starting from childhood (61). As well as exhibiting significant neurological symptoms, it is a disorder that consistently presents with GI tract disturbance, such as constipation or diarrhoea (61). Other gut-related symptoms include severe disruption of gut barrier permeability (62), detection of bacterial products (e.g. LPS) in the bloodstream (63; 64) and alterations in gut microbiota diversity as well as the loss of anti-inflammatory microbiota constituents (e.g. *Bacteroides*) (65).

Therapeutic interventions targeting the gut have proven effective in alleviating some symptoms of ASD. An important consequence of the cognitive symptoms of ASD is a difficulty in implementing a varied diet, thus leading to deficiencies in dietary fiber and anti-oxidant components (66). Diet supplementation with, for example, omega-3 fatty acids or levocarnitine was able to improve ASD symptoms (67; 68). Probiotic supplementation, i.e. the inoculation of living bacterial cocktails, with either simple (one/two species) or multi-bacteria cocktails was shown to improve gut barrier integrity and restore a normal immunomodulation of cytokines (69). In a six-month-long study testing probiotic efficacy, cognitive improvements were also observed independently of improvements observed in the gut (70). A more aggressive approach to modulating the gut microbiota is microbiota transfer therapy (MTT), involving fecal material transfer (FMT). This technique is controversial as its effectiveness in treating inflammatory bowel disease has been shown in isolated studies (71) but variability in efficacy and adverse effects remain of concern. Nevertheless, a recent trial performed MTT in children with ASD with a 2-year follow up that showed long-term improvements in both gastro-intestinal and ASD symptoms (72).

#### 1.3.2 Parkinson's disease

Parkinson's disease (PD) is the second-most prevalent form of neurodegenerative disease (73). Clinical symptoms center around motor dysfunction caused by nerve cell damage and a subsequent decrease in dopamine production in the basal ganglia (73), otherwise known as the control center for movement, balance and coordination. The gut-brain axis has been implicated in PD as dysregulation of the enteric nervous system, gastrointestinal symptoms such as constipation (74) and prolonged transit time (75), and gut microbiota dysbiosis have been shown to precede motor deficits (76; 77; 78). Evidence of specific microbial community alterations (79; 80; 81; 82) and short-chain fatty acid profiles (83) have been associated with PD severity and disease outcome.

The efficacy of targeting the gut microbiota as a therapeutic approach for Parkinson's disease has shown promise through the implementation of various techniques. Indirect efficacy was shown through the gut microbiome's capacity to modulate drug metabolism (84), which has been shown to influence pharmacokinetics in the treatment of Parkinson's disease (85). Direct modification of the gut microbiota, through fecal material transfer, was performed in

## Introduction

---

six PD patients with a two-year follow-up (86). Improvements in motor, non-motor and GI symptoms were observed in five out of six patients within four weeks, with adverse effects occurring in one of the six. Probiotic and prebiotic interventions have focused on the effect of supplementing the host-gut ecosystem with health-promoting short-chain fatty acids, such as butyrate (87; 88). Probiotic supplementation with *Clostridium butyricum* in a neurotoxic agent-induced PD animal model revealed the importance of glucagon-like peptide 1 (GLP-1) in rescuing gut microbiota dysbiosis whilst in parallel improving characteristic motor and cognitive functions (88). In PD patients, the administration of resistant starch as a prebiotic aimed to increase SCFA levels, that are typically depleted in PD (87). The 12-week-long intervention led to a stabilisation in fecal microbiota composition, an increase in fecal SCFA abundance (particularly butyrate) and a decrease in the bowel inflammation marker, calprotectin.

### 1.3.3 Alzheimer's Disease

The number of studies of the gut-brain connection in Alzheimer's disease grew exponentially, as shown in figure 1.5, as the direct impact of the gut on neuroinflammation and its involvement in other neurodegenerative diseases, such as Parkinson's disease (76), became clear. Unfortunately, this increase in publications is driven mostly by review articles describing the potential for the gut microbiota to provide new avenues in the field of neurodegenerative disease. This imbalance highlights the need for continued original research efforts ultimately required for novel insights to arise.

In humans, patients diagnosed with dementia due to AD exhibited a decrease in fecal microbiota diversity and a distinct composition compared to age- and sex-matched controls (89). More specifically, the ratio in the two most abundant phyla (Firmicutes and Bacteroidetes) was inverted in AD. Furthermore, specific genera, including *Akkermansia spp.*, *Bacteroides spp.* and *Turicibacter spp.*, showed significantly altered relative abundance. These also correlated with the presence of AD biomarkers in the cerebro-spinal fluid of patients. Furthermore, the presence and abundance of pro-inflammatory members of the gut microbiota positively correlated with amyloidosis in the brain of AD patients as well as peripheral inflammatory markers (90).

AD-associated gut microbiota alterations are also relevant in preclinical models of AD. Similar trends in diversity and phylum- and genus-level differences were observed in conventionally-raised aged APP/PS1 mice (91). The use of a germ-free APP/PS1 model proved the microbiome's capacity to affect model hallmarks of AD, having shown a significant reduction in the genetically-driven accumulation of amyloid- $\beta$  in the brain. Furthermore, the colonization of germ-free AD mice with cecal contents obtained from conventionally-raised AD mice significantly increased amyloid plaque burden compared to when colonized with the microbiota from healthy mice.

Microbial manipulations in the context of treating symptoms of Alzheimer's disease have been

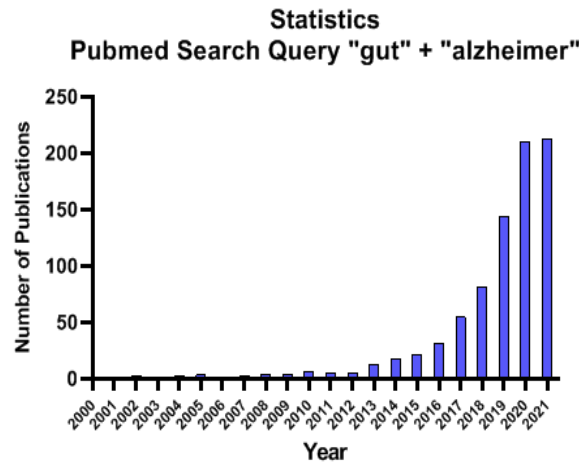


Figure 1.5 – *Growth of the field of gut-Alzheimer's disease research in number of publications*  
Number of publications per year in Pubmed database between 2000 and 2021 matching the search query of "gut" and "alzheimer". Data source: pubmed.ncbi.nlm.nih.gov

successful, though not widely prescribed. Approaches to dietary intervention should account for their positive impact on prominent risk factors of AD such as obesity. Thus, adhesion to a Mediterranean diet led to improvements in brain matter loss in cognitively normal individuals at risk of AD (92). In search of a diet-mediated modulation of inflammation in AD, several anti-inflammatory ingredients, including curcumin, vitamin D3 and caffeine, were shown to improve symptoms of AD (93). Probiotic treatments tested in two pre-clinical models of AD (3xTg-AD mice and rats injected with A $\beta$ ) successfully restored energy metabolism pathways in the brain, reduced levels of phosphorylated tau (94) and improved spatial learning deficits and synaptic plasticity (95).

In summary, the potential for therapies targeting the gut microbiota to be successful in neurodegenerative diseases remains promising but somewhat unclear. Today, we are in the early stages of implementing therapeutic strategies whilst continually assessing the variability of efficacy as well as controlling for adverse effects. The continued global research effort towards a better understanding of the gut-brain connection in diseases such as AD will provide novel options for early diagnosis and hopefully also for treatment.

## 1.4 Microscopy Tools to Study the Gut Ecosystem

In recent years, technological advances in microscopy and image processing have enabled scientists to probe biological processes through imaging. Due to these advances, microscopy has evolved from largely qualitative observations of cells and tissues to the production of high-throughput quantitative data sets in fixed or live tissues (96). A unique advantage brought by applying microscopy techniques to physiological contexts is the ability to generally retain native conformations of structural and functional components of interest. Three-dimensional

## Introduction

---

data provide the added benefit of contextualising biological signals within tissues in a way that improves interpretations of physiology. However, the availability of a wide range of microscopy techniques comes with inevitable technical constraints related to specimen preparation and staining that must be considered during modality selection and the resulting interpretation.

Traditionally, the study of biological processes focuses on interpreting molecular and/or cellular interactions using biochemical techniques. For example, our approach to assessing the gut-brain interaction in Alzheimer's disease entails studies of gut microbiota composition by 16S rRNA sequencing and of brain metabolites by mass spectrometry. Histopathological assessment of amyloid- $\beta$  plaque load is historically appropriate, but novel techniques, such as optical projection tomography, can provide a holistic view of molecular or cellular interactions at the organ scale. For example, an understanding of the spatial organisation of amyloid plaques throughout the brain in the 5xFAD model was revealed by OPT (97; 98).

Imaging modalities applied to the gut usually span the microscopic scale, with the ability to image epithelial and bacterial cells at varying resolutions (99; 100; 101; 102; 103). Recently, light-sheet microscopy (LSM) has garnered much interest for its capacity to produce 3-dimensional images with high resolutions (in the range of 2-15 micrometers (104)). Furthermore, its adaptation for the acquisition of fluorescent signals, known as light sheet fluorescent microscopy (LSFM), has made it compatible with previously established fluorescent labelling methods. Centimetric volumes can be acquired by LSM, though this requires the concatenation of microscopic acquisitions that is time-consuming and produces heavy data sets.

Within the host-gut ecosystem, an example of a spatially relevant entity composed of specialised structures is immunity. Gut-associated lymphoid tissues (GALT), which include Peyer's patches (PP) and isolated lymphoid follicles (ILF), form hubs for continuous monitoring of luminal signals and rapid pathogen detection and destruction within the intestinal mucosa (105). The relevance of these structures in understanding the host-gut ecosystem's immune network is underlined by the dependence of ILF maturation on gut microbiota training (106; 107). The distribution of GALTs throughout the intestine has mostly been described by 2D local visualization using methods such as brightfield microscopy, scanning electron microscopy, confocal microscopy and stereomicroscopy (108; 109; 110; 105; 111). Three-dimensional studies of lymphoid cells using LSFM have revealed the importance of cell trafficking in a mouse model of inflammatory bowel disease (112).

The functional relevance of intestinal structures such as GALTs cover distances that go beyond a few centimetres. The mesoscopic scale of optical projection tomography, as well as its capacity for fluorescence signal acquisition, make it an ideal modality for studying large volumes of intestine. Despite a reduced resolution relative to modalities such as LSM, reduced data acquisition and processing times are advantageous. However, immune disturbances are driven by coordinated clusters of cells and the importance of observing these at high resolution cannot be denied. Therefore, to address the need for high volume and high resolution observations of the gut's immune system, OPT is concatenated with confocal microscopy in our novel gutOPT



#### **1.4. Microscopy Tools to Study the Gut Ecosystem**

---

pipeline. Additionally, the procedure of clearing reversal should be compatible with other high-resolution imaging modalities, thus making gutOPT adequate for the development of a multi-modal imaging pipeline.

In this thesis, I will present a novel application of optical projection tomography developed to probe functionally pertinent structures in the gut. The rotational image acquisition of optical projection tomography proved to be suited to the tubular shape of the gut. Furthermore, an updated setup design aimed to optimize the resolution was achieved to the reduced depth of field of the gut compared to larger samples previously imaged by OPT (for example the mouse brain (97)).



## 2 Effect of Gut Microbiota Modulation in a Model of Alzheimer's Disease

The work presented in this chapter is the result of a multi-disciplinary research effort within the framework of the AD-gut Horizon 2020 Consortium ([adgut.eu](http://adgut.eu)). The goal of the project was to reach a better understanding of gut microbiota composition alterations resulting from early-onset Alzheimer's disease mutations in the 5xFAD mouse model. Furthermore, we aimed to investigate the therapeutic potential of gut microbiota modulation in AD using two methods. In one, the power of cohousing 5xFAD (Tg+) mice with healthy (Tg-) littermates was observed, whereby microbiota composition was altered in wild-type cohoused groups compared to those separately housed. In the other, strict germ-free and gnotobiotic conditions were put in place, with the aim to test the effects of two different low-complexity bacterial cocktails in the 5xFAD model. The gut ecosystem encompasses varied classes of metabolites that directly impact host health at the gut lining but also at distant sites. Thus, we hypothesised that one major axis by which the gut microbiota is modulating brain health is through metabolomic transport and signalling. Our investigation of brain metabolites revealed genotype-dependent differences in the abundance of a number of compounds derived from ingested products in conventionally-raised conditions. Low-complexity groups, whose AD phenotype is reduced, do not exhibit a genotype dependence in the abundance of these metabolites in the majority of cases.

Arielle L. Planchette, Alessio Mylonas, Francesca Ronchi, Terry Mueller, Monica Iacchizzi, Andrina Rutsch, Olena Prykhodko, Stephen Burleigh, Thao Duy Nguyen, Tannaz Ghaffarzadegan, Ling Cao, Raffaele Vitale, Katrin Freiburghaus, Cedric Bovet, Martina Zanella, Frida Fak-Hallenius, Andrew Macpherson, Aleksandra Radenovic, Mercedes Gomez de Agüero, "Effects of Gut Microbiota Modulation in a Model of Alzheimer's Disease" Submitted to Scientific Reports (October 2021)

A.L.P. wrote the bulk of the manuscript in close collaboration with A.M., E.R., M.G. and A.R.. The same team collaborated on the combined data analysis, synthesis and preparation of figures. The author contributions to the experiments in the manuscript can be found in the methods section. The project was supervised and guided by M.G., A.Mac. and A.R.

### 2.1 Introduction

Alzheimer's disease (AD) is the most common neurodegenerative disease and occurs most frequently in the elderly (113). Characteristic hallmarks of AD include the accumulation of amyloid-beta plaques and cognitive decline. Genetic mutations that alter the proteolytic processing of the amyloid precursor protein (APP) have been implicated in causing either an early (114) or late onset (115) familial form of Alzheimer's disease (fAD). Mutations in the APP (17) and its proteolytic processing lead to an increased deposition of amyloid-beta ( $A\beta$ ) in plaques. Despite important advances in our understanding of APP (116), we still lack a satisfactory understanding of the aetiology of AD.

Recently, the gut microbiome has been implicated in the development of neurodegenerative diseases including Multiple sclerosis (MS) (117; 118), Alzheimer's disease (AD) (91), Parkinson's disease (PD) (76) and Autism Spectrum Disorders (ASD) (119). These findings have made it relevant to investigate the gut microbiome as a potential source of diagnostic biomarkers and as a therapeutic route. Previously, it was shown that the lack of a microbiome is protective of plaque deposition in AD (91), demonstrating the functional role of the gut microbiota in Alzheimer's disease progression. It is established that as the microbiota composition is altered, so too are the host's microbial-derived metabolites (120). However, the extent of cognitive decline and the involvement of microbial metabolites in the brain have not yet been investigated.

Additionally, health- or disease-promoting mechanisms, such as biomarkers of AD and inflammatory processes, have been associated with the abundance of specific bacteria. Genera that are more prevalent in AD patients include *Blautia* and *Bacteroides*, both of which correlate with amyloid-beta and phosphorylated tau biomarkers measured in cerebrospinal fluid (CSF) (89). Conversely, health-promoting genera that are significantly less abundant in AD patients are *Bifidobacterium*, *Turicibacter* (89), *Parabacteroides* (91) and *Akkermansia* (121). The bacterium *Akkermansia muciniphila* has been of particular interest for its therapeutic impact as it is consistently less abundant in neurodegenerative diseases (122). For example, in aged conventionally-raised AD mice, *Akkermansia muciniphila* relative abundance was negatively correlated with levels of amyloid-beta 42 in the brain (91). Additional health-promoting bacteria identified in humans and in murine models that are of interest for probiotic formulations include *Roseburia intestinalis*, implicated in the production of anti-inflammatory products (123), *Bacteroides thetaiotaomicron* known to trigger immunological development in germ-free models (124), and *Lactobacillus reuteri* as an immunomodulator capable of reducing the production of pro-inflammatory cytokines (125). To increase the value of studying the microbiota in disease contexts, functional studies of the molecular signals that alter host physiology should be a priority.

In this study, we identify the bacteria characterizing dysbiosis in the conventionally-raised 5xFAD model (24) and follow the microbiome's evolution throughout AD development, together with an assessment of the brain metabolite signature at old age. The housing experi-

mental conditions, that significantly contribute to an organism's microbiome, are extremely important in studies of gut microbiota modulation (121; 126; 127; 128; 129; 130; 131; 132). We aimed to study how housing conditions could influence gut microbiota composition and neurological symptoms of AD in 5xFAD mice. We found that amyloid and cognitive symptoms of AD were significantly diminished in aged cohoused 5xFAD animals compared to non-cohoused groups. These occurred in conjunction with changes in the microbiota profile of both cohoused genotypes, with specific bacteria identified as significantly altered as a result of cohousing. Finally, we tested whether specific bacteria of the gut microbiota were effective in treating symptoms of AD in 5xFAD mice. The two cocktails that we used are Adgut (*Akkermansia muciniphila* YL44, *Parabacteroides distasonis* ASF519 and *Roseburia intestinalis* DSM14610) and Cuatro (*Escherichia coli* K12, *Bacteroides thetaiotaomicron* ATCC29148, *Lactobacillus reuteri* I49 and *Clostridium clostridioforme* YL32). In both gnotobiotic conditions, symptoms of AD pathology did not worsen compared to animals in germ-free conditions, even at old age.

## 2.2 Methods

### 2.2.1 Animal models

Animals were housed in two separate facilities based on their hygiene conditions. All conventionally-raised groups were specific pathogen free (SPF) at EPFL and experiments were run with the approval of the Canton of Vaud ethics and veterinary authorities (VD 3448). Standard food and water were available ad libitum. The gnotobiotic models (germ-free, Adgut and Cuatro) were housed in individual isolators at the clean mouse facility (CMF) in Bern (BE88/17 and BE35/2021), with an ad libitum supply of autoclaved food and water. Animal experiments were approved by the Bern cantonal ethics and veterinary authorities. Contribution: A.L.P. and A.M.

Two conventionally-raised cohorts were studied at EPFL. In one, animals were separated at weaning according to 5xFAD genotype, with two groups of cages containing only one genotype and a control group with co-housed animals. Non-cohoused groups are annotated WT-WT or Tg-Tg depending on the genotype present, whilst cohoused groups are WT-CH for cohoused wild-type littermates and Tg-CH for cohoused 5xFAD transgenic animals. The separately-housed cohort was performed once, whilst the cohoused cohort was repeated once (two iterations in total). Contribution: T.M., M.I., A.R., F.R. and M.G.

### 2.2.2 16S sequencing of the gut microbiota

Longitudinal feces collections were performed at time points designed to probe early (16 and 24 weeks) and late (32 and 42 weeks) stages of Alzheimer's disease. Individual mice were placed in a clean cage and fecal pellets were collected, flash frozen and stored at -20°C until sequenced. Contribution: A.L.P.

## **Chapter 2. Effect of Gut Microbiota Modulation in a Model of Alzheimer's Disease**

---

V4 16S rRNA sequencing was used to probe gut microbiota composition, with sample processing performed according to the Illumina sequencing pipeline requirements.

16S relative abundance data was interpreted using ANOVA-simultaneous component analysis (ASCA, (133)), with age and genotype as filtering factors. Ten thousand permutations were computed with the number of samples from the smallest group. Principal component separation for the group as a whole was observed and the corresponding loading values were analysed to identify bacteria significantly associated with genotype and/or age. Contribution: S.B., O.P., L.C., EF

Pearson correlation analysis was performed on the complete 16S profile of the selected groups and plotted using Graphpad Prism. Contribution: A.L.P.

### **2.2.3 Cognitive testing**

The Morris Water Maze was performed in conventionally-raised females at the four time-points selected for our study. The test is preceded by three days of 2-minute handling sessions by the experimenter. The test was performed over five days, with four days of training followed by one recall session. The training phase consisted of six 2-minute trials per mouse separated by a 30-minute period. During these trials, the mice freely explored the pool with no input from the experimenter. After two minutes, mice were guided to the platform and remained there at least 15 seconds before being returned to the cage. If the mice found the platform and remained on it at least 3 seconds, they were removed by the experimenter. The recall test consisted of a 2-minute trial during which the platform was absent and the experimenter assessed searching characteristics exhibited by the mouse. Gnotobiotic animals (germ-free, Adgut and Cuatro) were tested at 42 weeks of age under SPF conditions as a terminal experiment. Contribution: A.L.P.

### **2.2.4 Amyloid- $\beta$ plaque quantification**

Upon excision, a portion of the brain was fixed in 10% Formalin at room temperature for 4 hours and cryo-protected in 30% sucrose at 4°C overnight. The samples were frozen in optimal cutting temperature compound (OCT) on dry ice and 25 micrometre-thick sections were collected using a Leica CM3050S cryostat and mounted on charged glass slides. To stain the amyloid- $\beta$  plaques, slides were primed in 70% ethanol for 1 minute, followed by a 20-minute dark incubation in 0.1% Thioflavin S (CAS 1326-12-1, Acros Organics 213151000) dissolved in 70% ethanol filtered through a 0.22 $\mu$ m filter. After a wash step, slides were mounted with Fluoromount G (Southern Biotech 0100-35) and a 60x20mm glass coverslip. Slides were imaged in an Olympus VS120 slide scanner at 10X magnification illuminated with a DAPI filter for 200ms. Individual plaques and brain tissue regions were segmented using a pixel classifier in the Qupath whole-slide image processing software (134). The ratio of plaque relative to brain area is calculated within Qupath and extracted for all samples using a program

in python with Qupath integration. Contribution: A.L.P.

### 2.2.5 Metabolomic Analysis

The metabolic profile was probed in the brain by untargeted ultra-performance liquid chromatography high resolution mass spectrometry (UPLS-HRMS). Metabolites with high-quality peaks were cross referenced with an in-house database and annotated when the metabolite identity was certain. Standard fold change analysis was performed using the MetaboAnalyst tool, with a minimum threshold of 2-fold difference and a 95% confidence limit. Contribution: A.L.P., K.F., C.B., M.Z. and R.V.

## 2.3 Results

### 2.3.1 Gut microbiota composition is altered in the 5xFAD model

Animal rearing conditions were set up such that 5xFAD transgenic positive (Tg+) and negative (Tg-) littermates were born from a 5xFAD Tg+ father and a Tg- mother, as shown in figure 2.1 (A). At weaning, mice were separated according to the 5xFAD genotype so that the two groups were separately-housed (Tg+ SH and Tg- SH). Assessments of AD symptom severity were performed terminally, whilst feces collection and 16S rRNA sequencing occurred throughout ageing. The genetically-driven accumulation of amyloid- $\beta$  plaques in the 5xFAD model is able to induce symptoms of Alzheimer's disease, such as cognitive decline. Disease severity was probed at time points designed to span from young (16 and 24 weeks) to old age (32 and 42 weeks) testing both females and males. Amyloid plaques were stained with thioflavin S and imaged in order to quantify plaque burden dynamics throughout the evolution of AD (figure 2.1 (B)). This burden increases with age in Tg+ animals, with wild-type littermates remaining clear of plaques throughout (figure 2.1 (C)). Cognitive decline was measured using the Morris water maze and is prominent in females at 42 weeks of age (figure 2.1 (D)), with latency to the target platform being significantly increased in transgenic animals on day 2 of learning. Instead, at 32 weeks, the increase in latency in Tg+ SH animals is less pronounced and not statistically significant (figure 2.1 (D)).

The effect of the 5xFAD genotype on fecal microbiota composition was measured throughout ageing in littermates that were housed separately according to genotype. Using the multivariate analysis tool ASCA (133), we found that 5xFAD Tg+ genotype significantly influenced fecal microbiota composition regardless of age (figure 2.1 (E)) and that the greatest divergence in microbiota profile occurs at the latest stage of AD (figure 2.1 (F)). The 16S profiles of individual mice show a distinct separation at 42 weeks (figure 2.1 (G)). Using loadings values from the genotype only (figure 2.1 (H)) and the interaction between genotype and age (figure 2.1 (I)), we identify bacteria that associate with these parameters. We found that the bacteria *Bacteroides* spp., *Odoribacter* spp., *Alistipes* spp. and *Anaeroplasma* spp. were significantly associated with Tg+ SH mice, whereas *Turicibacter* spp., *Bifidobacterium* spp. and *Allobaculum* spp. were

## **Chapter 2. Effect of Gut Microbiota Modulation in a Model of Alzheimer's Disease**

---

associated with the Tg- SH group (figure 2.1 (H-I)). By plotting individual bacteria selected by the multivariate analysis (figure 2.1(J)), we observed the varying dynamics of their relative abundance due to age and 5xFAD genotype. In particular, the majority of bacteria associated with the Tg+ SH mice show a sudden increase at 42 weeks (figure 2.1(J)), at which time both plaque burden and cognitive decline are advanced.



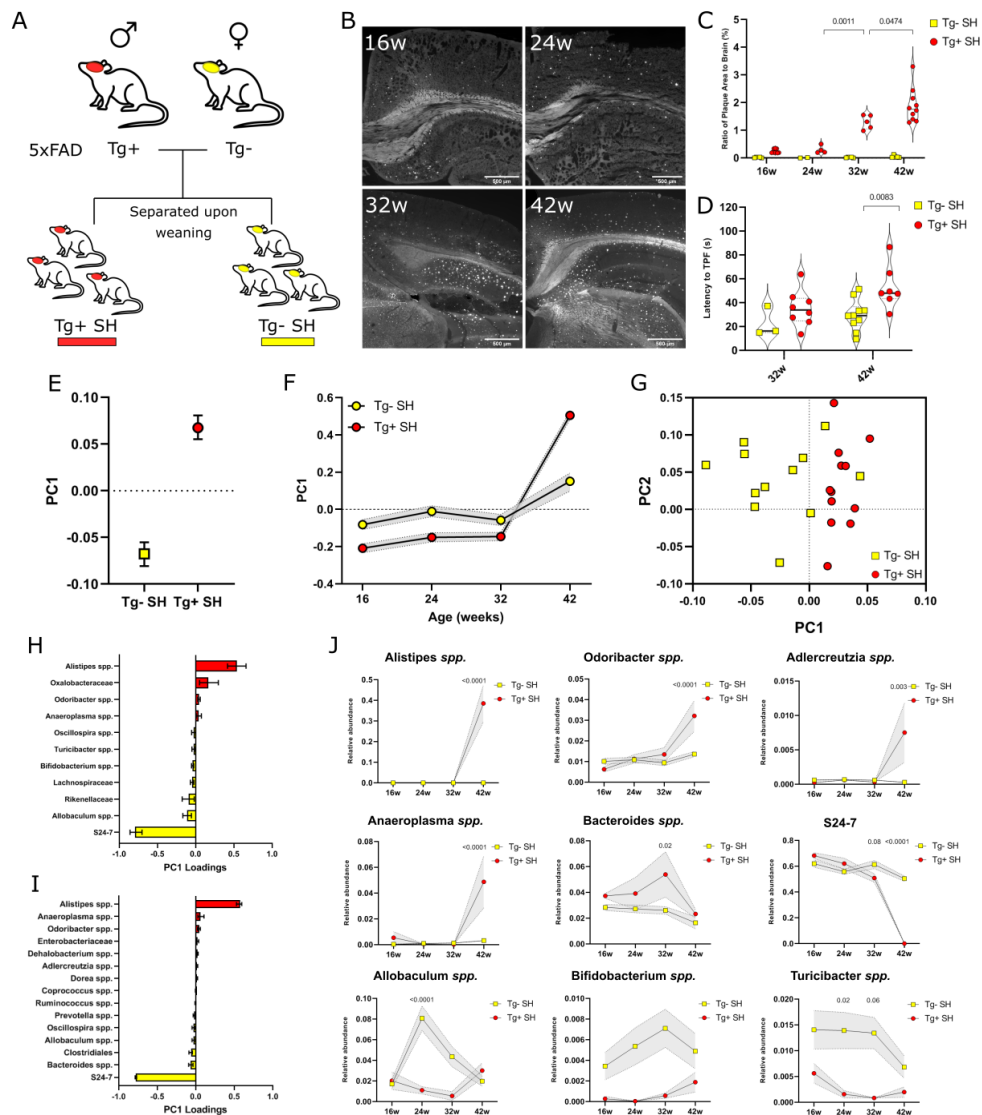


Figure 2.1 – Gut microbiota composition is altered in the 5xFAD model with age. Severity of Alzheimer's-like pathology in conventionally-raised 5xFAD model as well as 16S rRNA sequencing in fecal samples throughout ageing. (A) Experimental approach for breeding and housing 5xFAD littermates. (B) Amyloid- $\beta$  plaque aggregation is shown in representative images of thioflavin S-stained plaques for each time point in 5xFAD transgenic mice. (N= 9 at 16w, N=4 at 24w, N=5 at 32w and N=10 at 42w). (C) Ratio of plaque area to brain (%) from thioflavin S-stained sections throughout ageing. (D) MWM Latency to target platform (TPF) measured in 42-week old 5xFAD transgenic (Tg+) and wild type (Tg-) housed separately (single-house) according to genotype ((Tg- SH) or (Tg+ SH)). (E) Principal component analysis of faecal 16S profiles calculated by ASCA modelling (10'000 iterations) between Tg- (Tg- SH) and Tg+ (Tg+ SH) mice housed separately according to genotype and including all ages. (F) Principal component analysis of interaction between genotype and age. (G) Principal component analysis with individual point at 42 weeks only. (H) Association of bacteria to genotype in PC1 loadings. (I) Association of bacteria to genotype and age interaction in PC1 loadings. (J) Relative abundance of bacteria with genotype and/or age association. Statistics are two-way ANOVA with Bonferroni multiple comparisons. Experiment performed once.

### 2.3.2 Co-housing 5xFAD and control littermates alters microbiota composition and reduces severity of AD

Housing is an experimental factor known to significantly impact studies of gut microbiome composition (135; 136). We conducted experiments with the co-housing condition, as shown in figure 2.2, to understand how the microbiota and disease development (cerebral amyloid plaques formation and memory deficits) would be affected. At weaning, animals born from a 5xFAD transgenic positive (Tg+) father and negative (Tg-) mother were separated into three housing groups: a cohoused (Tg+ CH and Tg- CH) and two separately-housed (Tg+ SH and Tg- SH) groups (figure 2.2 (A)).

At 42 weeks, a Pearson correlation matrix of the fecal microbiota profile confirms that by cohousing 5xFAD littermates (Tg+ CH and Tg- CH), the microbiota of Tg- and Tg+ animals becomes similar to each other and very dissimilar to separately housed Tg- SH animals (figure 2.2 (B)). This distinct separation is further identified by ASCA modelling of the 16S data including all ages, whereby the significant difference between separately housed genotypes was lost when animals were cohoused (figure 2.2(C)). When the effect of genotype and age is analysed, we observed the grouping of Tg- CH, Tg+ CH and Tg+ SH animals from 16 weeks onwards that evolves into a larger divergence at 42 weeks (figure 2.2 (D)), whilst Tg- SH animals exhibited no variation throughout. Several genera previously changing due to 5xFAD genotype were found to be altered by co-housing at 42 weeks of age by plotting loadings along principal component 1 (figure 2.2 (E)). Individually plotting the bacteria *Bacteroides* spp., *Allobaculum* spp., *Alistipes* spp., *Prevotella* spp. and *Turicibacter* spp., confirmed the trend observed by multivariate analysis (figure 2.2 (F)). This effect is present but less prominent at 32 weeks (figure 2.6 in supplementary information).

Alongside altering gut microbiota composition, co-housing significantly reduced the cerebral amyloid plaque load at 42 weeks compared to levels observed in separately-housed individuals (figure 2.2 (G)). This is also the case for animals at 32 weeks of age (figure 2.6 in supplementary information). This suggests that gut microbiota modulation is capable of altering hallmarks of AD, in spite of the amyloid plaque load being genetically driven in these models. Furthermore, cognitive decline appears to be influenced by the housing condition. In the Morris water maze at 42 weeks (figure 2.2 (H)), the significant loss in cognition observed in separately-housed animals (Tg+ SH) is no longer significant in the cohoused group (Tg+ CH). At 32 weeks (figure 2.6 in supplementary information), cognitive decline is not observed in the Morris water maze. Our findings clearly suggest that the gut microbiota can modulate brain function under conventionally-raised conditions.

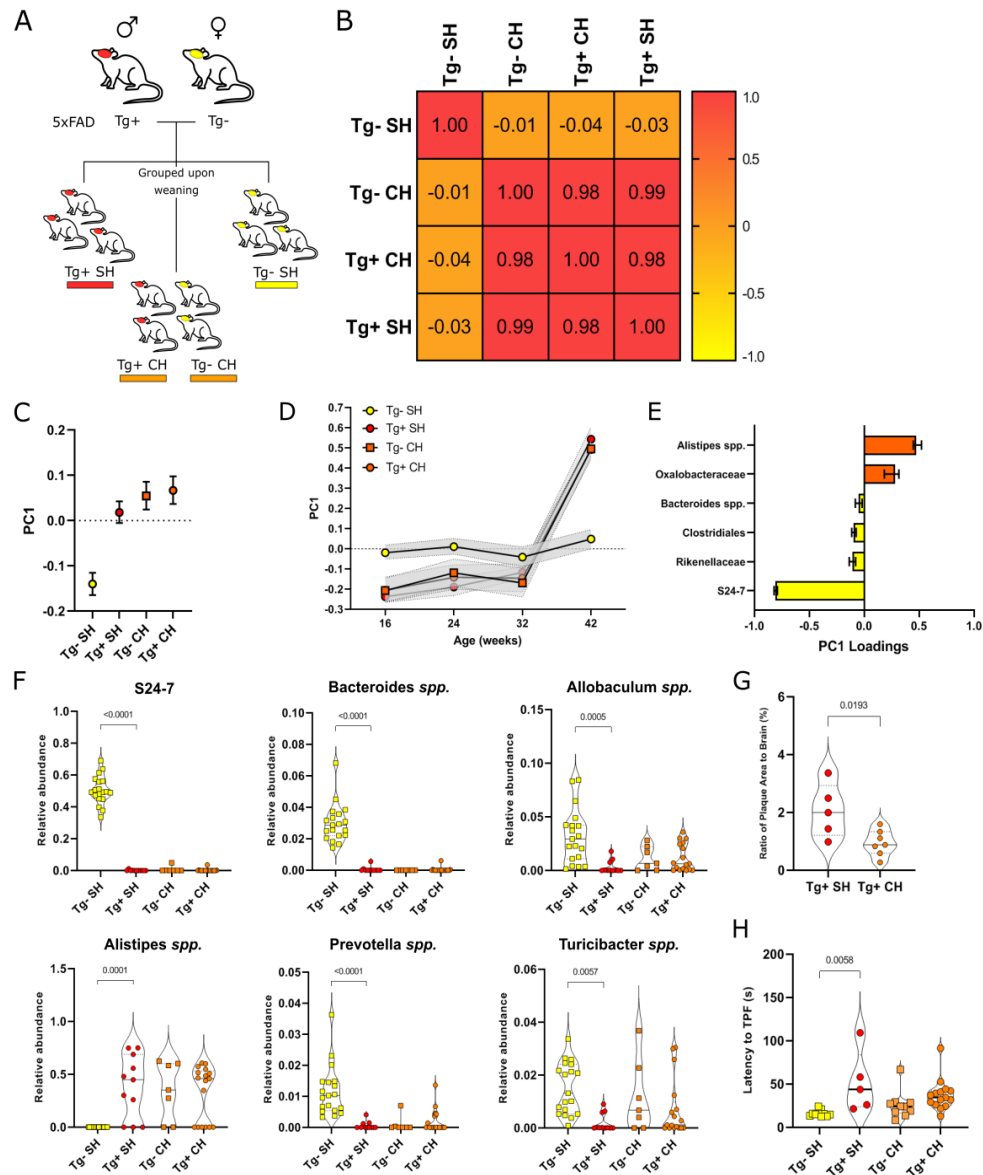


Figure 2.2 – Cohousing 5xFAD and control littermates alters gut microbiota composition and symptoms of AD. Comparative analysis of 16S rRNA fecal microbiota composition of cohoused and non-cohoused animals at 42 weeks, with assessment of changes in AD hallmarks. (A) Experimental approach for breeding and housing non-cohoused and cohoused 5xFAD littermates. (B) Pearson correlation of 16S profiles for the four housing groups at 42 weeks. (C) ASCA principal component analysis of the genotype and housing factor along PC1 with 10'000 model permutations. (D) ASCA PC1 values of interaction between housing condition and age. (E) Loadings values for individual bacteria with significant association along PC1. (F) Individual plots for bacteria of interest under the different housing conditions. (G) Amyloid-beta plaques measured at 42 weeks in cohoused (Tg+ CH) vs separately-housed (Tg+ SH) mice. (H) Latency to target platform (TPF) on day 2 of the Morris Water Maze in the different housing conditions. Statistics are two-way ANOVA with Bonferroni multiple comparisons. Cohousing experiment performed twice.

### 2.3.3 The metabolite profile is altered in the AD brain

Microbial communities and their metabolites are known to reach and affect the brain through the vagus nerve (137; 138) and circulation (139; 140). Therefore, we assessed the effect of microbiota on brain metabolites. An untargeted approach was implemented using ultrahigh-performance liquid chromatography combined with high-resolution mass spectrometry (UPLC-HRMS) to identify brain metabolites in separately-housed 5xFAD transgenic mice and littermate controls at 42 weeks. The metabolite profiles of Tg- SH and Tg+ SH animals are distinct and diverge mostly according to principal component 2 (figure 3A). By calculating fold change with a minimum 2-fold difference and a 0.05 statistical significance threshold, we identified 31 metabolites, of which 26 were reduced in Tg+ SH brain tissue relative to Tg- SH, and 15 were significantly more abundant in Tg+ SH animals (figure 2.3 (B)). Some of these metabolites are classed as pharmacological compounds with, for example, clomipramine having anti-depressant properties (141). Such metabolites associating with 5xFAD genotype is perplexing, as they may influence cognition characteristic of the AD phenotype. Thus, a relevant area of further research lies within the potential for the gut microbiome to influence the host's absorption of pharmacological compounds and downstream effects on pathology. Of those, 11 metabolites altered in 5xFAD brain tissue were found to be derived from dietary products (figure 2.3 (C)). The majority of these compounds, 9 out of 11, are less abundant in Tg+ brain tissue compared to the Tg- controls. Several food components and a metabolite linked to the gut microbiota, 5-(3',4'-Dihydroxyphenyl)-gamma-valerolactone, were identified (figure 2.3 (C)) (142). The full list of compound classes, exposure routes and known sources can be found in figure 2.7 in the supplementary information.

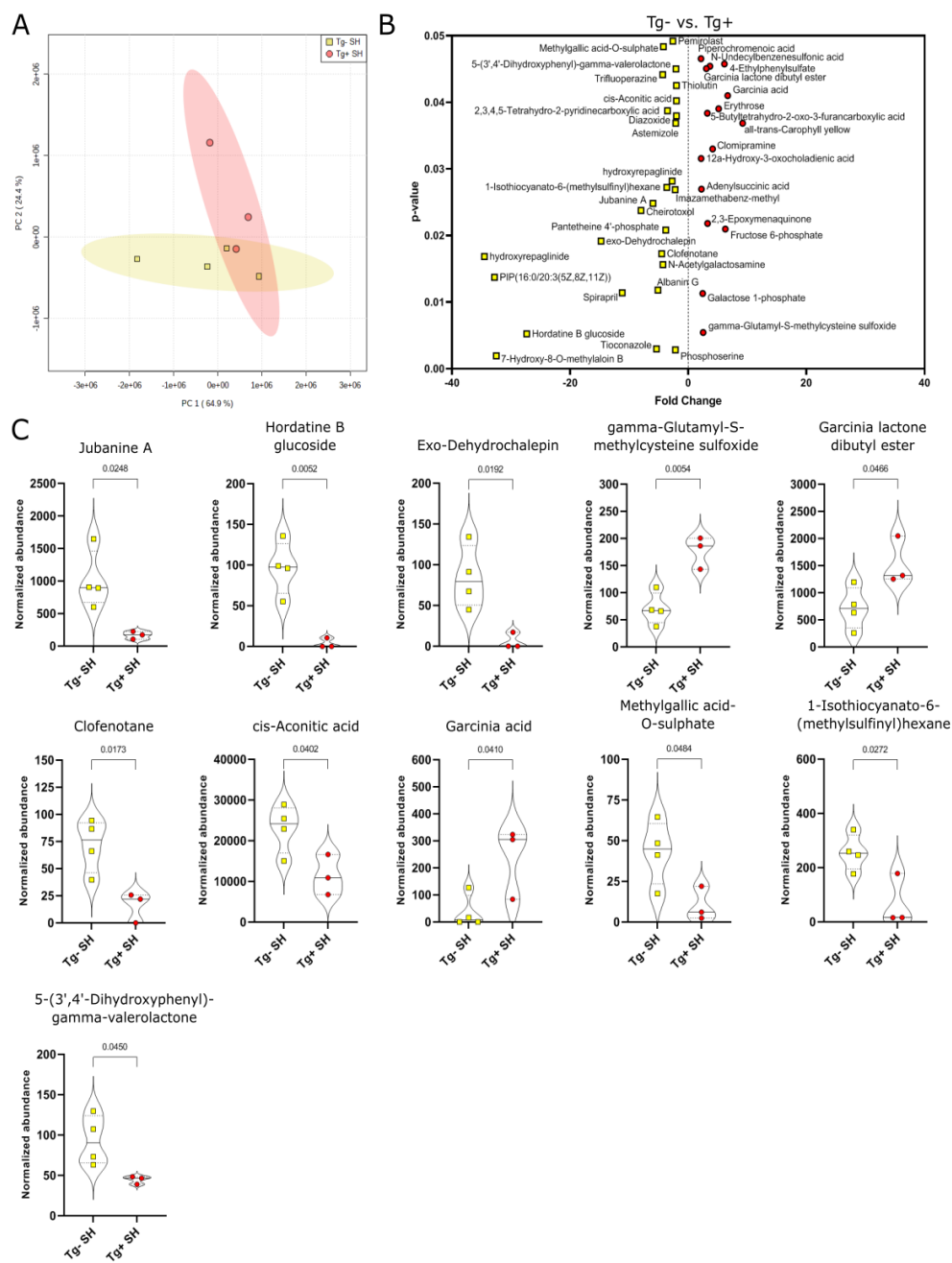


Figure 2.3 – *Food-derived metabolites in the brain are altered in the 5xFAD model* Untargeted metabolomic analysis of brain tissue from non-cohoused mice at 42 weeks. (A) PCA of metabolite profile with 95% confidence ellipse in non-cohoused (SH) 5xFAD (Tg+) and control littermates (Tg-). (B) Fold change analysis of metabolites with a significant greater than 2-fold increase or decrease in the 5xFAD animals. Metabolites with significant fold change between genotypes. (C) Significantly altered metabolites that were derived from food products. The first ten are components of foods whilst the last metabolite, 5-(3',4'-Dihydroxyphenyl)-gamma-valerolactone, is produced by microbiota metabolism. Statistics are two-tailed T-test.

### 2.3.4 Low-complexity gut microbiota compositions significantly influence hallmarks of AD

Gut microbiota modulation has been proposed as a potential therapeutic target for diseases affected by the gut microbiota, including neurodegenerative diseases (143). To test the effect of modulating microbiota composition on hallmarks of AD, we assessed disease severity at old age in a germ free 5xFAD model and in two models colonized with defined low-complexity bacterial cocktails known as Adgut (*Akkermansia muciniphila* YL44, *Parabacteroides distasonis* ASF519 and *Roseburia intestinalis* DSM14610) and Cuatro (*Escherichia coli* K12, *Bacteroides thetaiotaomicron* ATCC29148, *Lactobaccillus reuteri* I49 and *Clostridium clostridioforme* YL32). The Adgut cocktail was selected based on a previous study highlighting the loss of *Akkermansia muciniphila* and *Parabacteroides distasonis* in a model of AD (91), as well as, in particular, the association of *Akkermansia muciniphila* with health (121; 144; 145; 61).

Our findings showed that the low-complexity microbiota conditions do not aggravate AD severity, such as cerebral plaque formation and/or cognitive impairment. Representative images of brain sections stained with thioflavin S (figure 2.4 (A)) were processed to quantify amyloid plaque load as a percentage of brain area. Amyloid plaque load at 42 weeks was significantly reduced in the germ-free, Adgut and Cuatro microbiota conditions relative to age-matched conventionally-raised 5xFAD Tg+ mice (figure 2.4 (B)). In the Morris water maze (MWM) at 42 weeks, cognitive deficits are entirely absent in Tg+ compared to Tg-littermates in the groups colonized with the Adgut and Cuatro microbiota (figure 2.4 (C)). Conversely, germ-free animals have a delayed learning curve, whereby latency in Tg+ mice is significantly different from Tg- controls throughout the test (figure 2.4 (C)). This trend potentially represents an exacerbated phenotype in the germ-free 5xFAD mice as result of deficient neural development in the absence of a microbiota (146; 147). This is confirmed and more evident on day 2 (figure 2.4 (D)).

With the aim to deepen our understanding of the cerebral environment in 5xFAD animals colonized with low-complexity cocktails, we analysed the brain metabolite profile by untargeted mass spectrometry. The brain metabolome in the germ-free, Adgut and Cuatro microbiotas cluster together by partial least-squares discriminant analysis (PLS-DA) whilst the conventional microbiota forms a separate cluster (figure 2.5 (A)). For this reason, individually plotted metabolites (figure 2.5 (B)) only include the germ-free and low-complexity microbiota cocktails. Many of the food-derived metabolites identified as changing in conventionally-raised AD mice were no longer affected by genotype in the gnotobiotic groups shown here (figure 2.8 in supplementary information).

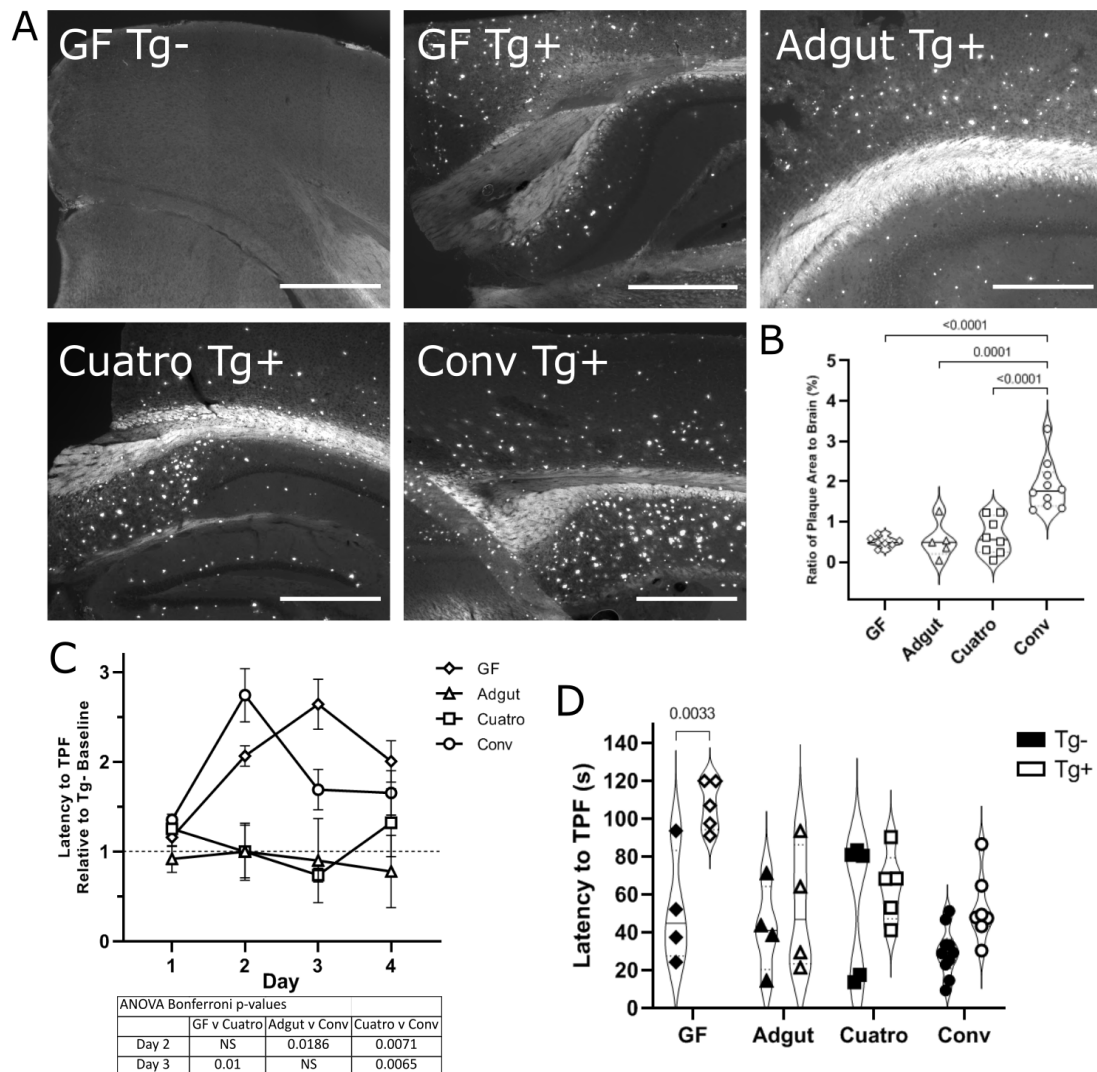


**Figure 2.4 – AD symptoms are altered in low-complexity microbiota models** Amyloid plaque burden and cognitive decline at 42 weeks in germ-free, Adgut and Cuatro microbiota conditions, compared to conventionally-raised model. (A) Representative images of amyloid plaques stained with thioflavin S at 42 weeks of age. Scale bars are 500 $\mu$ m. (B) Percentage of brain occupied by Amyloid- $\beta$  plaque at 42 weeks of age. Statistics are two-way ANOVA with Bonferroni multiple comparisons. (C) Latency to target platform relative to the healthy controls for each microbiota condition, with a Tg- baseline that equals 1 for each group. Statistics are two-way ANOVA with Bonferroni multiple comparisons. Table below plot highlight significant Bonferroni p-values, all others are NS. (D) Latency to target platform on day 2 of the MWM at 42 weeks. Statistics are two-way ANOVA with Bonferroni multiple comparisons. Experiments performed once.

Five food-derived metabolites changed in abundance in Tg+ animals (e.g. cis-aconitic acid, exo-dehydrochalepin, jubanine A, hordatine B glucoside in the germ-free group and Garcinia

## Chapter 2. Effect of Gut Microbiota Modulation in a Model of Alzheimer's Disease

acid in the Adgut) (figure 2.5 (B)). Interestingly, the trend observed here is inversed from the changes observed in conventional groups. For example, cis-aconitic acid is significantly reduced in conventional Tg+ mice (figure. 2.3 (C)), whereas it is more abundant in germ-free Tg+ animals. Another metabolite derived from food products that was not identified as significantly altered in conventionally-raised animals was pisumoside B, a component of pea plants (148). The full list of compound classes, exposure routes and known sources can be found in figure 2.9 in the supplementary information.

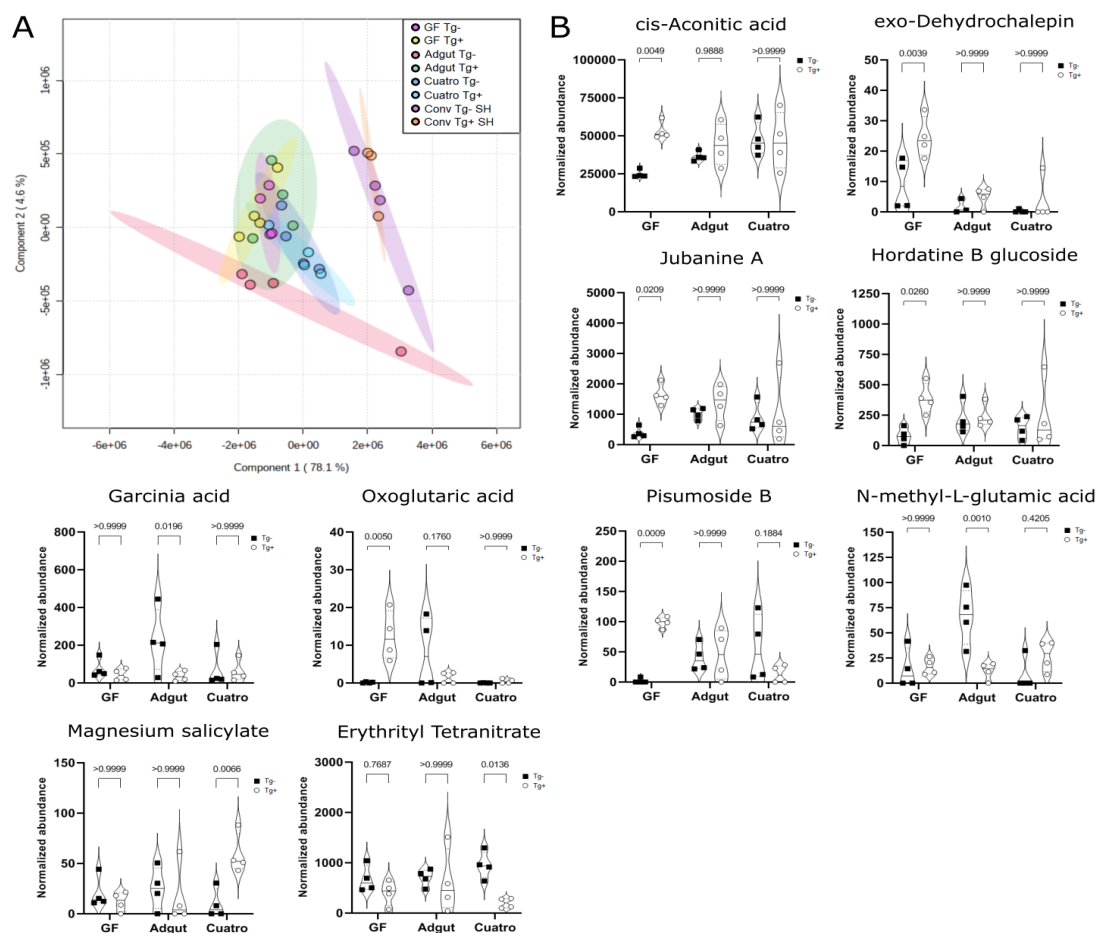


Figure 2.5 – *Brain metabolites in low-complexity microbiota compositions* Untargeted metabolomic analysis of brain tissue from germ-free and low-complexity microbiota conditions at 42 weeks. (A) PLS-DA of metabolite profile with 95% confidence ellipse in all microbiota groups and both genotypes: conventionally-raised, germ-free, Adgut and Cuatro. (B) Top 10 significantly altered metabolites, of which six are derived from food products. Statistics are two-way ANOVA with Bonferroni multiple comparisons.



## 2.4 Discussion

The gut microbiome is known to affect the development of multifactorial diseases such as Alzheimer's disease, and has increasingly attracted scientific interest in the search for microbiota-derived therapeutic solutions. In this study, we aimed to investigate gut microbiota dynamics in the 5xFAD model of Alzheimer's disease (AD) reared under varying living conditions. These aimed to (i) observe an unchallenged microbiota scenario in separately housed transgenic and wild-type littermates, (ii) examine the modulatory effect of co-housing on symptoms of AD and (iii) probe the capacity for low-complexity bacterial cocktails to ameliorate AD symptoms by old age.

In conventionally-raised separately-housed animals, we found significant alterations in the gut microbiota according to 5xFAD genotype and identified specific bacteria with previously reported associations in other studies of AD (91; 89; 149; 77). With the aim to observe metabolic alterations in the AD brain, we identified a panel of metabolites derived from ingested dietary products reaching the brain from the gut. The observed reduction of AD symptom severity in cohoused animals provides evidence for the bi-directional nature of host-gut modulation and supports gut microbiota modulation as a viable therapeutic avenue for disorders of the brain. As a preliminary test for future probiotic treatment, low-complexity microbiota compositions were implemented under gnotobiotic conditions. In the Adgut and Cuatro cocktails, amyloid plaque burden and cognitive deficits did not worsen, compared to germ-free conditions, at the latest stage of disease.

### 2.4.1 AD affects gut microbiota composition in a conventional environment

The 5xFAD genotype leads to the rapid onset of Alzheimer-like symptoms that evolve with age, including the accumulation of amyloid plaques and cognitive decline (figure 2.1). Thus, this model is an effective pre-clinical model of neurodegeneration that may be used to test gut-brain interactions in this context. To demonstrate the relevance of the 5xFAD as a viable model for host-microbiome studies, we characterized AD-associated shifts in feces (figure 2.1). We report microbial dysbiosis in the 5xFAD model, in line with previous reports in the APP/PS1 mouse model (91; 149; 77; 150) and in humans (89). Specifically, we find an increase in the abundance of *Bacteroides* and decrease in *Allobaculum* similar to that seen in feces of the APPPS1 model (149). We also find considerable overlap with genera identified in humans. These include the wild-type-associated *Turicibacter* and *Bifidobacterium* and the AD-associated *Adlercreutzia* and *Alistipes* (89). Several studies have tested the effect of direct microbiota modulation on gut dysbiosis and symptoms of AD in the 5xFAD model. In one example, inoculating the *Bifidobacterium longum* strain effectively reduced gut dysbiosis and cognitive symptoms (151). In a separate study, sustained antibiotic treatment led to a reduction in amyloid plaque load and nesting behaviour (152). Thus, the potential for therapeutic avenues to be found in gut microbiota modulation has begun to be explored in AD models.

Our results corroborate that gut microbiota composition is altered in a model of AD. Certain altered genera, namely *Allobaculum*, *Turicibacter* and *Bifidobacterium*, diverge according to genotype starting in young mice and prior to the presentation cognitive decline. In addition, consistently identified bacterial associations across different murine models and in humans suggest that fundamental biological processes implicated in disease are conserved. Shifts in gut microbiota composition may be symptomatic of dysbiosis of the gut environment as a whole, thus we believe the associated microbial metabolites are a compelling biological process to be further investigated.

### 2.4.2 Evidence for the bi-directional gut microbiota modulation through cohousing

Cohousing is useful in reducing cage- or littermate-related bias for microbiome studies as well as a robust method for standardizing a model's microbiota (130; 131; 136). In this study, we test if by cohousing 5xFAD animals (Tg+ CH) with wild-type littermates (Tg- CH) symptoms of AD would be different than the ones assessed in non-cohoused groups (Tg+ SH and Tg- SH). Cohousing was found to significantly alter fecal 16S profile (figure 2.2), most importantly at the latest measured stage of AD (42 weeks). At this age, the gut microbiota composition of cohoused wild-type animals (Tg- CH) is indistinguishable from cohoused and non-cohoused transgenic littermates (Tg+ CH and Tg+ SH). The age-dependence of this trend suggests a co-evolution of microbiota modulation with AD symptom severity. Bacteria that were altered due to genotype in non-cohoused groups, namely *Alistipes*, *S24-7*, *Allobaculum*, *Bacteroides*, *Prevotella* and *Turicibacter*, were also influenced by cohousing. Thus, we substantiate the genotype-associated gut microbiota modulation via cohousing and show a directionality effect with transgenic individuals affecting wild-type microbiota composition.

Co-housing has been assessed as a method for microbiome intervention in other contexts. In a model of ConA-induced hepatitis, biomarkers for liver damage showed a co-housing-dependent amelioration in diseased animals (153). Co-housing was also found to exert a protective effect in NLRP3 -deficient mice by alleviating depressive behaviour (154). In another example, co-housing modified the gut microbiota composition of type-1-diabetes-susceptible NOD mice, but did not alter physiological characteristics of the model (155). As well as affecting the gut microbiota, we found that cohousing led to a significant decrease in amyloid plaques in cohoused 5xFAD individuals (Tg+ CH) compared with the non-cohoused group (Tg+ SH). Cognition was altered, with an observed loss of cognitive deficit in cohoused animals (Tg- CH and Tg+ CH) compared to the separately housed groups in the Morris water maze. Trends observed in younger mice, at 32 weeks, further implicate the gut microbiota in the modulation of cognition. At that age, the significant reduction in amyloid plaque burden is reproduced. However, in the absence of significant divergence in microbiota composition, cognitive decline is not apparent.

### 2.4.3 Altered Brain Metabolite Profile Reveals Pathological Hallmarks of AD

The brain metabolome is known to be influenced by the gut microbiota (119; 156). To investigate the effects of altered gut microbiota composition in the brain, we aimed to identify metabolites with potential associations with the gut environment. The animal models studied here had equal access to food and water, thus the changes we observed in food-derived metabolites may be due to changes in satiety and/or in metabolism.

A pathological axis of Alzheimer's that could be linked to changes we observed in brain metabolite profile and the gut environment is inflammation. The compound 1-Isothiocyanato-6-(methylsulfinyl)hexane (6-MSITC) is found in foods in the Brassicaceae vegetable family, including cabbage, mustard and wasabi root (148). Functional analyses of 6-MSITC extracted from the wasabi root have revealed its potent anti-inflammatory and anti-microbial properties (157). The anti-inflammatory mode of action is mediated by 6-MSITC's suppression of cyclooxygenase-2 (COX-2) and downstream cytokine activation (158). Thus, the significant reduction of 6-MSITC levels in Tg+ brain tissue may signal increased tissue inflammation as a result of overexpressed inflammatory factors.

In our model, indirect evidence of mitochondrial dysfunction and cell survival is suggested by AD-dependent changes in the abundance of two key players in the citric acid cycle, cis-aconitic and garcinia acid (also known as hydroxycitric acid, HCA). Cis-aconitic was increased in Tg+ separately housed animals and is an intermediate metabolite in the Krebs cycle (159), levels of which have been used as a metric for mitochondrial respiratory chain deficiency (160). Cis-aconitic acid regulates the enzymatic activity of itaconate, a decarboxylase enzyme responsible for modulating cell growth and survival and exhibiting immune regulatory function (161). Garcinia acid, found to be less abundant in Tg+ SH brain, is a competitive inhibitor of ATP citrate lyase, an enzyme responsible for the extramitochondrial catalysis of citrate to oxaloacetate and acetyl CoA (162), both of which are key compounds in the Krebs cycle. Furthermore, garcinia acid is a potent modulator of appetite by its ability to increase the availability of serotonin (163) in the brain. Interestingly, serotonin is also produced in the gastrointestinal tract by enterochromaffin cells upon stimulation by microbiota-derived short-chain fatty acids (53). In the 5xFAD brain, we observed a relative decrease in cis-aconitic and an increase in garcinia acid which strongly suggests changes in mitochondrial function. This being one of the well-described hallmarks<sup>51</sup> and perhaps triggers (164) of Alzheimer's disease in patients and in pre-clinical models of AD (165).

Our results suggest that the metabolic processing of dietary products, such as food rich in cis-aconitic acid and garcinia acid, is a potential source of influence in the development of mitochondrial pathology, as well as uncontrolled inflammatory processes in Alzheimer's disease.

### 2.4.4 Low-complexity cocktails influence amyloid plaque burden and cognition

Having established the capacity for gut microbiota modulation to influence hallmarks of AD under conventional rearing conditions, we tested the efficacy of low-complexity bacterial cocktails in reducing AD severity. Evidence of probiotic-associated improvements of stress (166), host immune function (167) and neurological health (168; 169) is given in studies of pre-clinical models and humans. Since the start of our study, probiotic treatments have been tested in AD patients and animal models, having shown an effect on cognition, synaptic plasticity and other physiological mechanisms such as metabolic status (169). However, the composition of previously tested probiotic cocktails relies on select bacteria that are easy to culture and have shown an ability to modulate the established microbiota (167) to influence host health (166). In most cases, probiotic cocktails include mixtures of one to several strains of *Lactobacillus* and *Bifidobacterium* (167; 169; 95; 170).

Our approach to probiotic supplementation differed in that we designed cocktails with the aim to restore balance and replenish the microbiome with species that have been shown to be depleted as a result of disease (91). Furthermore, in order to improve our ability to test their efficacy in ameliorating symptoms of AD, the cocktails were used in gnotobiotic conditions. In the gnotobiotic environment, no evidence was found of AD-related gut microbiota dysbiosis. Furthermore, amyloid plaque burden and cognitive deficits were not worsened by supplementing with the two low-complexity bacterial cocktails we present, compared to germ-free conditions.

The Adgut cocktail contains *Akkermansia muciniphila* YL44, *Parabacteroides distasonis* ASF519 and *Roseburia intestinalis* DSM14610, which were selected based on their association with a healthy phenotype in various disease models, including AD (91). In another study, supplementation with *A. muciniphila* led to a reduction in amyloid-beta plaques and an amelioration of cognitive impairments in a model of AD (121). Alone, *P. distasonis* was able to influence metabolic status, which plays a role in AD (171; 172) and in obese pre-clinical models (173). In conjunction, an elevation of *A. muciniphila* and *P. distasonis* abundance resulted in alterations in the brain metabolome, especially affecting amino acid transport essential to neurotransmitter biosynthesis (174). This trend is confirmed in the 5xFAD model treated with the Adgut and Cuatro cocktails, as we observe no worsening of plaque burden compared to germ-free-raised 5xFAD group.

The constituents of the Cuatro probiotic cocktail were selected based on their known associations with health in gnotobiology and in humans. The combination of *Escherichia coli* K12, *Bacteroides thetaiotaomicron* ATCC29148, *Lactobacillus reuteri* I49 and *Clostridium clostridioforme* YL32 in this cocktail is based on the implementation of low-diversity gnotobiotic models that improve metabolic microbial capacity with a resulting physiological function similar to that of complex microbiomes (175). *B. thetaiotaomicron* was associated with healthy individuals (176) and shown to enhance epithelial and immunological development when introduced into a germ-free model (124). *L. reuteri* is a known immunomodulator

that reduces the production of pro-inflammatory cytokines (177) and has been successfully implemented as one of twelve species in the stable Defined Moderately Diverse Mouse Microbiota (178; 134) known to reconstitute a healthy phenotype in gnotobiotic conditions (178). The capacity for the Cuatro microbiota to not exacerbate symptoms of AD pathology in the 5xFAD model could support the hypothesis that supplementation with health-promoting bacteria can significantly shift host-gut interactions towards a healthy phenotype. However, these statements will need to undergo careful *in vivo* testing in more diverse both defined and undefined hygiene conditions.

The power of gut microbiota composition to influence brain biochemistry is exemplified in the separated clustering of gnotobiotic brain metabolomic profile from conventionally-raised animals. Furthermore, the majority of genotype-dependent metabolite variation observed in conventional rearing conditions not observed in germ free or low-complexity microbiota settings. This is evident in trends displayed by *cis*-aconitic acid. Levels of this metabolite are increased in the conventional Tg<sup>+</sup> SH relative to Tg<sup>-</sup>, whereas a significant decrease is observed in the germ-free Tg<sup>+</sup> mice. Meanwhile, levels remain unchanged in Tg<sup>-</sup> groups regardless of the microbiota composition. These differences suggest that the absence of a microbiota modulates the effect of genotype on physiological markers, such as metabolites.

## 2.5 Conclusion

Our findings demonstrate that in AD, gut dysbiosis occurs and influences specific genera whose sensitivity to AD is conserved across multiple pre-clinical models and in humans. In conjunction with gut dysbiosis, we observed variations in brain metabolites and identified numerous metabolites derived from ingested products as candidates for microbiota-modulated brain metabolites in AD. We present two methods of gut microbiota modulation, one being cohousing mediation and the other through strict gnotobiotic control. With these, we confirm the role of microbiota composition as a key player in influencing the severity of AD pathology. Our findings support gut microbiota modulation as a therapeutic intervention in diminishing amyloid plaque formation and cognitive decline. The colonization with genera known to impact general health benefits did not exacerbate plaque load and cognition in the A<sub>g</sub>gut and Cuatro cocktails, this could suggest the importance of gut microbiota population dynamics and the resulting microbiome's capacity to improve host health; however further studies are necessary.

Though the majority of experimental results were individually convincing, the overall interpretation of the physiological interactions encountered certain limitations. The implicitness of directionality in the system is minimal, likely as a result of the system's multidimensionality and the big-picture approach taken in this study. Furthermore, the complexity of physiological networks at the whole organism level makes effect directionality in any biological system challenging to identify. In some cases, as in the gnotobiotic brain metabolites, experiments would benefit from increased power. This is particularly pertinent in light of inherent inter-individual

## Chapter 2. Effect of Gut Microbiota Modulation in a Model of Alzheimer's Disease

---

variability.

**Funding.** H2020 Framework Program of the European Union (grant no 686271) and Innosuisse (grant no 31434.1 IP-ICT).

**Disclosures.** The authors declare no conflicts of interest.

**Data availability.** Data underlying the results presented in this paper are available upon request.

## 2.6 Supplementary Information (SI)

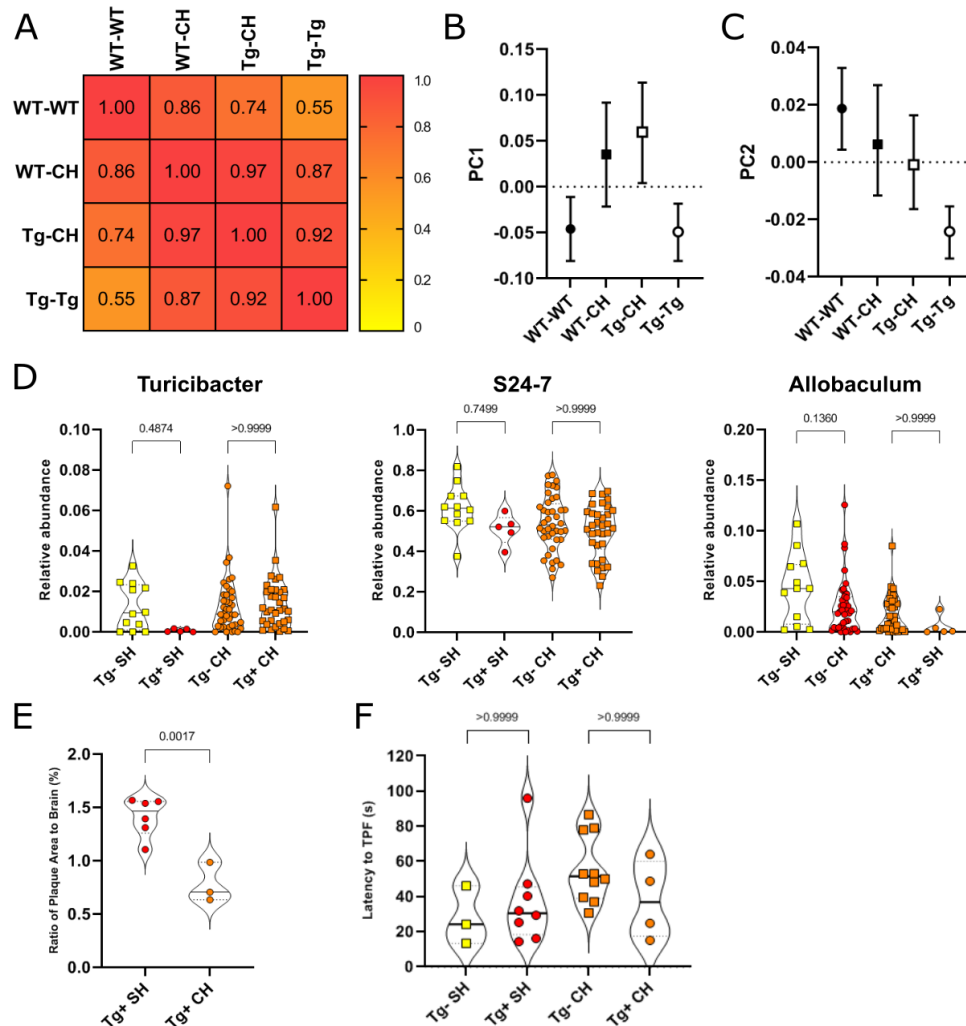


Figure 2.6 – *The prominence of the cohousing effect is diminished at 32 weeks* Comparative analysis of 16S rRNA fecal microbiota composition of cohoused and non-cohoused animals at 32 weeks, with assessment of changes in AD hallmarks. (A) Pearson correlation of 16S profiles for each housing group at 32 weeks. (B) ASCA model PCA of the genotype and housing factor along PC1 and (C) PC2. (D) Relative abundance of a subset of bacteria identified at 42 weeks in the 32-week old group. (E) Percentage of brain tissue occupied by plaques in separately housed and cohoused mice at 32 weeks. (F) Latency to target platform (in seconds) on day 3 of the Morris water maze. Statistics in D are two-way ANOVA with Bonferroni multiple comparisons. Statistics in E are two-tailed t test. In F, statistics are one-way ANOVA with Bonferroni multiple comparisons.

## Chapter 2. Effect of Gut Microbiota Modulation in a Model of Alzheimer's Disease

Name	Metabolite ID	Compound class	Exposure route	Source	Literature
Jubanine A	HMDB0030205	Oligopeptides	Ingestion	Component of jujuba root	1
Hordatine B glucoside	HMDB0030460	2-arylbenzofuran flavonoids	Ingestion	Component of cereal products	2
exo-Dehydrochalepin	HMDB0039071	Psoralens	Ingestion	Component of herbs and spices	1
gamma-Glutamyl-S-methylcysteine sulfoxide	HMDB0031863	N-acyl-alpha amino acids	Ingestion	Component of foods in the onion family	1
Garcinia lactone dibutyl ester	HMDB0040462	Tricarboxylic acids and derivatives	Ingestion	Component of fruits	1
Clofenotane	HMDB0032127	Diphenylmethanes	Ingestion	Component of cow's milk	1
cis-Aconitic acid	FGCZ-C00417	Tricarboxylic acids and derivatives	Ingestion	Found in several foods, including cow's milk, japanese pumpkins, purple mangosteens root veg and shallots.	3
Garcinia acid	HMDB0031159	Tricarboxylic acids and derivatives	Ingestion	Component of plants such as Garcinia cambogia and Hibiscus sabdariffa	4
Methylgallic acid-O-sulphate	HMDB0060005	Methyl ester of gallic acid	Ingestion	Found in gallnuts, sumac, witch hazel, tea leaves, oak bark, and other plants	5
1-Isothiocyanato-6-(methylsulfinyl)hexane	HMDB0038461	Sulfoxides	Ingestion	Component of brassicas - cabbage and mustard family	1
5-(3',4'-Dihydroxyphenyl)-gamma-valerolactone	HMDB0029185	Catechols	Gut-microbiota derived	Metabolised from flavan-3-ols in food	6

SI Figure 2 List of metabolites identified in conventionally-raised brain samples and their dietary product origin

Figure 2.7 – List of metabolites identified in conventionally-raised brain samples and their dietary product origin

1. Yannai, edited by S. Dictionary of food compounds with CD-ROM: additives, flavors, and ingredients. (Boca Raton, Fla.: Chapman and amp; Hall/CRC, 2004).
2. Piasecka, A. et al. Phenolic metabolites from barley in contribution to phenome in soil moisture deficit. *Int. J. Mol. Sci.* 21, 1–23 (2020).
3. Hayamizu, K. et al. Effects of garcinia cambogia (Hydroxycitric Acid) on visceral fat accumulation: a double-blind, randomized, placebo-controlled trial. *Curr. Ther. Res. Clin. Exp.* 64, 551–567 (2003).
4. van der Hooft, J. J. J. et al. Structural elucidation and quantification of phenolic conjugates present in human urine after tea intake. *Anal. Chem.* 84, 7263–7271 (2012).
5. Sánchez-Patán, F. et al. Synthesis, Analytical Features, and Biological Relevance of 5-(3,4-Dihydroxyphenyl)- $\gamma$ -valerolactone, a Microbial Metabolite Derived from the Catabolism of Dietary Flavan-3-ols. *J. Agric. Food Chem.* 59, 7083–7091 (2011).
6. Shaner, D. L. and O'Connor, S. L. The Imidazoline Herbicides. (1991). doi:https://doi.org/10.1201/9780203709993



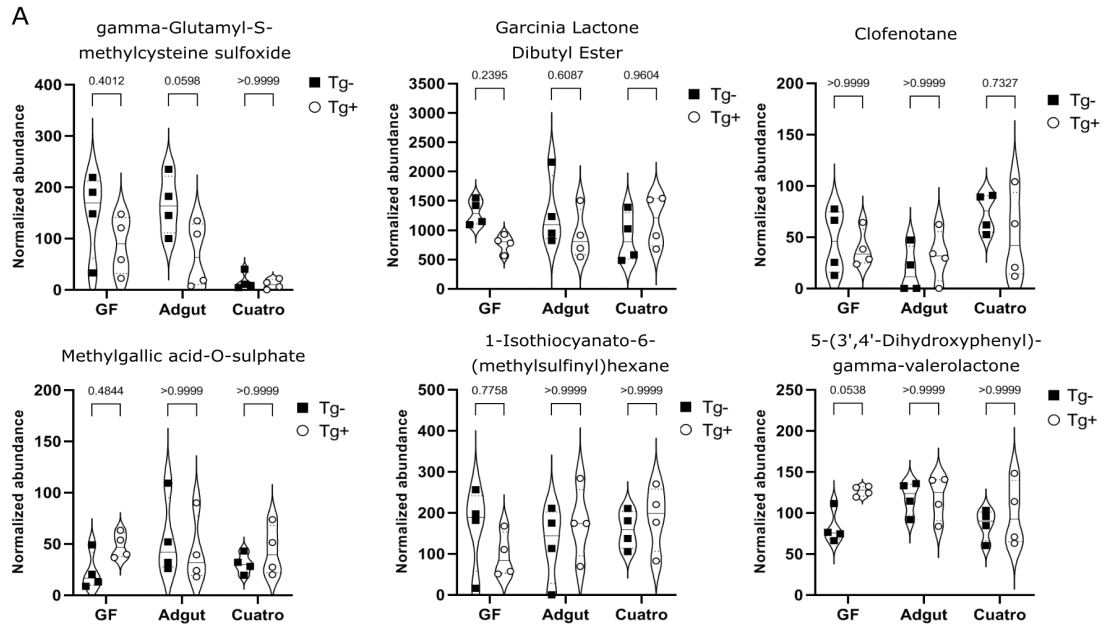


Figure 2.8 – *Brain metabolites in low-complexity microbiota compositions* Untargeted metabolomic analysis of brain tissue from germ-free and low-complexity microbiota conditions at 42 weeks. (A) Metabolites whose abundance is significantly different in conventionally-raised Tg+ mice and that are no longer different in the germ-free and gnotobiotic models. Statistics are two-way ANOVA with Bonferroni multiple comparisons.

## Chapter 2. Effect of Gut Microbiota Modulation in a Model of Alzheimer's Disease

Name	Metabolite ID	Compound class	Exposure route	Source	Literature
cis-Aconitic acid	FGCZ-C00417	Tricarboxylic acids and derivatives	Ingestion	Found in several foods, including cow's milk, Japanese pumpkins, purple mangosteens root veg and shallots.	3
exo-Dehydrochalepin	HMDB0039071	Psoralens	Ingestion	Component of herbs and spices	1
Jubanone A	HMDB0030205	Oligopeptides	Ingestion	Component of jujuba root	1
Hordatine B glucoside	HMDB0030460	2-arylbenzofuran flavonoids	Ingestion	Component of cereal products	2
Garcinia acid	HMDB0031159	Tricarboxylic acids and derivatives	Ingestion	Component of plants such as Garcinia cambogia and Hibiscus sabdariffa	4
Pisumoside B	HMDB0037125	Diterpene glycosides	Ingestion	Component of pea plant	1
Magnesium Salicylate	HMDB0015469	Non-steroidal anti-inflammatory drug (NSAID)	Synthetic	NA	8
Erythrityl Tetranitrate	HMDB0015551	Alkyl nitrates	Synthetic	NA	9
Oxoglutaric acid	HMDB0000208	Gamma-keto acid and source of glutamate	Endogenous	NA	10
N-methyl-glutamic acid	HMDB0062660	Glutamic acid derivatives	Endogenous	NA	11

SI Figure 4 List of metabolites identified in germ-free and gnotobiotic brain samples and their dietary product origin

Figure 2.9 – Brain metabolites in low-complexity microbiota compositions

1. Yannai, edited by S. Dictionary of food compounds with CD-ROM: additives, flavors, and ingredients. (Boca Raton, Fla.: Chapman andamp; Hall/CRC, 2004).
2. Piasecka, A. et al. Phenolic metabolites from barley in contribution to phenome in soil moisture deficit. *Int. J. Mol. Sci.* 21, 1–23 (2020).
3. PubChem Compound Summary for CID 643757, cis-Aconitic acid. National Center for Biotechnology Information. Available at: <https://pubchem.ncbi.nlm.nih.gov/compound/cis-Aconitic-acid>. (Accessed: 1st October 2021)
4. Hayamizu, K. et al. Effects of garcinia cambogia (Hydroxycitric Acid) on visceral fat accumulation: a double-blind, randomized, placebo-controlled trial. *Curr. Ther. Res. Clin. Exp.* 64, 551–567 (2003).
5. van der Hooft, J. J. J. et al. Structural elucidation and quantification of phenolic conjugates present in human urine after tea intake. *Anal. Chem.* 84, 7263–7271 (2012).
6. Sánchez-Patán, F. et al. Synthesis, Analytical Features, and Biological Relevance of 5-(3,4-Dihydroxyphenyl)- $\gamma$ -valerolactone, a Microbial Metabolite Derived from the Catabolism of Dietary Flavan-3-ols. *J. Agric. Food Chem.* 59, 7083–7091 (2011).
7. Shaner, D. L. and O'Connor, S. L. The Imidazoline Herbicides. (1991). doi:<https://doi.org/10.1201/9780203709993>
8. PubChem Compound Summary for CID 64738, Magnesium 2-hydroxybenzoate. National Center for Biotechnology Information Available at: <https://pubchem.ncbi.nlm.nih.gov/compound/Magnesium-salicylate-anhydrous>. (Accessed: 1st October 2021)
9. National, C. for B. I. PubChem Compound Summary for CID 5284553, Erythrityl tetranitrate. Available at: <https://pubchem.ncbi.nlm.nih.gov/compound/Erythrityl-tetranitrate>. (Accessed: 1st October 2021)
10. PubChem Compound Summary for CID 51, 2-Oxoglutaric acid. National Center for Biotechnology Information Available at: <https://pubchem.ncbi.nlm.nih.gov/compound/2-Oxoglutaric-acid>. (Accessed: 1st October 2021)
11. PubChem Compound Summary for CID 439377, N-Methyl-L-glutamic acid. National Center for Biotechnology Information. Available at: <https://pubchem.ncbi.nlm.nih.gov/compound/N-Methyl-L-glutamic-acid>. (Accessed: 1st October 2021)

### 3 High resolution optical projection tomography platform for multispectral imaging of the mouse gut

Optical projection tomography (OPT) is a mesoscopic imaging modality that relies on the three-dimensional reconstruction of sequential acquisitions over a 360° sample rotation. In order to detect structures within the depth of field, samples must be transparent. Fluorescent labels can be used to target structures of interest, as has been demonstrated for whole-brain imaging of amyloid- $\beta$  plaques in a model of Alzheimer's disease (97), functional gene activity characterization in plant structures (179), cell proliferation tracking in zebrafish embryos (180) and more.

Whilst OPT has been applied to various large samples as cited above, this work aimed to describe the first iteration of an OPT setup optimized to image the mouse gut. The longitudinal and cylindrical shape of the gut is particularly appropriate for the rotational nature of OPT acquisitions, which inspired the application of the technique described in this chapter. Furthermore, the implications of observing the localisation of tissues or cells of interest were of particular interest as the study described in chapter 2 was ongoing. However, the development and implementation of this OPT modality could not be performed on 5xFAD tissues due to time limitations.

This section consists of a published manuscript in which we describe the OPT setup we developed to address the need to image the mouse gut environment. We implemented an optimized resolution and field of view, adapted acquisition settings and channel management tools for imaging sections of mouse intestinal tissue. We also demonstrate the resulting 3D reconstructions of the autofluorescent mucosal tissue of the gut as well as the stained vascular network.

Cédric Schmidt, Arielle L. Planchette, David Nguyen, Gabriel Giardina, Yoan Neuenschwander, Mathieu Di Franco, Alessio Mylonas, Adrien C. Descloux, Enrico Pomarico, Aleksandra Radenovic, and Jérôme Extermann, "High resolution optical projection tomography platform for multispectral imaging of the mouse gut," *Biomed. Opt. Express* 12, 3619-3629 (2021)

C.S. and A.L.P. contributed equally to the writing of the manuscript, with contributions from

all authors, and initiated the project. C.S. designed and built the setup in collaboration with D.N., G.G., Y.N., M.D.F., E.P. and J.E.. A.L.P. and A.M. selected targets of interest and performed sample preparations. A.L.P., C.S. and G.G. acquired the data and implemented 3D reconstruction. A.R. and J.E. supervised the project.

## 3.1 Introduction

Mesoscopic imaging focuses on samples typically ranging from a few millimeters up to several centimeters in at least one dimension (181). This range is generally not accessible to optical microscopy techniques such as confocal and multiphoton microscopy which use raster scanning to produce volumetric images, thus limiting the sample size to less than 1 mm for a reasonable acquisition time (181). At the mesoscopic scale imaging whole animal organ portions becomes possible, thus providing the opportunity to investigate their global structural organization, as well as biological functionalities. In particular, systematic longitudinal imaging of intact gut tissues is a desirable tool to advance our understanding of the fundamental interactions between the enteric nervous system, the immune system, the epithelial barrier and microbes. Such imaging range can also be exploited for the molecular diagnosis of Parkinson's disease. Recent studies using conventional microscopy have revealed the presence of Lewy Bodies in the intestine, and highlighted their usefulness as early reliable biomarkers of the disease (182; 183; 184). However, this method is challenging to apply in routine diagnostics because of poor tissue sampling in standard histological methods occurring when dealing with elongated specimens. The added advantages of using whole-tissue imaging are reliable and global biological marker characterization and quantification, therefore decreasing the need for repeated endoscopic interventions.

While mesoscopic imaging is mainly conveyed by light sheet fluorescence microscopy (LSFM) (185), optical projection tomography (OPT) (186) differs in that it comes with reduced complexity, lower cost, and an alternative scanning geometry. In LSFM, the illumination consists of a well-defined sheet of light generated by a laser and that is orthogonal to the detection path. Recently, LSFM has been used in a humanized mouse model to image Human T cells in the ileocolic artery of colitic immunodeficient mice and demonstrated the translational value of the 3D imaging of the inflamed murine gut (112). On the other hand, OPT can be understood as the optical equivalent of the x-ray computed tomography (CT) (187; 188) or the micro-CT (189) for smaller specimens: a camera acquires a sequence of bright-field or fluorescence images (or projections) of the sample upon rotation at equally spaced angular orientations. The sample is then reconstructed using a suitable algorithm (190). Both LSFM and fluorescent OPT allow spectral decomposition of the measured signal. This feature provides enhanced tissue specificity as compared to higher-energy scanning techniques such as x-ray imaging, where tissue identification is performed via light attenuation measurements. Although LSFM can provide a higher lateral resolution with respect to OPT (typically sub- $\mu\text{m}$  in at least one dimension), its intrinsic anisotropy between axial and lateral resolution could induce ambiguity in 3D analysis (191). For this reason, and because of its rotational scanning geometry, we

consider OPT to be competitive for imaging long samples with cylindrical symmetry, such as the mouse gut.

Since its first demonstration, the OPT scheme has been adopted for a variety of applications, including imaging of zebrafish embryos (192; 193) and their cardiovascular system (194; 195), mouse organs (196; 197), as well as plants (198; 199), in both transmission and epi-detection geometries. In preclinical research, pancreas imaging via OPT (196; 200) has been shown to play a key role in diabetes research, providing scientists with a quantitative overview of the disease progression in the entire mouse organ. Similarly, whole mouse brain imaging was performed with OPT for the study of Alzheimer's disease (201; 98). Technical advances have come with the growth of OPT applications in preclinical research. For instance, helical scanning has been proposed to increase the field of view (FOV) (202), fluorescence lifetime measurements has demonstrated enhanced tissue specificity (193; 203), coherent LASER illumination has enabled measurement of blood flow (204; 205) and tomography acquisition has been combined with LSFM in hybrid instruments for artefact correction (206; 207; 208). At the same time, advanced reconstruction algorithms based on light field retrieval (209; 210; 211), resolution improvement using point-spread-function (PSF) deconvolution (212; 213; 214), tissue absorption measurements (215) and iterative reconstruction allowing reduced acquisition time (202; 216; 217), have been developed.

Here, we present the first multispectral fluorescent OPT platform suited to mouse gut imaging. To this end, we introduce a new sample preparation technique, based on a virtually cut-free specimen embedding procedure via molding in cylindrical tubes. This method allows one to uniformize sample shape, as well as reduce sample damage and imaging artefacts as compared to standard sample preparation (218; 180). In addition, we design our setup to optimize the trade-off between the sample size and the lateral resolution induced by visible light diffraction limitations (219). We provide accurate measurements of the resolving power of the instrument based on the reconstructed PSF of 1  $\mu\text{m}$  diameter fluorescent microspheres and demonstrate a sub-28  $\mu\text{m}$  resolution along the 3 dimensions. Finally, we present a reconstructed 3-cm long gut portion with two spectral channels to emphasize the vascular system network surrounding the intestinal villi structure.

## 3.2 Methods

### 3.2.1 Sample Preparation Protocol

#### Trans-cardiac Perfusion and Fixation

Mice were generated and housed at the École Polytechnique Fédérale de Lausanne and handled in accordance with the guidelines and regulations of the institution and of the state of Vaud (authorization number VD3448). Animals are deeply anesthetized by intra-peritoneal injection of 50 mg/kg of sodium pentobarbital. Upon disappearance of reflexes, the mice are perfused with 10 ml of heparinized PBS (5 I.U./ml Liquemin) followed by 10 ml of 4

### **Chapter 3. High resolution optical projection tomography platform for multispectral imaging of the mouse gut**

---

% paraformaldehyde (CAS 30525-89-4, Carl Roth AG 0964.1). Once samples of interest are collected, they undergo post-fixation overnight at 4°C.

#### **Tissue Fluorescence Quenching and Permeabilization**

Samples are washed in PBS at room temperature for 30 minutes to remove excess paraformaldehyde. Tissue fluorescence quenching is performed by incubating the samples in a solution of MetOH:DMSO:H<sub>2</sub>O<sub>2</sub> (as a 2:1:3 ratio) overnight. This is followed by tissue permeabilization, which is carried out by cycling through three freeze-thaw cycles (1hr at -80°C and 30 minutes at room temperature).

#### **Antibody Staining**

The principle of staining whole organ samples is based on immuno-histochemical staining on a large scale. The samples are blocked in a buffer for 24 hours at room temperature followed by a 48-hour primary antibody incubation and a 24-hour wash in 0.1 % TBS-Triton X-100 (UN3082, Applichem). Then, the samples undergo a 48-hour secondary antibody incubation and another 24-hour wash. Organ vasculature is stained by post-excision infusion staining of a rat anti-CD31 primary antibody targeting the murine platelet-endothelial cell adhesion molecule (Abcam ab7388). The secondary antibody is a goat anti-rat AlexaFluor 647 (Thermofisher A21247).

#### **Mounting and Clearing**

The samples are mounted in 1.5 % agarose using cylindrical open-ended molds made from 10 ml serological pipettes cut to optimal length. In order to center and straighten the intestinal tissue, the samples are pierced with strings on either end, which are used to adjust the sample's position within the cylinder. One end of the mold is closed using parafilm, to be filled with 1.5 % agarose and allowed to set at room temperature. The agarose-enclosed samples are dehydrated for 24-hour in pure methanol (CAS 67-56-1, Sigma-Aldrich 322415), with two solution changes. Then, they are cleared using a 1:2 ratio of benzyl alcohol (CAS 100-51-6, Sigma-Aldrich 305197) and benzyl benzoate (CAS 120-51-4, Sigma-Aldrich B6630) (BABB). Clearing takes at least 72 hours prior to OPT acquisition. All the steps above are performed in the dark to prevent photo bleaching.

#### **Fluorescent Microsphere**

For calibration and resolution analysis, we used 1  $\mu$ m fluorescent FITC-labeled microspheres based on melamine resin (90305-5ML-F, Sigma). The sample preparation follows the previous steps with the beads as specimen. Approximately 0.01 ml of particle solution is mixed to 10 ml of 1.5 % agarose before molding to achieve a nearly colloidal solution. The acquisition is

performed shortly after the clearing process to avoid undesired fluorescence quenching of the signal induced by chemical reaction with either the methanol or the BABB.

### 3.2.2 Acquisition setup

The optical design of our platform has been realized with commercially available optics. The imaging depth of field (DOF), FOV and optical resolution have been optimized for imaging a mouse gut with a diameter up to 5 mm over the whole visible range using OpticStudio 21.1 (Zemax LLC). In order to reduce the number of sections during sample preparation, the positioning mechanism allows specimens up to 10 cm in length to be acquired. A schematic of the setup is shown in Fig. 3.1. Sample illumination is provided by several LEDs on metal-core PCBs (MxxxD2,3 series, Thorlabs) of different central wavelengths, mounted on heat dissipators and filtered out using bandpass filters. An aspheric condenser lens (ACL25416U, Thorlabs) in front of the LEDs combined with a spatial mask allow for a nearly homogenous beam of 7 mm in diameter at the sample position after being reflected on a dichroic beam splitter (Chroma). The sample illumination, as well as the fluorescence detection, relies on an achromatic doublet (AC300-080-A, Thorlabs) and a meniscus (LE4484, Thorlabs) composing the objective lens set. The implementation of the meniscus reduces the spherical aberration induced by the successive air-glass-BABB planar interfaces (220). The interaction with the sample takes place in a quartz cuvette (Hellma, HELL704001-30-10) with 3 mm wall thickness filled with BABB acting as an index-matcher. The tip and tilt fine-tuning of the position of the rotation axis has been carried out using aluminum thin sheets following the procedure provided by Watson et al. (221). The sample embedded in agarose is glued to the lower end of a cylinder magnet facilitating its positioning onto the rotation stage. The sample positioning and projection acquisition process is driven by a custom MATLAB interface for sequential measurement of multiple regions.

Sample fluorescence is transmitted through a dichroic beam splitter, passes through an aperture stop of 2.24 mm diameter and a spectral filter, before being focused onto a sCMOS sensor (ORCA-Flash 4.0, Hamamatsu; pixel size of  $6.5 \mu\text{m}$ ) by a tube lens (TTL200-A, Thorlabs). The whole imaging system has a 2.66x magnification and a numerical aperture of 0.03 resulting in a Huygens PSF (222) that spans from 15 to  $20 \mu\text{m}$  FWHM over the visible range. These characteristics lead to an isotropic voxel size of  $2.44 \mu\text{m}$ . The camera sensor can capture a  $5 \times 5 \text{ mm}^2$  FOV, meaning a 5 mm-long specimen region of interest. The images are saved in 16 bit TIFF format and compressed around 8:1 ratio using an efficient lossless compression method (223) to reduce data transfer and storage. The fixed sample is mounted on a stage assembly to perform x and z translation (PT1/M-Z8, Thorlabs), as well as a  $\theta$  rotation (PRM1/MZ8, Thorlabs). The sample y-axis is scanned vertically using a 300 mm linear translation stage (LTS300/M, Thorlabs) allowing to image specimens up to 10 cm in length in 25 sequential acquisitions (assuming 1 mm overlap). The setup has been designed to allow ease and speed in changing the LED light source, dichroic beam splitter and spectral filters by implementing a custom filter cube slider. Up to five channels are currently available, spanning UV to red

### Chapter 3. High resolution optical projection tomography platform for multispectral imaging of the mouse gut

wavelengths. Typical measurements are performed with an illumination power density of  $0.1 \text{ W/cm}^2$  (at 415 nm) and a camera integration time spanning from 0.01 s to 0.5 s. When imaging with multiple spectral channels, the filter slider is moved manually after the complete acquisition of the sample. Channels are acquired opposite to the excitation wavelength number, from red to UV, in order to reduce photobleaching. The tissue's autofluorescence is excited with a LED centered at 415 nm and spectrally filtered between 400 nm and 440 nm while the emission is measured between 455 nm and 520 nm. Under these conditions, a complete set of 1200 projections spanning  $360^\circ$  can be acquired within 12 minutes. Currently, half of this time is taken by the final positioning step of the rotational stage before projection acquisition and we are currently working on implementing a video acquisition mode to reduce imaging time. Moreover, we plan to adopt a similar scanning approach as reported by A. Arranz et al. (202) in order to reduce the risk of unnecessary photobleaching of the sample when measuring overlapping regions for stitching.

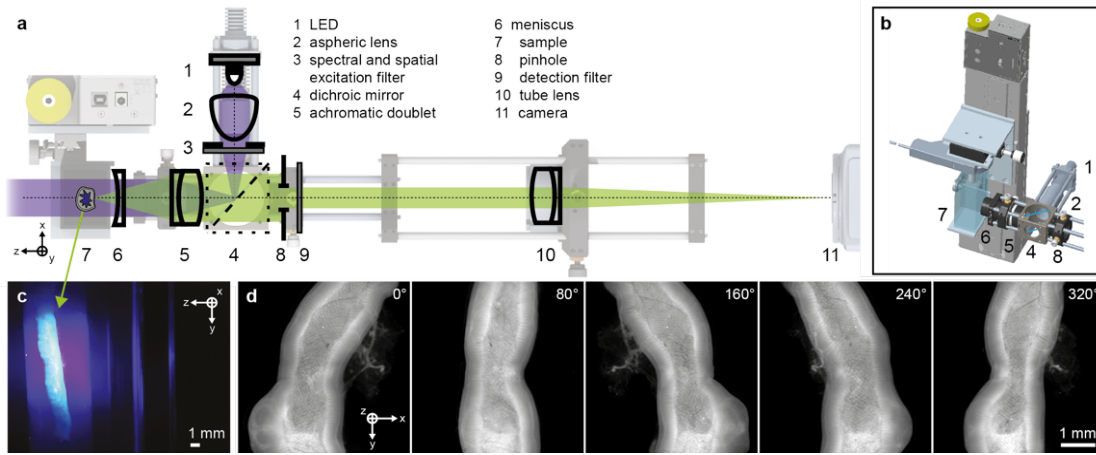


Figure 3.1 – *OPT design* a) Optical layout superimposed with the corresponding mounting system (view from the top). Optical components are numbered from 1 to 11. The optical path of the excitation and detection beams are represented in purple and green, respectively. b) A three-quarter view of the motorized sample positioning stages, as well as the transparent cuvette filled with BABB. c) Photograph taken from the side of the cuvette. A 30 mm long mouse gut sample is embedded into a cylinder of agarose gel submerged in the BABB cuvette. The gel cylinder is glued to the sample holder, which is held together with the rotating motor using a magnet. The gut sample is excited by a LED centered at 415 nm and the fluorescent signal is acquired by the camera for multiple angular positions of the specimen. d) A selection of five projections showing the characteristic acquisitions of cleared samples over  $360^\circ$  in OPT imaging.

#### 3.2.3 Image reconstruction algorithm

2.3 Image reconstruction algorithm Our reconstruction process relies on the filtered back-projection (FBP) algorithm (224) for its minimal computational costs. The software is written in Python and calls ASTRA library (225) functions for reconstruction. The full process handles



16-bit data and heavy tasks are all GPU accelerated. Briefly, the measured background signal is first subtracted from all projections. The upper and lower limits of the reconstruction area are defined according to the specimen by applying an intensity threshold value after averaging over all projections. The center of rotation is determined at the 10 % top and 10 % bottom of the specimen limits by iterating over a guessed interval and maximizing the variance of the reconstruction, as suggested in (226). After complete FBP reconstruction, a circular mask is applied to the data to remove the out-of-FOV diverging values and the voxels with negative values are set to zero (224). The 3D image is finally exported as a 3D TIFF file ready for visualization. The full process typically takes less than 5 min with a 3.5 GHz CPU and an enabled 4 Gb GPU (GeForce GTX 750 Ti) acceleration. The script is provided in Dataset 1.

The filtering step in FBP consists in applying a band pass filter to reduce the blurring induced by oversampling the sample near the rotation axis. Such numerical filtering can be applied in the spatial or spectral domain and multiple filter designs have been implemented in the ASTRA toolbox (225). To select the most appropriate filter type for our application, we rely on the no-reference image quality assessment (NR-IQA) BRISQUE model (227) and the measurement of the spatial resolution determined with fluorescent microspheres. We computed the BRISQUE test on a typical reconstructed gut with a selection of the most common filters used in OPT. As given in table 1, we obtained better results with the Hamming filter, which confirms our qualitative impression. The stitching of multiple sub-regions and the registration of multiple spectral channels are realized after volume reconstruction using BigStitcher (228), an ImageJ (229) plugin.

Table 3.1 – No-reference image quality assessment for the most common FBP filters used in OPT

Filter type	BRISQUE score <sup>a</sup>	PSF FWHM <sup>b</sup>
No filter	87.2	No data
Ram-Lak	69.4	31 $\mu\text{m}$
Shepp-Logan	59.2	34 $\mu\text{m}$
Cosine	41.3	36 $\mu\text{m}$
Hamming	38.4	28 $\mu\text{m}$
Hann	38.8	29 $\mu\text{m}$

<sup>a</sup>Evaluated after reconstruction of a mouse gut. A lower BRISQUE score means a better-evaluated scene. <sup>b</sup>Lateral resolution measured using the PSF of reconstructed fluorescent microspheres. The value corresponds to the FWHM of a Gaussian fit realized after intensity integration in the XZ-plane.

### 3.3 Results

#### 3.3.1 Instrument resolution and optimization

To improve the resolution power of a standard OPT scheme, the DOF needs to be adapted to cover at least half of the specimen along the optical axis (186). This strategy allows for the use of higher NA objective lenses, while acquiring the entire sample over a  $360^\circ$  rotation. The smallest achievable lateral resolution  $R_{lat}$  of the optical assembly therefore depends on the radius of the sample  $r_{sample}$ . Indeed, the confocal parameter is given by  $DOF = 2\pi \frac{n\omega_0^2}{\lambda_0}$ , where  $n$  is the effective refractive index of the medium between the objective lens and the sample,  $\omega_0$  the Gaussian beam waist, and  $\lambda_0$  the vacuum wavelength. By using the relation that converts  $1/e^2$  beam waist into  $R_{lat}$  FWHM dimension  $2\omega_0 = \sqrt{\frac{2}{\ln 2}} R_{lat}$ , one can derive Eq. (3.1):

$$R_{lat} \geq \sqrt{\frac{(\ln 2 \lambda_0 DOF)}{(\pi n)}} = \sqrt{\frac{((\ln 2 \lambda_0 r_{sample}))}{(\pi n)}} \quad (3.1)$$

providing the diffraction limit achievable with a standard OPT instrument for a given sample dimension. For our application, given  $n = 1.54$ ,  $\lambda_0 = 525$  nm and  $r_{sample} = 2.5$  mm, the smallest achievable  $R_{lat}$  is  $14 \mu\text{m}$ .

To optimize the alignment and characterize the resolution of the instrument, we have selected  $1 \mu\text{m}$  fluorescent microspheres as emitting point sources to measure the point spread function (PSF) in the projection space (230) and in the reconstructed volume. These particles are more than five times smaller than the theoretical PSF, thus satisfying the sampling theorem (231), and are sufficiently bright to be imaged by the OPT instrument (232). Examples of acquired beads are shown in Fig. 3.2 (a) and (b), in the projection space and after reconstruction, respectively. According to previously reported works (214; 233), we observe that the lateral resolution given by the reconstructed PSFs decreases radially away from the axis of rotation, as shown by Fig. 3.2 (f). Moreover, as detailed by Chen et al. (233) this effect is strongly enhanced when the angular resolution is reduced (see  $0.6^\circ$ ,  $0.9^\circ$ ,  $1.8^\circ$  and  $3.6^\circ$  data), and  $0.3^\circ$  angular steps (1200 projections) are required to satisfy the minimal number of projections (233) and maintain the PSF optimal over the whole FOV. Similarly, the position of the rotational axis with respect to the focal plane must be finely adjusted in order to remove the seagull shape of the PSF shown by Fig. 3.2 (f). This artefact was previously reported by Watson et al. (221) and was attributed by the authors to a refractive index mismatch between the BABB and the agarose matrix or by a too small DOF. Here, we were able to correct the insufficient sampling of the single emitter by optimally positioning the rotation axis with respect to the DOF using five sets of beads acquired with  $0.3^\circ$  angular resolution for different positions of focus, as shown by Fig. 2e. After optimization, and by selecting the beads positioned inside a 2 mm radius from the rotational axis, we have measured a mean PSF FWHM of  $17 \mu\text{m}$  in the y-axis and  $28 \mu\text{m}$  in the x- and z-axis (see Fig. 2c and 2d). The PSF FWHMs are measured after integrating over the corresponding axis. These PSF values demonstrate a sub- $28 \mu\text{m}$  resolution along all

3 dimensions and over more than  $60 \text{ mm}^3$  in a single acquisition. As compared to a similar setup dedicated to the mouse brain imaging with a claimed  $50 \mu\text{m}$  isotropic resolution (201), we succeed in improving the resolution by a factor of almost 2. While the y-axis resolution confirms the computed theoretical estimation ( $15\text{--}20 \mu\text{m}$ ) and is slightly superior to the system diffraction limit ( $14 \mu\text{m}$ ), the x- and z-axis suffer from a resolution loss introduced by the FBP reconstruction. We are currently investigating the implementation of PSF deconvolution (212; 213; 214) during FBP to reduce this drawback.

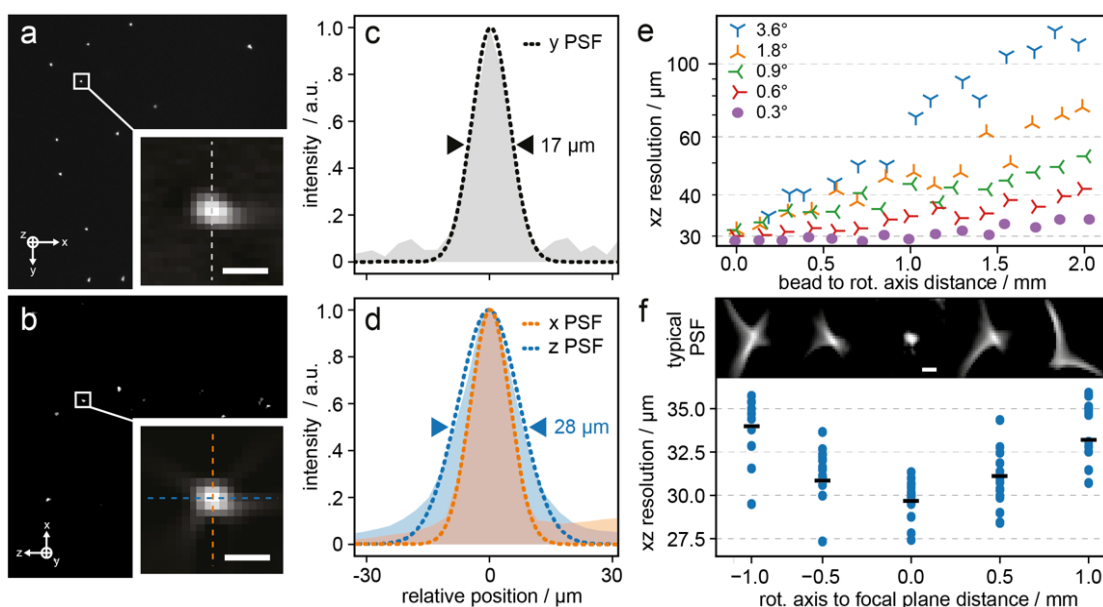


Figure 3.2 – *OPT PSF characterization* a) Single projection of the acquired fluorescent microspheres. The close-up shows an in-focus microsphere (scale bar =  $20 \mu\text{m}$ ). b) Y-projection over the reconstructed volume of microspheres to show the XZ-plane PSF. The close-up shows a typical microsphere (scale bar =  $20 \mu\text{m}$ ). c) Gaussian fit of the PSF integral represented in a) along the Y-axis. The given value is the Gaussian FWHM. d) Gaussian fits of the PSF integrals represented in b) along the X- and Z-axis. The given value is the Gaussian largest FWHM. e) XZ-plane lateral FWHM of the reconstructed PSF as a function of the distance to the rotation axis for multiple angular resolutions. Each data point is the mean of microspheres included in a  $0.1 \text{ mm}$  interval. f) XZ-plane mean lateral resolution (black line) measured from the reconstructed PSF of fluorescent microspheres as a function of the distance of the rotation axis to the focal plane. 15 PSFs (blue dots) are represented by axis position. A typical PSF for each position is represented at the top of the graph. A seagull shape of the PSF is visible as the distance of the rotation axis to the focal plane increases (scale bar =  $20 \mu\text{m}$ ).

### 3.3.2 Mouse gut imaging

We have imaged a 3-cm long portion of a mouse gut with the use of 2 spectral channels. In addition to the tissue autofluorescence dominated by flavin adenine dinucleotide, we stained the vasculature to emphasize the penetrating vessel network and demonstrate the specificity

### **Chapter 3. High resolution optical projection tomography platform for multispectral imaging of the mouse gut**

---

of our approach. The CD31-mediated vasculature staining is excited at 625 nm and recorded at 690 nm. The full acquisition has been performed by sequentially measuring 8 sub-regions of 5-mm length and 0.5-mm reciprocal overlap (used for stitching) for each spectral channel. The data acquisition and processing took approximately 190 minutes. The intestinal tissue's macroscopic structure is well preserved after OPT sample processing and details can be observed after volumetric reconstruction. At the centimeter scale, we are able to resolve the mesentery-associated vasculature, which surrounds and supports the gastrointestinal tract (Fig. 3.3 (a)) (234). In the autofluorescence channel (shown in cyan), individual villi appear as an evenly distributed speckled pattern, as shown in Fig. 3.3 (b). With a cross-sectional view as in Fig. 3.3 (c), we are able to distinguish the submucosa and muscularis layers of the tissue as a distinct ring surrounding the villi structures. When exciting the sample at 625 nm, we observe regions (shown in magenta) with a high density of blood vessels stained by anti-CD31 within the submucosa, where the blood and lymph vasculature networks as well as the enteric nervous system are situated (Fig. 3.3 (c)). This signal is also present in the villi themselves, with an increased concentration of the signal at the ends of the villi closest to the lumen (Fig. 3.3 (c) and (d)). This is due to the convergence of the vascular network resident within each individual villus. Thus, OPT can be used as a powerful tool to cross-sectionally image the mouse gut whilst keeping the longitudinal structure intact for subsequent analysis and interpretation in any desired angle and plane (see Visualization 1).

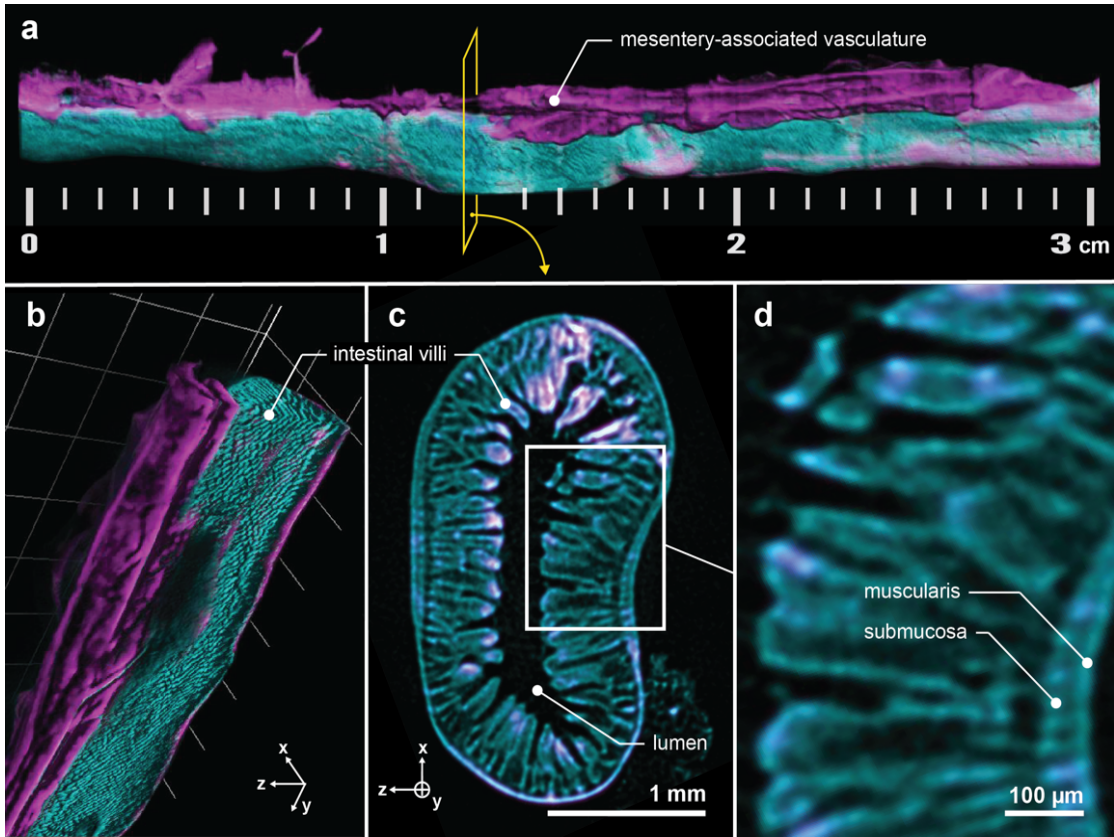


Figure 3.3 – *Mouse small intestine portion imaged by multispectral OPT* a) 3D blend rendering of a 3-cm long mouse gut portion acquired using 2 spectral channels. The vasculature (magenta) is stained using an anti-CD31 antibody combined with an anti-rat Alexa Fluor 647 secondary antibody and is excited at 625 nm. The tissue is imaged using autofluorescence of flavin adenine dinucleotide excited at 415 nm. b) Sliced perspective view of the gut portion emphasizing the intestinal villi structure, as well as the penetrating vessels, and highlighting the 3D advantage of the technique. c) OPT cross-section view of the gut showing the submucosa and muscularis layers of the tissue surrounding the villi structures. d) Close-up of the typical villi structure with the increased concentration of the vasculature visible close to the lumen as well as in the submucosa and muscularis layers.

### 3.4 Conclusion

We described a new multispectral OPT setup optimized for the imaging of the mouse gut and capable of spanning 3 orders of magnitude in size along the 3 dimensions, from a few micrometers to centimeters. We used fluorescent microspheres to optimize the instrument performance and to demonstrate sub- $28\ \mu\text{m}$  resolution along the 3 axes. We showed that the adoption of a multispectral fluorescence approach on cleared samples subject to specific stainings allow to extract anatomic and structural information within a whole organ structure. Our multispectral OPT setup enables the investigation of the spatial organization of the villi structures, as well as the identification of the vasculature network, of a 3-cm long mouse gut.

### Chapter 3. High resolution optical projection tomography platform for multispectral imaging of the mouse gut

---

Besides visualizing the peripheral intestinal vasculature, we observe a high density of blood vessels within the submucosa, as well as clear traces of vasculature at the villi ends closest to the lumen. We consider this technique a powerful tool for translational gastroenterological research, as it can overcome the typical downsides of conventional techniques, such as limited penetration depth, FOV or resolution. Moreover, it is likely that OPT can be performed with whole-mount stained human specimens obtained from biopsies or surgery, for research and diagnostics in fields like inflammatory bowel disease or cancer immunotherapy. The advantage of OPT as a diagnostic tool is that it is time-efficient, cost-effective and it enables the observation of large volumes with a single acquisition, thus reducing misinterpretations based on poor tissue sampling while using standard histological methods. Moreover, the unique advantage of OPT in enabling bright-field illumination to the mesoscopic range allow 3D imaging from unlabeled samples (206). Specimen-adapted multispectral OPT imaging has the potential to set the basis for major advances in translational research and patient care, leading to the optimization of current diagnostics.

**Funding.** Innosuisse - Schweizerische Agentur für Innovationsförderung (31434.1 IP-ICT); Horizon 2020 Framework Programme (686271).

**Acknowledgments.** The authors are grateful to Theo Lasser for useful discussions and overall support and to François Bugnon and Charles Brack for technical support. AR and AD acknowledge the support from the EPFL Open Science fund.

**Disclosures.** The authors declare no conflicts of interest.

**Data availability.** Setup design files, microsphere data and FBP reconstruction code underlying the results presented in this paper are available in Dataset 1. Data underlying the mouse gut results may be obtained from the authors upon reasonable request.

## 4 Optical Imaging of the Small Intestine Across Scales

This section presents a submitted manuscript in which I outline a novel pipeline for imaging the small intestine across scales. The gutOPT workflow encompasses fluorescence labelling of millimetre-long sections of small intestine, 3-dimensional imaging by optical projection tomography and region-of-interest referencing in confocal microscopy. An important application of such a technique lies in the characterization of gut tissue structure in autofluorescence OPT imaging, including villous density. Observations of the gut immune compartment, consisting here of isolated lymphoid follicles, offers a unique large-scale visualization with quantitative parameters available. This pipeline can be applied to pre-clinical samples, as shown here, and there is hope for this technique to be useful in the characterization of clinical biopsies.

Arielle L. Planchette, Cédric Schmidt, Alessio Mylonas, Olivier Burri, Mercedes Gomez de Agüero, Aleksandra Radenovic and Jérôme Extermann, "Optical Imaging of the Small Intestine Across Scales" Submitted to Nature Biotechnology (October 2021)

A.L.P. wrote the manuscript with contributions from all authors, and initiated the project. A.M., C.S. and A.L.P. performed sample preparations, acquired OPT scans and performed 3D reconstructions. A.R. and J.E. supervised the project.

### 4.1 Introduction

The intestine forms an interface between the external environment and the rest of the body, fulfilling many essential functions in the process. Among these are immune system education, and the regulation of the microbiome – which are incidentally interdependent (235; 236). Indeed, we now know that the microbiome is necessary for the correct education of the immune system (237; 238) and that this has long-term repercussions on immunity in the gut. As such, the gut microbiome has been linked to distinctly immune-related disorders ranging from obesity (239) and diabetes (240) to auto-immune (241) and allergic diseases (242; 243; 244). Importantly, significant advances in the aetiology of such disorders were

made through studying gut structure (28; 245; 246). For example, deficits in gut morphology and barrier permeability have been implicated in both obesity (247; 248) and diabetes (249), with the latter showing signs of decline prior to type-1-diabetes onset in non-obese diabetic mice (NOD). The relevance of observing cell localization within tissue regions of the gut is further exemplified by microscopic observations of intraepithelial lymphocytes localisation, which highlighted the impact of high-fat-diet-induced obesity on the control of pathogen transepithelial migration and the mediation of intestinal epithelial repair (248).

Secondary lymphoid structures are strategically positioned along the gastrointestinal tract to orchestrate immuno-surveillance against pathogens and invading microorganisms. These are known to develop during early life (250), and to require stimuli from the microbiome (251; 252). Peyer's patches (secondary LT) and isolated lymphoid follicles (ILFs, tertiary LT) form key networks where microbial antigens are presented to T- and B-cells, effectively dictating both regulation and tolerance to commensals. While new methods are continuously being developed for immuno-phenotyping and isolation of immune cells from ILFs (253; 111), their function – deriving from their location at the interface with the microbiota – also necessitates further research in their natural context.

Optical projection tomography (OPT) is a 3D imaging modality that is ideal for mesoscale imaging, offering broad applicability while maintaining compatibility with other microscopy techniques. With fields of view spanning from a few millimetres to 60mm in length (246) and full 3D-volume acquisition times ranging from minutes to an hour (254), OPT is a time- and cost-effective technique with which large-scale structural and functional parameters can be imaged. OPT has been leveraged for concatenated, functional multi-channel plant imaging (246), functional cell proliferation imaging in zebrafish (255), multi-orientation digital sectioning of whole mouse embryos (256) and mouse organs imaging of liver, pancreas (254) and brain (257).

Recently, we developed a multi-spectral OPT modality to image the mouse gut (258) with a 3D resolution of  $28\mu\text{m}$  allowing distinction of mucosal layers and villi in samples several centimetres in length. To demonstrate the wide range of applications for this method, we present a workflow that enables mesoscale observation of signal distribution throughout millimetre-long gut sections with autofluorescent contextualization, as well as the identification of regions of interest that can be characterized at higher-resolution following reverse OPT (RevOPT) processing. We apply this workflow to visualise the gut immune compartment and present the first observation of isolated lymphoid follicle (ILF) distribution in a single acquisition spanning several millimetres of gut tissue. Furthermore, we confirm the lack of large organised lymphoid structures in young and germ-free mice, likely reflecting the age- and microbiome-dependence of the gut immune system development. Finally, by implementing OPT reversal and confocal microscopy, we show the feasibility of tracking regions of interest (ROIs) initially selected in 3D for subsequent higher resolution imaging using traditional histology methods. This method is a powerful approach to characterize tissues at multiple scales while providing high resolution data with ready-to-use processing pipelines optimized



for the mouse gut.

## 4.2 Methods

### 4.2.1 Animal Handling

Specific pathogen free C57BL/6J mice were purchased and housed at the École Polytechnique Fédérale de Lausanne (Switzerland) under specific pathogen free conditions with *ad libitum* access to food and water, according to guidelines and regulations of the state of Vaud, Switzerland (authorization VD3448). Germ-free C57BL/6J mice were obtained from the Clean Mouse Facility, University of Bern (Switzerland). Germ-free status was routinely monitored by culture-dependent and -independent methods and confirmed to be microbial-free. Experiments were performed in accordance with regulations approved by the ethical and veterinary committee of the Canton of Vaud, Switzerland. As was described previously (258), mice were deeply anesthetised by intra-peritoneal injection of 50mg/kg sodium pentobarbital prior to a transcardiac perfusion of 10ml heparinised PBS (5 I.U./ml Liquemin). Tissues were fixed by perfusing with 10ml of freshly-prepared 4% paraformaldehyde (CAS 30525-89-4, Carl Roth AG 0964.1) and an overnight post-fixation step at 4°C.

### 4.2.2 Sample preparation

All the following steps took place in the dark. Samples were washed for 30 minutes in PBS after the overnight fixation. A 45-minute step-wise dehydration in methanol precedes overnight autofluorescence quenching in a 2:1:3 ratio solution of MetOH:DMSO:H<sub>2</sub>O<sub>2</sub> overnight at room temperature. The samples are washed twice in pure MetOH in preparation for three freeze-thaw cycles between -80°C and room temperature (1 hour and 30 minute cycles respectively) in order to permeabilize the tissue before antibody-mediated staining. A step-wise rehydration to TBS-Tween prepares the samples for antibody-mediated staining of targets. This begins with blocking for 24h, is followed by a primary antibody incubation for 48h and a 24h washing step and ends with a 48h incubation in a secondary antibody and a final 24h washing step. To stain immune cells, we used a rat anti-mouse CD45 monoclonal antibody conjugated to APC (BioLegend 147708) and a goat anti-rat IgG (H+L) Alexa Fluor 647 (Invitrogen A21247). The samples were mounted in custom cylindrical moulds in 1.5% agarose, dehydrated in pure methanol (CAS 67-56-1, Sigma-Aldrich 322415) for 24 hours and rehydrated in a 1:2 benzyl alcohol:benzyl benzoate mixture for a minimum of 48h before acquisition (BA: CAS 100-51-6, Sigma-Aldrich 305197; BB: CAS 120-51-4, Sigma-Aldrich B6630).

### 4.2.3 Microscopy

#### OPT

##### Reverse OPT

After OPT imaging, the samples were dehydrated in pure methanol and rehydrated in PBS for 24h each. At this stage, it is possible to carefully track regions of interest identified in the 3D OPT images to be specifically observed using other imaging modalities downstream. The samples were extracted from the agarose moulds and frozen in optimal cutting temperature (OCT) medium on dry ice. Using a Leica CM3050S cryostat, 25 micrometre-thick sections were collected and mounted on coated glass slides (Eppredia J1800AMNZ). The sections were counterstained with DAPI (Thermofisher D1306) at a concentration of 5 $\mu$ g/ml for 10 minutes with a 5 minute pre- and post-wash with 0.3% Triton-X100 in PBS.

##### Confocal Microscopy

Confocal microscopy was performed using a Leica SP8 inverted microscope, producing two-channel images encompassing the CD45-positive and nuclei signals. Sequential acquisition began with the AlexaFluor647 channel followed by the DAPI channel. Exposure times were determined according to live observation of pixel intensities in order to avoid over-exposure of the tissue. Tiled acquisitions of whole-gut sections were performed using the automated tile function in the LAS-X software.

### 4.2.4 Image Processing

#### Virtual unfolding

The image processing pipeline for virtual unfolding was inspired by previous reports (104) applied using Fiji and is available in the form of a macro algorithm. All steps outlined below are applied to all of the sections within the filtered-back-projection stacks. First, the gut tissue is segmented from the lumen and surrounding background and a mask is created. For each section, the segmented tissue outline is added to the ROI manager. The centroid coordinates within the tissue outline are calculated and used as an origin for the identification of a sectioning origin at a 45° angle from the centre. From this point, we interpolate a polygon shape to draw the line along which the unfolding takes place. A stack of the straightened images is produced and re-sliced orthogonally to create the unfolded image whose field of view include the entire surface of the sample, spanning the lumen in the innermost slice to the outermost layers of the gut. From this image, the apex of each villus is identified by applying a Laplacian filter and extracting local maxima ROIs, whose density can then be calculated within a defined area.

### 4.2.5 Isolated Lymphoid Follicle Segmentation

Quantifiable characteristics were extracted from FBP reconstructions showing the isolated lymphoid follicles using the surface tool in Imaris. The smoothing of surface areas was set to  $2\mu\text{m}$  and thresholding based on absolute intensity, whose values were set visually by the user. Larger structures were segmented by implementing the “number of voxels” filter. Volume and distance statistics were exported in csv format for data plotting.

## 4.3 Results

### 4.3.1 Sample preparation pipeline and the power of tissue autofluorescence

To achieve the multi-scale observation of spatially-distributed biological signals of interest, we developed a sample preparation pipeline that includes two imaging modalities: high-volume optical projection tomography and high-resolution confocal microscopy after reverse OPT (RevOPT, figure 4.1). The pipeline is divided into four phases, sample preparation (figure 4.1 (a-k)), imaging and image processing (figure 4.1 (l-m)), reverse OPT (figure 4.1 (n-r)) and secondary imaging (figure 4.1 (s)), spanning a duration of approximately three weeks. First, tissue preservation, autofluorescence quenching and tissue permeabilisation are performed to prepare the samples for staining. This is followed by fluorescent antibody staining of select markers. A clearing step precedes the acquisition of optical projections over a  $360^\circ$  sample rotation. Next, a filtered back-projection algorithm is used to reconstruct the projections into a 3D image as described previously (258). Using RevOPT we revert the sample to a state compatible with freezing in Optimal Cutting Temperature (OCT) compound, allowing for cryostat sectioning and counterstaining (figure 4.1 (p-r)). Finally, in amongst several methods requiring thin sectioning including electron microscopy or single-molecule FISH, we selected confocal microscopy to image regions of interest identified by OPT with improved resolution.

Tissue autofluorescence is an inherent signal produced by extracellular matrix components and certain pigmented cell types. In OPT, autofluorescence quenching is required to reduce noise and retain targeted fluorescent signals (258) (figure 4.1, steps a and c). However, low levels of autofluorescence enable the discrimination of the outer and inner layers of the gut when samples are illuminated at 415nm spectrally filtered between 400-440nm, whilst emission is collected within the range of 455-520nm (258). A longitudinal portrayal of the gut (figure 4.2 (a)) provides an overview of the structures present in the tissue. In reconstructions made up of 1200 projections, well-resolved villi can be observed in a 3D visualisation software (figure 4.2 (b)). When taking a cross-sectional view, the mucosal layers can be distinguished from the villi in the OPT scan (figure 4.2 (c); mu = muscularis, sm = submucosa, m = mucosa and L = lumen) whilst a greater resolution is achieved by confocal microscopy on the same sample having undergone RevOPT (figure 4.2 (d)). During RevOPT, counterstaining is possible and demonstrated here by the staining of DNA with DAPI (figure 4.2 (d)). The improved preservation of cross-sectional structure in OPT is evident when comparing the virtual section

(figure 4.2 (c)) and its histological counterpart (figure 4.2 (d)), with loss of tissue and distortion being apparent in the confocal image.

We implemented a virtual unfolding technique (104) (for more detail, see supplementary figure 4.6) to observe the gut tissue from within the lumen, with sections spanning from this point to the serosa (figure 4.2 (e), section closest to lumen). Villous density could be calculated by segmenting the unfolded image and finding local maxima (figure 4.2 (f)). This can be performed for the whole tissue region or applied to smaller regions of interest to probe different areas of the tissue. In this healthy tissue, overall villous density is mostly homogeneous (figure 4.2 (f)). This data can be transformed into a quantitative visualisation of different sectors (figure 4.2 (g)). Virtual unfolding also yields a straightened image (figure 4.2 (h)) of the tissue cross section seen in figure 4.2 (c).

Virtual unfolding of 3D-reconstructed data can lead to detailed visualizations of structures that are difficult to visualise in a 3D image such as figure 4.2 (a) or in a virtual cross-section as in figure 4.2 (c). We found a suspected lymphoid follicle in the autofluorescence channel of a different sample (top view figure 4.2 (i), side view figure 4.2 (j)), whose structural context is made clear by virtual unfolding (figure 4.2 (k) and straightened figure 4.2 (l)). The follicle is made up of three lobes, with a concentration of fluorescent vessels in the centre. In the areas surrounding the follicle, gaps in the villi suggests the potential presence of lymphatic vasculature. Typically, large vascular networks are difficult to observe by visualization of cross-sections. In figure 4.2 (m), an example of such a network is shown, highlighting the added value that processing the autofluorescence channel can bring to gut structure characterization.

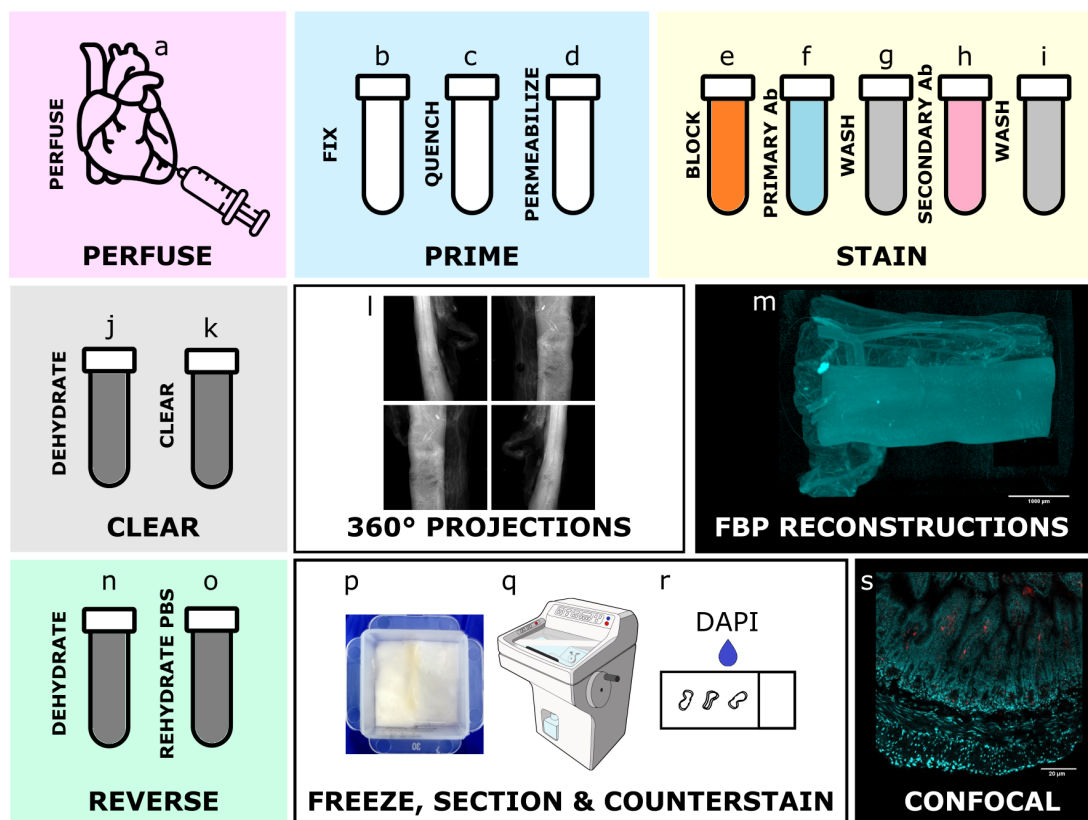


Figure 4.1 – *gutOPT* Workflow Sample preparation and handling in four steps: sample preparation (**a-k**), imaging and image processing (**l-m**), reverse OPT (**n-r**) and secondary imaging (**s**). The experimental steps for sample preparation are: transcardiac perfusion of PBS and 4% PFA (**a**); 4-hour PFA fixation (**b**); overnight autofluorescence quenching with methanol, DMSO and hydrogen peroxide 1:3:2 mixture (**c**); permeabilisation by three freeze-thaw cycles between  $-80^{\circ}\text{C}$  (1h) and room temperature (30min) (**d**); 24-hour tissue blocking (**e**); 48-hour primary antibody incubation (**f**); 24-hour wash (**g**); 48-hour secondary antibody incubation (**h**); 24-hour wash (**j**); 36-hour dehydration in pure methanol with two solution changes (**j**) and clearing in 1:2 ratio of benzyl alcohol and benzyl benzoate (**k**). Optical projections are acquired over a  $360^{\circ}$  rotation of the sample (**i**) and a 3D image is reconstructed using filtered back projection (**m**). OPT processing may be reversed in order to image sections of the same sample using alternative imaging modalities. To do so, samples are dehydrated in pure methanol for 36 hours (**n**), rehydrate in PBS (**o**), mounted in cryomatrix (**p**), cryo-sectioned (**q**) and counterstained with DAPI (**r**). High-resolution imaging modalities such as confocal microscopy (**s**) may be applied to samples whose large-scale volume has been observed.

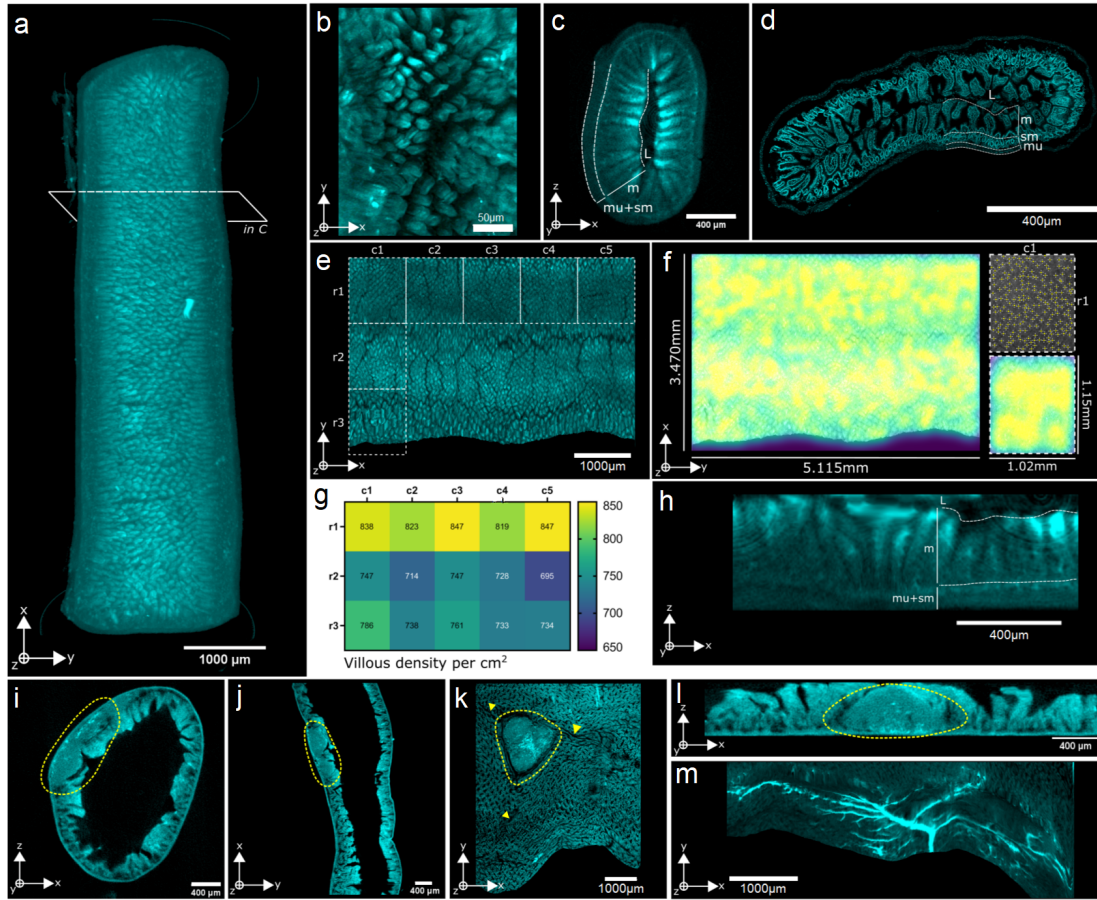


Figure 4.2 – *Visualization and characterization of the autofluorescence signal* (a) FBP reconstruction from a single acquisition of gut in the autofluorescence channel. (b) Close-up of the villi structures from within the lumen. (c) Cross-sectional view of the 3D reconstruction, with visible layers labelled mu = muscularis, sm = submucosa, m = mucosa and L = lumen. (d) High-resolution tiled acquisition of the same gut sample using confocal microscopy, with concurrent layers labelled. (e) Innermost layer of the same reconstruction that was virtually unfolded (104). (f) Use of unfolded image to perform whole gut segment quantification of villus density by applying a Laplacian filter and the find maxima function. (g) Villi density quantified within sub-regions of the unfolded scan. (h) Cross-sectional view of unfolded image, with mucosal layers labelled as before. (i-m) Images of secondary lymphoid structures from a cross-section view (i and j) or top to bottom (l) (encircled in yellow). (j) Side view of the same structure as in i. (k) Unfolded image reveals tri-lobular structure and possible vascularisation (arrow). (l) Straightened cross section of structure in i. (m) Widespread network of large vessels in an unfolded image.

#### 4.3.2 Cell-type specific signal distribution throughout the gut volume

OPT can also be used for visualisation of cell types according to stainings of selective markers. To demonstrate this, we chose to stain the gut immune compartment, due to its structured

organisation under healthy conditions and its common deregulation in intestinal diseases (e.g. IBD (259)) and other systemic disorders (e.g. metabolic diseases (260; 261), autoimmunity (262) and neurodegeneration (65; 263)). For this we stained CD45-positive cells using fluorescently labelled antibodies. In healthy adult mice, immune cells are found interspersed at regular intervals or compartmentalised in gut-associated lymphoid structures (GALTs) known as isolated lymphoid follicles (ILFs, figure 4.3 (a) triangle). Overlaying the autofluorescence channel reveals other adjacent structures such as blood vessels and luminal dietary fibers (figure 4.3 (a), cross and square respectively). It is known that age- and microbiota-dependent education of the immune system is responsible for the formation of structures such as GALTs and Peyer's patches (264; 107). We confirm that with OPT, we are able to identify differences in the immune cell compartments in the contexts of young (14 days) SPF mice and old (30+ weeks) germ-free mice (figure 4.3 (b) and 4.3 (c) respectively), compared to the old SPF sample shown in figure 4.3 (a). At young age under normal rearing conditions, no dense regions of immune cells are observed (figure 4.3 (b)). Intestines of older, germ-free mice also exhibit reduced CD45-positive cell clusters in the mucosal layers. A two-channel cross-sectional view of these samples (figure 4.3 (d-f)) frames the immune signal with the structured layers of the gut. An isolated lymphoid follicle is located within the sub-mucosal layers and is surrounded by smaller, less dense CD45-positive clusters in figure 4.3 (d). Conversely, in both germ-free and young animals, there is no specific fluorescence thus indicating a lack of well-defined GALT structures in these mouse models (figure 4.3 (b), (c), (e), and (f)).

OPT reconstructions can thus be used for broader, organ-scale characterisation of the mouse intestine. Furthermore, current 3D image processing tools allow for accurate quantification of different parameters. We segmented the ILFs in the 625nm channel alone (figure 4.3 (g)) and found their size ranges from approximately 1 to 5 million  $\mu\text{m}^3$  (figure 4.3 (h)). Their spatial distribution along the small intestine is uniform, averaging at  $500\mu\text{m}$  in between ILFs (figure 4.3 (i)).

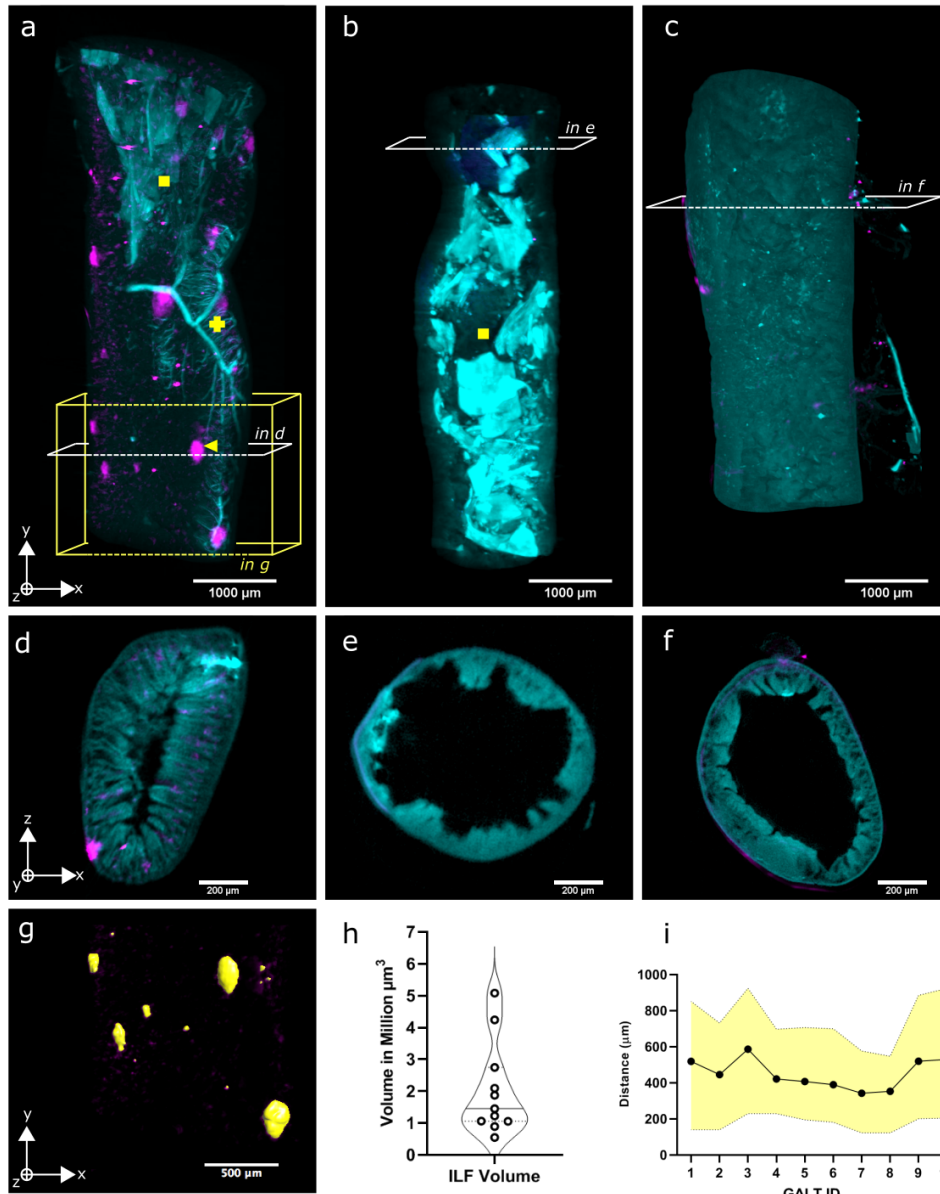


Figure 4.3 – *Multi-channel OPT reconstructions and segmentation of gut immune component* (a-c) Longitudinal views of two-channel OPT renders with tissue autofluorescence in cyan and CD45-positive cell clusters in magenta. Age- and microbiota-dependent development of gut-associated lymphoid structures (GALTs) is evident in a healthy old conventionally-raised gut (a) versus young conventionally-raised (b) and adult germ-free (c) gut samples. Structures of interest include the positive cell clusters (triangle), vascular network (cross) and luminal dietary fibers (square). (d-f) Cross-sectional view of 3D reconstructions for samples shown A-D. (g) 3D segmentation of isolated lymphoid follicles (ILFs) signal using Imaris. (h) Measured volume occupied by individual CD45-positive regions in a healthy old C57BL/6 mouse, measured in million  $\mu\text{m}^3$ . (i) Spatial distribution of ILFs throughout the tissue seen in A as measured by minimum, mean and maximum distance in  $\mu\text{m}$  between each follicle. C57BL/6J mice were used.



### 4.3.3 gutOPT pipeline for multi-modal imaging and high resolution characterisation of the gut

Because sample preparation for optical projection tomography is compatible with downstream processing for additional imaging modalities, we wondered whether we could incorporate a single pipeline for imaging at different scales. We performed reverse-OPT (figure 4.1 (n) and (o)) on the samples shown in figure 4.3 and imaged them using confocal microscopy (figure 4.4). We wondered whether we could use OPT to pre-select regions of interest, and retrace them and image them using high resolution techniques. To do this, we selected isolated lymphoid follicles in the OPT reconstruction and calculated their distance from the edge of the sample (figure 4.4 (a) i and ii). Once samples had undergone RevOPT and were mounted in optimal cutting temperature (OCT) compound, the depth of each cryosection was used to track the localization of the ROIs. We find that the fluorescence signal was maintained from the OPT staining, and sections do not require further immuno-staining for confocal imaging.

Specifically, we find that preselected ILF regions observed by OPT are high-density cell clusters rich in Cd45-positive cells (figure 4.4 (b) and (c)). In both ROIs containing ILFs, the calculated distances were accurate, and we find the immune cell-dense region situated within the submucosa as expected from the OPT reconstructions and their known localisation (265; 106). Areas lacking GALTs in 3D (figure 4.4 (a) iii) only contain sparse positive cells in the lamina propria at higher resolution (figure 4.4 (d)). By measuring the immune cell density in the whole-sectioned GALT regions we find that the signal density threshold for visibility in OPT is approximately 400 fluorescent cells per  $\text{mm}^2$  of DAPI signal (figure 4.4 (e)). We imaged the adult germ-free mice that display no GALTs by OPT (figure 4.4 (f)). Here, we find no Cd45+ cells along the length of the villi nor in the submucosa, confirming that no ILFs are present, and suggesting that the lack of a microbiome indeed alters the immune compartment in the gut (figure 4.4 (f), triangle). The number of immune cells is also significantly reduced compared to that observed in the gut of conventionally-raised mice (figure 4.4 (g)). Thus, OPT can be used to identify specific structures and markers of interest using tissue-wide staining, and given a sufficiently dense fluorescent signal ROIs can be traced by confocal microscopy using RevOPT and cryosectioning.

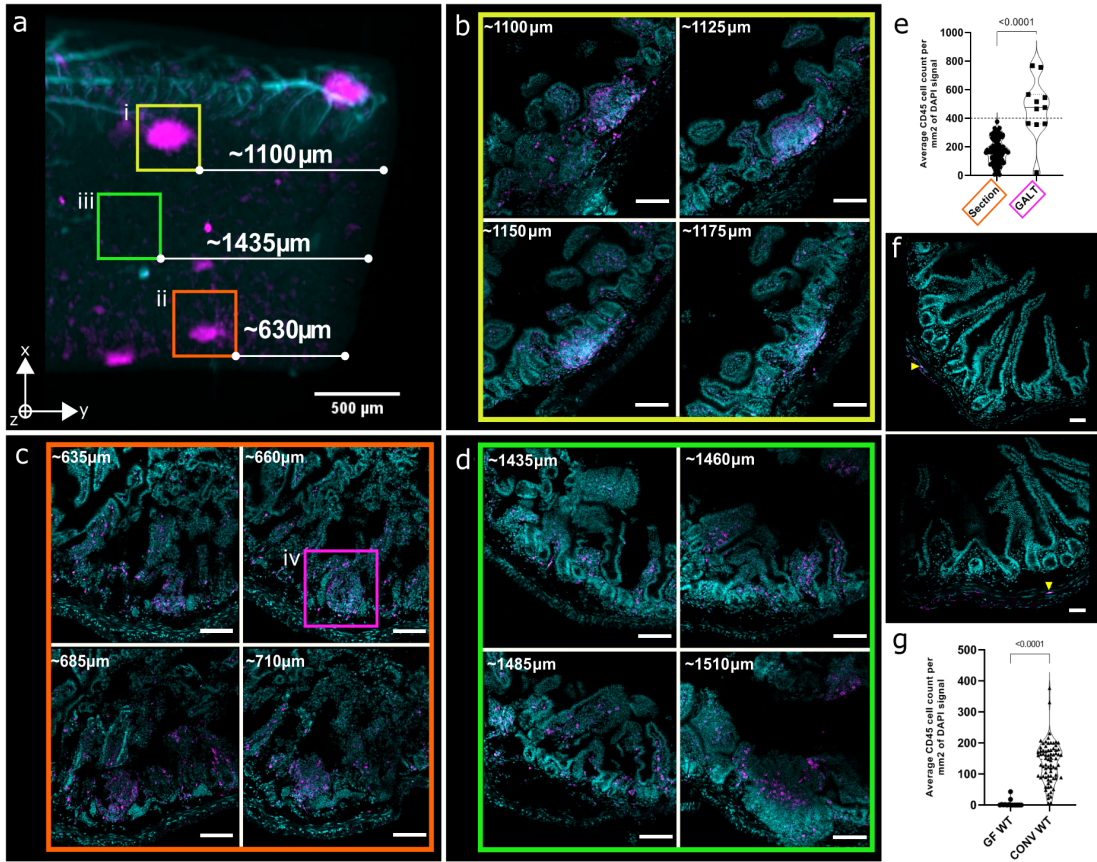


Figure 4.4 – *Reverse OPT for tracking of ROIs in high-resolution imaging modalities* (a) Close-up and selection of two GALT ROIs in OPT reconstruction, with calculation of distance from the end of the tissue. (a-d) Images come from a healthy conventionally-raised adult mouse gut. Regions i-iii are regions shown in b-d, with sectors i and ii containing CD45 signal and iii being empty. (b-d) Scale bars are 200 μm. (b) Two-channel confocal images of reverse-OPT sections within the depth of (i) in (a), with distance from the end of the tissue calculated based on the number of 25 μm-thick sections collected. Nuclei were stained with DAPI and Cd45 signal comes from pre-OPT staining. High Cd45+ cell density regions are the ILFs visible by OPT and are surrounded by sparse Cd45+ cells. (c) Confocal depths in the second ROI (ii) selected in (a). (d) Confocal depth in a region with no observed ILFs in (a) showing only sparse CD45 signal. (e) Comparison of CD45-positive cell density within GALT region and surrounding tissue measured in sections from four gut samples. The signal density threshold above which structures are visible in OPT reconstructions is estimated at 400 fluorescent cells/mm<sup>2</sup> of DAPI signal. (f) Confocal acquisitions from an old germ-free mouse gut, with no ILF signal observed in OPT and a visibly reduced presence of CD45-positive cells throughout the tissue. Scale bars are 200 μm. (g) Comparison of whole-section area density of CD45-positive cells in conventionally-raised and germ-free gut samples (example images b-d and f), showing significant reduction in immune cell presence in the gut lining of germ-free animals.

## 4.4 Discussion

The choice of microscopy technique for gut characterization relies on certain features of the signal of interest, including the scale, the required resolution, the need for staining, the sample preparation and its application in-vivo or ex-vivo. The heterogeneity of gut tissue structure and the dynamic recruitment and trafficking of cells involved in gut health makes 3D microscopy particularly adapted for this setting. Volumetric imaging modalities are continually being developed in parallel with advanced image processing techniques (266; 267; 268), as the weight of data grows rapidly with 3D imaging. Volumes are reconstructed from sections imaged at multiple depths, the number of which is one of the determinants of resolution. As such, common techniques include confocal microscopy, light sheet fluorescence microscopy and two-photon microscopy whose applications range from studying villous vascularisation (269), structural integrity (104; 270), local inflammatory status (112) and microbial community dynamics (100).

The multi-scale and multi-modal gutOPT pipeline we describe uses a customizable staining method to fluorescently label targets of interest, thereby permitting the imaging of tissues at the millimetre-scale. Furthermore, RevOPT can be readily concatenated for higher-resolution imaging of reference ROIs across different modalities. The data acquisition can extend beyond a single 5 millimetre section of gut to several centimetres with overlapping regions, as was demonstrated in previous work (258). The ability to assess multiple fluorescent signals within deep tissue, with minimal distortion, enables the co-localised imaging of different cellular structures in whole intestinal tissue segments. While the methodology can last up to three weeks, the high data yield and wide field of view is attractive for studying the distribution and localisation of distinct cellular structures.

Tissue autofluorescence serves multiple roles in the interpretation of microscopy images. It can provide crucial contextualization for fluorescent labels within tissues and facilitate the interpretation of functionality based on fluorescent signals. In addition, the intestinal architecture observed by autofluorescence imaging provides a label-free method for the characterization of diverse parameters (106) which may be used as comprehensive measures of gut integrity and leakiness (102). The 3-dimensional nature of OPT data provides the opportunity to observe the connectivity of structures from multiple perspectives, as we have shown with the addition of virtual unfolding and the observation of large vascular networks in the submucosa.

Such a technique could be applied to pathological contexts where structural deformation is symptomatic of disease. For example, coeliac disease (CD) is characterized by a destruction of the intestinal epithelium driven by gluten-activated inflammation, resulting in observed villous atrophy and lymphocytic infiltration of the epithelium (271). With the capacity to accurately reconstruct mesoscale volumes, the presented optical projection tomography pipeline offers an approach that maintains structural integrity whilst multiplying the field of view available for diagnostic observation.

## Chapter 4. Optical Imaging of the Small Intestine Across Scales

---

The gastrointestinal tract constitutes the richest site for crosstalk between external stimuli and the host, with numerous signalling pathways mediating the symbiotic relationship made up of neural, endocrine and immune responses as the main functional contributors (272). As is exemplified in most gut-associated disorders, gut immunity is a major mediator of homeostasis which if deregulated can lead to disease directly in the gut, e.g. inflammatory bowel disease (IBD) (273), and to systemic disorders beyond the GI tract ranging from metabolic diseases including diabetes (274) to neurodegenerative diseases (263). The gut is thus equipped with well-developed sensory mechanisms that are organised into gut-associated lymphoid structures (GALT). Though functional studies of these systems at the cellular level are widespread and constitute multiple fields of research, the spatial distribution of immune structures in the gut is not well documented at the mesoscale. Here, we present a novel method for the visualization of GALTs in 3D with subsequent high-resolution 2D ROI referencing in the mouse gut. We demonstrate the ability of our multi-modal OPT pipeline to characterize specific regions of interest at multiple scales and relate our findings to the histological and functional landscape of research that concur with the distribution of GALTs we observe in the mouse gut.

In order to show the applicability of OPT to address the mesoscale organization of cell-types within tissues, we explored the development of GALTs in models where age and the microbiota are manipulated. We stained the CD45 antigen that is found on hematopoietic cells (275) from which almost all immune cell types are derived (276). CD45-rich regions identified as isolated lymphoid follicles (ILF) were found in the gut of a 30-week-old conventionally-raised C57BL6 mouse. ILFs are a sub-category of gut-associated lymphoid tissues (106) whose functions are to limit contact between luminal microbiota and the epithelium via IgA secretion, and to sense epithelial breaching by bacteria and signal the need for phagocytosis to surrounding macrophages (277). For the first time, we are able to measure the variation in volume and the spatial distribution of ILFs in 3D throughout an uninterrupted section of tissue at the millimetre scale. Furthermore, with concatenated overlapping data acquisition, this could easily be extended to the centimetre scale.

The age- and microbiome-dependence of the maturation and regulation of gut immune responses has become evident in recent years (278). Initial exposure to the environment during the neonatal period begins the process of microbiome colonization that in turn shapes the immune system throughout development (279). In accordance with this knowledge, the sparse immune signal observed in the gut of a young conventionally-raised mouse, specifically with no developed GALTs, is expected. In addition, the study of germ-free and gnotobiotic models has proven that the gut microbiota is necessary for the development of a mature and complete immune system (280), with post-gnotobiotic colonization with commensal bacteria resulting in the acute induction of lymphoid tissue genesis (252). Thus, the lack of isolated lymphoid follicles in the small intestine of old germ-free mice observed in OPT is indicative of the expected stunted immune germ-free phenotype.

We also demonstrate the traceability of ROIs between imaging modalities by selecting ILFs in OPT reconstructions and performing RevOPT and confocal microscopy. The distances

measured by image processing and by tracking the number of sectioning depths leads to an accurate correlation of signal localization. With signal density quantification, we are able to determine a limit of detection for regions of interest in OPT scans that may become a benchmark for the selection of targets of interest for OPT imaging. RevOPT adds value to our pipeline as it addresses the need for microscopic analysis of biological landscapes whilst offering the opportunity to interpret signals at the mesoscale.

This multi-modal method presents several advantages that are adaptable to the study's needs. For example, cut-free sections reduce the presence of common artefacts that distort the sample and impede large-scale histopathological interpretations. The virtual sections also simplify the registration of multiple imaging depths for 3D or concatenated 2D segmentation of regions of interest as we have demonstrated here. In studies where points of interest are sparsely distributed throughout the tissue, as is the case with ILFs in the gut, OPT and RevOPT enable the empirical selection of optimal regions for high-resolution downstream imaging that is exemplified in our results. We believe ease of implementation and the resulting possibilities of analysis in large volumes and at high resolution make the gutOPT pipeline an attractive method for both preclinical characterization of gut tissues and in gastroenterological clinical diagnostic settings. Thus, gutOPT addresses the need for a detailed yet holistic approach to understanding the complex physiological interactions involved in gut health and disease.

**Funding.** H2020 Framework Program of the European Union (grant no 686271) and Innosuisse (grant no 31434.1 IP-ICT).

**Acknowledgments.** The authors are grateful to Theo Lasser for useful discussions and overall support and to BIOP imaging facility for technical support and access to confocal microscopes.

**Disclosures.** The authors declare no conflicts of interest.

**Data availability.** Data and code underlying the results presented in this paper are available on SRM website.

## 4.5 Supplementary Information

### 4.5.1 Supplementary Figure 4.5



Figure 4.5 – *gutOPT Movie* Representative movie of three-dimensional image acquired by optical projection tomography, of samples shown in figure 4.3 (a) and (d). Image consists of two channels, the autofluorescent (cyan) and isolated lymphoid follicles stained with an anti-Cd45 antibody (magenta). The movie may be viewed on the SRM EPFL website.

## 4.5.2 Supplementary Figure 4.6

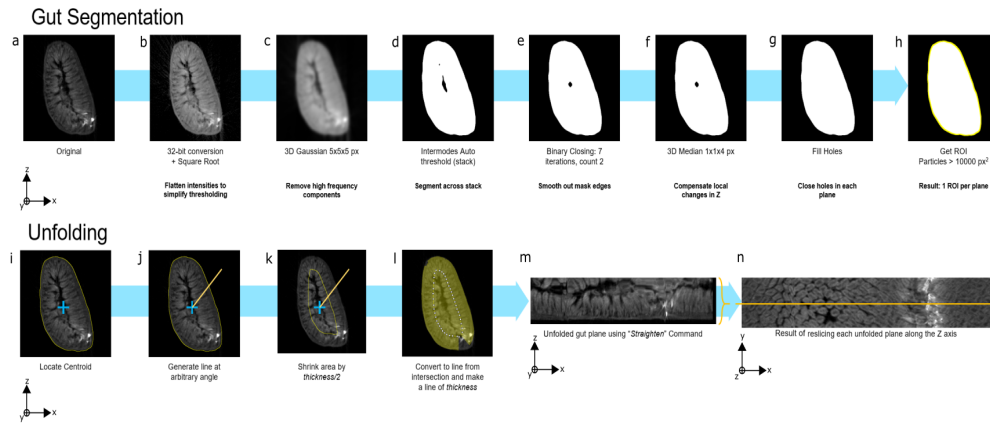


Figure 4.6 – *Segmentation and Unfolding of OPT filtered back projections of mouse intestine*  
 Image processing is performed in ImageJ, using a macro written by the authors. (a-h) Initial segmentation of the gut sample and background throughout the depths of the imaged sample. (i-n) Unfolding and reslicing of the intestinal lining, starting from the centroid. (m) top view of unfolded sample. (n) orthogonal view from within the lumen, making villi cross sections visible.





## 5 Conclusion and Outlook

In summary, in my thesis I have explored the host-gut environment and its importance in neurodegenerative development using multiple approaches. I provide new insights into the effects on health of the bi-directional gut-brain communication in the context of Alzheimer's disease and present a novel microscopy pipeline for host-gut interaction characterizations in 3D. The capability for gut microbiota modulation to alter and to itself be altered by this communication is shown, thus highlighting the need for studies to encompass the organism as a whole.

In this chapter, I reflect on the implications of my work and provide perspectives on the future of research in these fields.

### 5.1 Experimental Approach and Open Questions

The exploratory nature of the AD-gut and gutOPT projects meant a broad scientific approach was necessary. The neurodegenerative disease and gut microbiome research fields have grown significantly since the start of this thesis, meaning much less was known when I designed the experimental approach that would forge the work presented in this thesis.

With the mindset of identifying key players in the bi-directional gut-brain communication in Alzheimer's disease, I outlined a number of experimental readouts to guide my research (figure 5.1). I hoped these would describe the effects of the gut-brain connection on brain health and the gut microbiome, and perhaps point to physiological networks of interest for further investigation. As was shown in the manuscript in chapter 2, I was able to paint a picture of the brain and gut environments as well as test their changeability in response to microbiota modulation.

The majority of the experimental readouts outlined in figure 5.1 were observed, and led to the gut-brain characterization of the 5xFAD model given in chapter 2. In addition to implementing this experimental approach to the model being reared under specific pathogen free condition, my collaborators and I also characterized the 5xFAD model having undergone gut microbiota

## Chapter 5. Conclusion and Outlook

modulation (i.e. germ-free and gnotobiotic cocktails). Some of the readouts for which data were either inconclusive or not collected include the microbial metabolome and mucosal microbial populations, respectively. In the case of the microbial metabolome, we measured levels of short-chain fatty acids and bile acids in the cecum of conventionally-raised 5xFAD animals at multiple time points. Unfortunately, technical difficulties in the experimental execution led to limited data collection and the observation of no significant differences across the groups. The important signalling role played by SCFAs and BAs in the host-gut ecosystem, as was discussed in chapter 1 of this thesis, means this area of the model characterization is highly relevant and warrants further investigation.

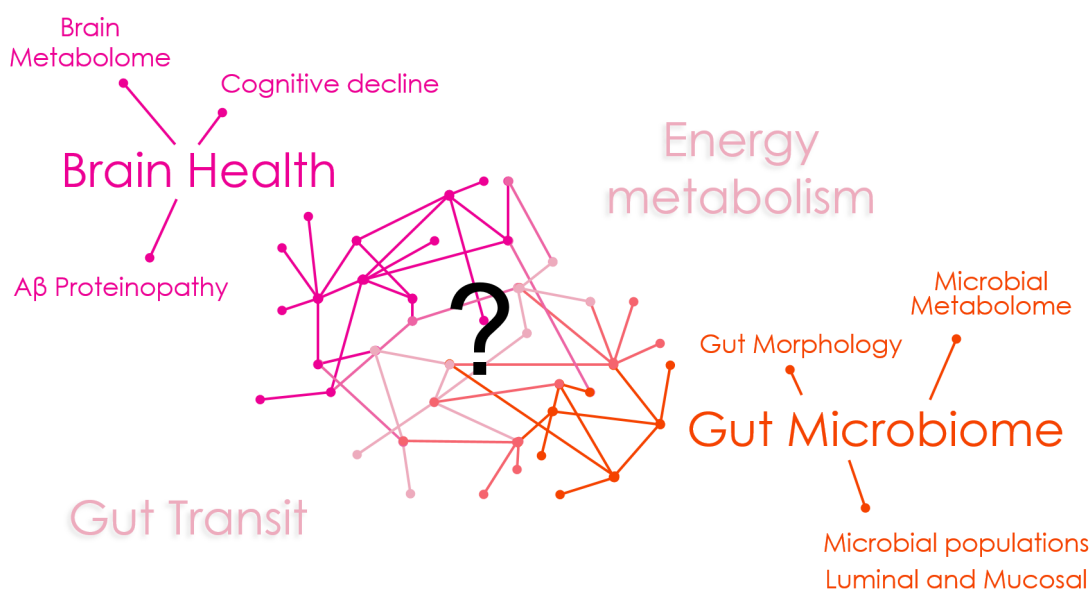


Figure 5.1 – *Plan of readouts for the study of the gut and the brain ecosystems* Mind map of the experimental approach outlined at the start of the thesis. By observing changes at the two major sites of focus, the brain and the gut, we hoped to deepen our knowledge of the routes that connect them. Energy metabolism and gut transit were identified as potentially deregulated in the conventionally-raised 5xFAD model, thus leaving open questions in this areas.

Some findings encountered during the course of the ADgut project pointed to additional physiological systems of interest. Indeed, evidence of deregulation in energy metabolism (with a sex-dependent element) and in gut transit with potential impact on nutrient absorption was uncovered in the 5xFAD model raised under conventional conditions (figure 5.2).

The two major findings that pointed to the involvement of energy metabolism and nutrient absorption were:

- Body weight was significantly reduced in old 5xFAD females, with a mean loss of 14% in body weight at 42 weeks compared to wild-type littermates (figure 5.2 (A)).

## 5.1. Experimental Approach and Open Questions

- Gut transit time was significantly reduced at old age in 5xFAD animals (males and females), with a 3.6-fold average decrease at 42 weeks in transgenic mice compared to wild-type littermates (figure 5.2 (B)).

Two recent studies have reported detailed characterizations of metabolic dysfunction in the 5xFAD model (281; 282), including a confirmation of the body weight loss I observed in aged 5xFAD females. In addition to changes in body weight associated with age and sex, these studies show that food intake, home cage activity and frailty were all altered in the 5xFAD genotype (281). Losses in energy expenditure accompanied the weight loss, as well as modified markers of hypothalamic and peripheral energy balance (including insulin, leptin and GLP-1) (282).

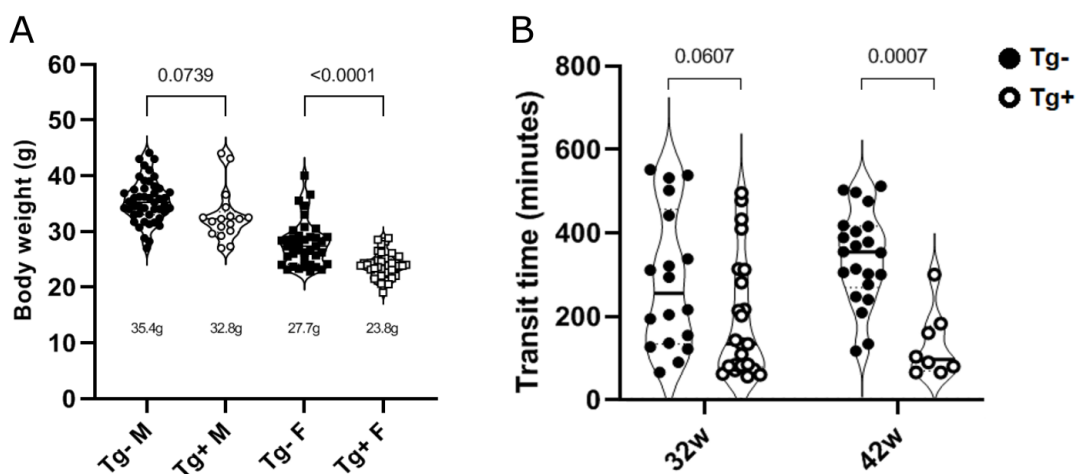


Figure 5.2 – *Effect of 5xFAD genotype on parameters of energy metabolism and nutrient absorption* Open questions remain as to the involvement of energy metabolism and nutrient absorption in the 5xFAD model, since the required follow-up experiments to those shown here were not performed. **A** Body weight measurements for 5xFAD Tg+ and Tg- mice at 42 weeks. p-values for **A** are one-way ANOVA with Bonferroni multiple comparison. **B** Transit time, measured as the time from ingestion of green food to excretion of the first green feces, in 5xFAD Tg+ and Tg- mice at 32 weeks and 42 weeks. p-values are two-way ANOVA with Bonferroni multiple comparison.

Gut motility is a known indicator of gastro-intestinal health (283; 284), is one of the major effectors of gut microbiota signalling in the host and has been described as a marker of intestinal dysfunction (285). Thus, the alterations in gut transit time observed in the aged 5xFAD model are indicative of a disturbance in gut function that is potentially associated with gut microbiota dysbiosis and is likely to affect nutrient uptake, subsequently influencing energy metabolism as a whole. A recent report of reduced gut transit time in the 5xFAD concurs with the observations made here (286), however there is a generally limited discussion of gut transit time in this model.

The numerous approaches applied to study the 5xFAD model highlight the fact that neurodegenerative disease, even in 'simplified' pre-clinical models, involves physiology as a whole. It appears that all physiological systems show alterations in the disease model, including neurology, immunology, energy metabolism, endocrinology and microbiome symbiosis, to name a few. Thus, it is now unequivocal that multi-disciplinary research is necessary for a continued exploration of this disease's development. The open questions discussed here point to some research avenues that need to, and in some cases have been, included in studies of neurodegenerative disease in order to appropriately encompass systemic influences. These may eventually grant us the understanding required to design multi-system treatment strategies.

### 5.2 Perspectives On Microbiota Modulation in Alzheimer's Disease

In this thesis, I have demonstrated that gut microbiota composition is altered in the 5xFAD model of Alzheimer's disease and that bidirectional gut-brain modulation can be experimentally observed. Two methods of gut microbiota modulation were implemented that were able, to varying extents, to influence amyloid plaque formation and cognitive deficits at old age. In addition, the metabolite landscape of the 5xFAD brain revealed that metabolites derived from dietary products are significantly altered by AD genotype.

The greatest challenge we face in treating brain disorders is an as of yet incomplete understanding of brain health in amongst physiology as a whole. In short, the inherent complexity of physiological networks make it difficult to paint a clear bigger picture. Traditional treatment ventures have targeted specific pathways identified as being potentially involved in the development in Alzheimer's disease in the form of hypotheses. As such, several critical hypotheses have proposed since the mid- to late-twentieth century have led the direction of clinical research, examples of which include the Cholinergic hypothesis (287) and more famously the Amyloid Cascade hypothesis (288). In the case of the Amyloid Cascade hypothesis, treatment strategies have focused on inhibiting the production (289) and aggregation (290) of amyloid- $\beta$ , increasing  $A\beta$  clearing (291) and immunotherapy (292). Unfortunately, the majority of anti-amyloid clinical trials have failed (191) for reasons ranging from a lack of efficacy (Solanezumab) to toxicity and a resulting worsening of cognition (Atabecestat) (293). The specificity of these targeted therapies may be incompatible with treating complex diseases like Alzheimer's. Thus, therapies with the ability to broadly impact physiology may lead to more successful outcomes.

The implication of the host-gut ecosystem in the development of Alzheimer's disease, evidence of which was shown in this thesis, not only deepens our understanding of the disease's etiology but also offers new therapeutic avenues. Gut microbiota modulation approaches make it possible to induce shifts in the entire system, including energy metabolism, immunity and nervous system activity. The organ systems, signalling pathways, and even specific bacterial genera associated with improvement or deterioration of AD symptoms across several model

---

### 5.3. Value of the gutOPT Pipeline for Host-Gut Investigation

systems are in many cases conserved, as was discussed in chapter 2. Thus, with a better understanding of the composition of a health-promoting microbiome, including its downstream effects on physiology, we may be able to design widely effective gut-associated therapies.

Implementing microbiota modulation in humans is faced with logistical limitations that cannot be ignored. An important symbiotic function of the microbiota is to produce a stable colonization of the host, whose role is to create an overwhelming competition for pathogenic colonizers. In the hopes of replacing microbiota composition, one must diminish or remove the original gut microbiota. This is achievable with the use of antibiotics, though the widespread and potentially deleterious effects of such a radical treatment are considerable, especially in terms of immunity. Furthermore, the aforementioned uniqueness of one's microbiome may lead to unpredictable patient responses to microbiota modulation in a clinical setting. In the case of fecal microbiota transfer (FMT) therapy, its success is established with 90% cure rates in recurrent *Clostridium difficile* infections (294). However, attempts at implementing FMT therapy in cases of ulcerative colitis (UC) and inflammatory bowel syndrome (IBS) have yielded conflicting reports (294). The unavoidable variation in gut microbiome composition and function within and between populations is likely an underlying contributor to the difficulty encountered in the interpretation of microbiota modulation results (294). Natural gut microbiota modulation occurs throughout one's lifetime, as a result of a host of modulators encompassed within lifestyle, for example. In studies of population-wide parameters influencing the healthy microbiome, lifestyle was identified as one of seven major covariates with a significant effect size (295). Thus, ensuring long-lasting positive effects of a modified microbiome is likely dependent on the adoption of long-term lifestyle changes that may otherwise skew the microbiota population towards an unhealthy phenotype.

### 5.3 Value of the gutOPT Pipeline for Host-Gut Investigation

Today, a pre-clinical researcher's toolbox inevitably holds one or multiple microscopy techniques. The ability to see where signals of interest localize is a vital complement to high-throughput molecular or cell-based quantitative approaches. In particular, microscopy often enables the observation of the structural and/or physiological context surrounding signals of interest, thus improving a researcher's capacity to interpret changes in the observed system.

As a result of immensely varied observational parameter needs (ranging from field of view, resolution, staining requirements, morphological modification and more), a vast number of microscopy techniques have been and continue to be developed. Thus, no single microscopy technique is universally applicable and the concatenation of multiple techniques can widen the possibilities for optimal pipelines to be applied in a chosen setting.

In this thesis I present the gutOPT pipeline, which offers the opportunity to image host-gut interactions at multiple scales by concatenating two imaging modalities: optical projection tomography and confocal microscopy. This pipeline is particularly adapted to the gastrointestinal tract due to this tissue's large-scale heterogeneity in structure, cellular composition

## Chapter 5. Conclusion and Outlook

---

and signalling exchanges involved in the host-gut ecosystem (see figure 1.3). As was demonstrated, simple image processing techniques can be applied to reconstructed 3-dimensional data and result in powerful qualitative and quantitative observations of a complex structure such as the gut. Thus, the gutOPT pipeline provides a bigger picture of volumetric sections of intestine that is adapted to gaining a better understanding of local host-gut ecosystem interactions. Furthermore, by concatenating OPT and a high-resolution modality like confocal microscopy, I fulfill a researcher's need to scan large volumes of tissue to identify regions of interest that can subsequently be imaged at high resolution.

I have demonstrated this pipeline's capacity for multi-channel OPT acquisitions of tissue autofluorescence and fluorescently-labelled signals of interest. By doing so, I have provided a concrete example of gutOPT's usefulness for physiological research in the gut environment. As was discussed in chapters 1 and 4, the immune compartment is intricately linked with gut microbiome homeostasis and a wide range of physiological mechanisms in the host. A recent thorough characterization of the cellular composition of isolated lymphoid follicles (ILF) has revealed their role as adaptive-immune inductive sites that contribute to region-specific immune responses in the gut (253; 111). As was corroborated in our results, the development of gut-associated lymphoid structures, including the ILFs we identified by OPT, is guided by host-gut interactions, thus cementing their relevance for further investigation.

An interesting future avenue for the gutOPT pipeline lies in the observation of the spatial organization of bacterial colonies within the gut lumen. Alterations in colony characteristics, such as size and diversity, alongside simultaneous observations of intestinal morphology, may reveal structural changes involved in the dynamics of host-gut communication. Aptamers present a novel opportunity for staining unconventional targets such as bacterial colonies. Indeed, the selective production of aptamers to specifically bind to targets of interest has been demonstrated in bacteria (296) and for the detection of *Listeria monocytogenes* by flow cytometry (297). In such a scenario, the power of OPT to identify regions of interest in large sectors of intestine is particularly interesting, as high-resolution observations of bacterial colony localization along the length of the gut are relevant to the homeostasis of the host-gut ecosystem and its impact on health and disease (298; 299).

The future of the gutOPT pipeline is open-ended. Throughout the development of what I present in this thesis, design choices were made according to the direction in which we wanted to take the project. Thus, the presently outlined setup and experimental procedure is but one example of how such a pipeline can be put to use. Parameters such as the selected sections of GI tract, the chosen staining targets, the number of overlapping sections imaged and reconstructed, and more are all tunable according to the user's experimental needs.

# Bibliography

- [1] World Health Organization. Dementia. <https://www.who.int/news-room/fact-sheets/detail/dementia>, 2021. Accessed: 2021-10-12.
- [2] Willa D. Brenowitz, Peter T. Nelson, Lilah M. Besser, Katherine B. Heller, and Walter A. Kukull. Cerebral amyloid angiopathy and its co-occurrence with Alzheimer's disease and other cerebrovascular neuropathologic changes. *Neurobiology of Aging*, 36(10):2702–2708, 2015.
- [3] Tong Li, Kerstin E Braunstein, Juhong Zhang, Ashley Lau, Leslie Sibener, Christopher Deeble, and Philip C Wong. The neuritic plaque facilitates pathological conversion of tau in an Alzheimer's disease mouse model. *Nature Communications*, 7(1):12082, 2016.
- [4] Steven M. Greenberg, Brian J. Bacskai, Mar Hernandez-Guillamon, Jeremy Pruzin, Reisa Sperling, and Susanne J. van Veluw. Cerebral amyloid angiopathy and Alzheimer disease — one peptide, two pathways. *Nature Reviews Neurology*, 16(1):30–42, 2020.
- [5] Michael T. Heneka, Monica J. Carson, Joseph El Khoury, Gary E. Landreth, Frederic Brosseron, Douglas L. Feinstein, Andreas H. Jacobs, Tony Wyss-Coray, Javier Vitorica, Richard M. Ransohoff, Karl Herrup, Sally A. Frautschy, Bente Finsen, Guy C. Brown, Alexei Verkhratsky, Koji Yamanaka, Jari Koistinaho, Eicke Latz, Annett Halle, Gabor C. Petzold, Terrence Town, Dave Morgan, Mari L. Shinohara, V. Hugh Perry, Clive Holmes, Nicolas G. Bazan, David J. Brooks, Stéphane Hunot, Bertrand Joseph, Nikolaus Deigendesch, Olga Garaschuk, Erik Boddeke, Charles A. Dinarello, John C. Breitner, Greg M. Cole, Douglas T. Golenbock, and Markus P. Kummer. Neuroinflammation in Alzheimer's disease. *The Lancet Neurology*, 14(4):388–405, 2015.
- [6] Carsten Henneges, Catherine Reed, Yun Fei Chen, Grazia Dell'Agnello, and Jeremie Lebrech. Describing the Sequence of Cognitive Decline in Alzheimer's Disease Patients: Results from an Observational Study. *Journal of Alzheimer's Disease*, 52(3):1065–1080, 2016.
- [7] Qianhua Zhao, Bin Zhou, Ding Ding, Satoshi Teramukai, Qihao Guo, Masanori Fukushima, and Zhen Hong. Cognitive decline in patients with Alzheimer's disease and its related factors in a memory clinic setting, Shanghai, China. *PLoS ONE*, 9(4), 2014.

## Bibliography

---

- [8] Michael A DeTure and Dennis W Dickson. The neuropathological diagnosis of Alzheimer's disease. *Molecular neurodegeneration*, 14(1):32, 2019.
- [9] Alzforum. 5xFAD (C57BL6). <https://www.alzforum.org/research-models/5xfad-c57bl6>, 2021. Accessed: 2021-10-12.
- [10] Irene Piaceri, Benedetta Nacmias, and Sandra Sorbi. Genetics of familial and sporadic Alzheimer's disease. *Frontiers in Bioscience*, 5(1):167–177, 2013.
- [11] Marta Crous-Bou, Carolina Minguillón, Nina Gramunt, and José Luis Molinuevo. Alzheimer's disease prevention: from risk factors to early intervention. *Alzheimer's research and therapy*, 9(1):71, 2017.
- [12] Xiaojuan Sun, Wei-Dong Chen, and Yan-Dong Wang.  $\beta$ -Amyloid: The Key Peptide in the Pathogenesis of Alzheimer's Disease. *Frontiers in Pharmacology*, 6:221, 2015.
- [13] Chris De Jonghe, Cary Esselens, Samir Kumar-Singh, Katleen Craessaerts, Sally Serneels, Frédéric Checler, Wim Annaert, Christine Van Broeckhoven, and Bart De Strooper. Pathogenic APP mutations near the  $\gamma$ -secretase cleavage site differentially affect  $A\beta$  secretion and APP C-terminal fragment stability. *Human Molecular Genetics*, 10(16):1665–1671, 2001.
- [14] Evelin L Schaeffer, Micheli Figueiro, and Wagner F Gattaz. Insights into Alzheimer disease pathogenesis from studies in transgenic animal models. *Clinics (Sao Paulo, Brazil)*, 66 Suppl 1(Suppl 1):45–54, 2011.
- [15] Richard J O'Brien and Philip C Wong. Amyloid precursor protein processing and Alzheimer's disease. *Annual review of neuroscience*, 34:185–204, 2011.
- [16] R E Tanzi, J F Gusella, P C Watkins, G A Bruns, P St George-Hyslop, M L Van Keuren, D Patterson, S Pagan, D M Kurnit, and R L Neve. Amyloid beta protein gene: cDNA, mRNA distribution, and genetic linkage near the Alzheimer locus. *Science*, 235(4791):880–884, 1987.
- [17] A Goate, M C Chartier-Harlin, M Mullan, J Brown, F Crawford, L Fidani, L Giuffra, A Haynes, N Irving, and L James. Segregation of a missense mutation in the amyloid precursor protein gene with familial Alzheimer's disease. *Nature*, 349(6311):704–706, 1991.
- [18] P H St George-Hyslop, R E Tanzi, R J Polinsky, J L Haines, L Nee, P C Watkins, R H Myers, R G Feldman, D Pollen, D Drachman, and et Al. The genetic defect causing familial Alzheimerand039;s disease maps on chromosome 21. *Science*, 235(4791):885 LP – 890, 1987.
- [19] Jürgen Götz, Liviu-Gabriel Bodea, and Michel Goedert. Rodent models for Alzheimer disease. *Nature Reviews Neuroscience*, 19(10):583–598, 2018.



- [20] Leo Tsuda and Young-Mi Lim. *Alzheimer's Disease Model System Using Drosophila*, pages 25–40. Springer Singapore, Singapore, 2018.
- [21] Kate M Van Pelt and Matthias C Truttmann. Caenorhabditis elegans as a model system for studying aging-associated neurodegenerative diseases. *Translational Medicine of Aging*, 4:60–72, 2020.
- [22] Salvatore Oddo, Antonella Caccamo, Jason D Shepherd, M Paul Murphy, Todd E Golde, Rakez Kaye, Raju Metherate, Mark P Mattson, Yama Akbari, and Frank M LaFerla. Triple-transgenic model of Alzheimer's disease with plaques and tangles: intracellular Abeta and synaptic dysfunction. *Neuron*, 39(3):409–421, 2003.
- [23] Rebecca Radde, Tristan Bolmont, Stephan A Kaeser, Janaky Coomaraswamy, Dennis Lindau, Lars Stoltze, Michael E Calhoun, Fabienne Jäggi, Hartwig Wolburg, Simon Gengler, Christian Haass, Bernardino Ghetti, Christian Czech, Christian Hölscher, Paul M Mathews, and Mathias Jucker. Abeta42-driven cerebral amyloidosis in transgenic mice reveals early and robust pathology. *EMBO reports*, 7(9):940–946, 2006.
- [24] H. Oakley, S. L. Cole, S. Logan, E. Maus, P. Shao, J. Craft, A. Guillozet-Bongaarts, M. Ohno, J. Disterhoft, L. Van Eldik, R. Berry, and R. Vassar. Intraneuronal beta-Amyloid Aggregates, Neurodegeneration, and Neuron Loss in Transgenic Mice with Five Familial Alzheimer's Disease Mutations: Potential Factors in Amyloid Plaque Formation. *Journal of Neuroscience*, 26(40):10129–10140, 2006.
- [25] Sadim Jawhar, Anna Trawicka, Carolin Jenneckens, Thomas A. Bayer, and Oliver Wirths. Motor deficits, neuron loss, and reduced anxiety coinciding with axonal degeneration and intraneuronal A $\beta$  aggregation in the 5XFAD mouse model of Alzheimer's disease. *Neurobiology of Aging*, 33(1):196.e29–196.e40, 2012.
- [26] Bernhard Clemens Richard, Anastasiia Kurdakova, Sandra Baches, Thomas A Bayer, Sascha Weggen, and Oliver Wirths. Gene Dosage Dependent Aggravation of the Neurological Phenotype in the 5XFAD Mouse Model of Alzheimer's Disease. *Journal of Alzheimer's disease*, 45(4):1223–1236, 2015.
- [27] Lihua Gu, Di Wu, Xiang Tang, Xinyang Qi, Xiaoli Li, Feng Bai, Xiaochun Chen, Qingguo Ren, and Zhijun Zhang. Myelin changes at the early stage of 5XFAD mice. *Brain Research Bulletin*, 137(June 2017):285–293, 2018.
- [28] Liang Zhang, Craig D. Wallace, Jamie E. Erickson, Christine M. Nelson, Stephanie M. Gaudette, Calvin S. Pohl, Samuel D. Karsen, Gricelda H. Simler, Ruoqi Peng, Christopher A. Stedman, F. Stephen Laroux, Marc A. Wurbel, Rajesh V. Kamath, Bradford L. McRae, Annette J. Schwartz Serman, and Soumya Mitra. Near infrared readouts offer sensitive and rapid assessments of intestinal permeability and disease severity in inflammatory bowel disease models. *Scientific Reports*, 10(1):1–12, 2020.

## Bibliography

---

- [29] Patrizia Giannoni, Margarita Arango-Lievano, Ines Das Neves, Marie Claude Rousset, Kévin Baranger, Santiago Rivera, Freddy Jeanneteau, Sylvie Claeysen, and Nicola Marchi. Cerebrovascular pathology during the progression of experimental Alzheimer's disease. *Neurobiology of Disease*, 88:107–117, 2016.
- [30] S M O'Mara, S Commins, M Anderson, and J Gigg. The subiculum: a review of form, physiology and function. *Progress in neurobiology*, 64(2):129–155, 2001.
- [31] Naomi Hartopp, Paul Wright, Nicola J Ray, Tavia E Evans, Claudia Metzler-Baddeley, John P Aggleton, and Michael J O'Sullivan. A Key Role for Subiculum-Fornix Connectivity in Recollection in Older Age. *Frontiers in Systems Neuroscience*, 12:70, 2019.
- [32] Elena Zenaro, Enrica Pietronigro, Vittorina Della Bianca, Gennj Piacentino, Laura Marongiu, Simona Budui, Ermanna Turano, Barbara Rossi, Stefano Angiari, Silvia Dusi, Alessio Montresor, Tommaso Carlucci, Sara Nani, Gabriele Tosadori, Lucia Calciano, Daniele Catalucci, Giorgio Berton, Bruno Bonetti, and Gabriela Constantin. Neutrophils promote Alzheimer's disease-like pathology and cognitive decline via LFA-1 integrin. *Nature Medicine*, 21(8):880–886, 2015.
- [33] Véréna Landel, Kévin Baranger, Isabelle Virard, Béatrice Loriod, Michel Khrestchatisky, Santiago Rivera, Philippe Benech, and François Féron. Temporal gene profiling of the 5XFAD transgenic mouse model highlights the importance of microglial activation in Alzheimer's disease. *Molecular Neurodegeneration*, 9(1):1–18, 2014.
- [34] Sung Hoon Baik, Seokjo Kang, Woochan Lee, Hayoung Choi, Sunwoo Chung, Jong Il Kim, and Inhee Mook-Jung. A Breakdown in Metabolic Reprogramming Causes Microglia Dysfunction in Alzheimer's Disease. *Cell Metabolism*, 30(3):493–507.e6, 2019.
- [35] Elizabeth E. Spangenberg, Rafael J. Lee, Allison R. Najafi, Rachel A. Rice, Monica R.P. Elmore, Mathew Blurton-Jones, Brian L. West, and Kim N. Green. Eliminating microglia in Alzheimer's mice prevents neuronal loss without modulating amyloid- $\beta$  pathology. *Brain*, 139(4):1265–1281, 2016.
- [36] Wenzhang Wang, Fanpeng Zhao, Xiaopin Ma, George Perry, and Xiongwei Zhu. Mitochondria dysfunction in the pathogenesis of Alzheimer's disease: recent advances. *Molecular Neurodegeneration*, 15(1):30, 2020.
- [37] Xiang Tang, Di Wu, Li Hua Gu, Bin Bin Nie, Xin Yang Qi, Yan Juan Wang, Fang Fang Wu, Xiao Li Li, Feng Bai, Xiao Chun Chen, Lin Xu, Qing Guo Ren, and Zhi Jun Zhang. Spatial learning and memory impairments are associated with increased neuronal activity in 5XFAD mouse as measured by manganese-enhanced magnetic resonance imaging. *Oncotarget*, 7(36):57556–57570, 2016.
- [38] Timon N. Franke, Caroline Irwin, Thomas A. Bayer, Winfried Brenner, Nicola Beindorff, Caroline Bouter, and Yvonne Bouter. In vivo Imaging With 18F-FDG- and 18F-Florbetaben-PET/MRI Detects Pathological Changes in the Brain of the Commonly Used 5XFAD Mouse Model of Alzheimer's Disease. *Frontiers in Medicine*, 7:1–12, 2020.

- 
- [39] Filip Kosel, Jacob S. Hamilton, Sarah L. Harrison, Victoria Godin, and Tamara B. Franklin. Reduced social investigation and increased injurious behavior in transgenic 5xFAD mice. *Journal of Neuroscience Research*, 99(1):209–222, 2021.
- [40] T.P. O’Leary, H.M. Mantolino, K. Stover, and R.E. Brown. Age-related deterioration of motor function in male and female 5xFAD mice from 3-16 months of age. *Genes, Brain and Behavior*, (902):e12538, 2018.
- [41] Katherine Kaylegian, Amanda J. Stebritz, Aldis P. Weible, and Michael Wehr. 5xFAD mice show early onset gap detection deficits. *Frontiers in Aging Neuroscience*, 11:1–9, 2019.
- [42] Jack A Gilbert. Our unique microbial identity. *Genome biology*, 16(1):97, 2015.
- [43] Khan Academy. What is an ecosystem? <https://www.khanacademy.org/science/biology/ecology/intro-to-ecosystems/a/what-is-an-ecosystem>, 2021. Accessed: 2021-10-12.
- [44] Michelle G. Rooks and Wendy S. Garrett. Gut microbiota, metabolites and host immunity. *Nature Reviews Immunology*, 16(6):341–352, 2016.
- [45] Roberta Caruso, Bernard C Lo, and Gabriel Núñez. Host–microbiota interactions in inflammatory bowel disease. *Nature Reviews Immunology*, 20(7):411–426, 2020.
- [46] Xin Zong, Jie Fu, Bocheng Xu, Yizhen Wang, and Mingliang Jin. Interplay between gut microbiota and antimicrobial peptides. *Animal Nutrition*, 6(4):389–396, 2020.
- [47] Daniel Erny, Anna Lena Hrabě de Angelis, Diego Jaitin, Peter Wieghofer, Ori Staszewski, Eyal David, Hadas Keren-Shaul, Tanel Mahlakovic, Kristin Jakobshagen, Thorsten Buch, Vera Schwierzeck, Olaf Utermöhlen, Eunyoung Chun, Wendy S Garrett, Kathy D McCoy, Andreas Diefenbach, Peter Staeheli, Bärbel Stecher, Ido Amit, and Marco Prinz. Host microbiota constantly control maturation and function of microglia in the CNS. *Nature Neuroscience*, 18(7):965–977, 2015.
- [48] V Hugh Perry, James A R Nicoll, and Clive Holmes. Microglia in neurodegenerative disease. *Nature reviews. Neurology*, 6(4):193–201, 2010.
- [49] Karpagam Srinivasan, Brad A Friedman, Ainhua Etxeberria, Melanie A Huntley, Marcel P van der Brug, Oded Foreman, Jonathan S Paw, Zora Modrusan, Thomas G Beach, Geidy E Serrano, and David V Hansen. Alzheimer’s Patient Microglia Exhibit Enhanced Aging and Unique Transcriptional Activation. *Cell Reports*, 31(13):107843, 2020.
- [50] Alyce M. Martin, Emily W. Sun, Geraint B. Rogers, and Damien J. Keating. The influence of the gut microbiome on host metabolism through the regulation of gut hormone release. *Frontiers in Physiology*, 10:1–11, 2019.
- [51] Shadi S Yarandi, Gautam Hebbar, Cary G Sauer, Conrad R Cole, and Thomas R Ziegler. Diverse roles of leptin in the gastrointestinal tract: modulation of motility, absorption, growth, and inflammation. *Nutrition (Burbank, Los Angeles County, Calif.)*, 27(3):269–275, 2011.

## Bibliography

---

- [52] Christina N. Heiss and Louise E. Olofsson. Gut Microbiota-Dependent Modulation of Energy Metabolism. *Journal of Innate Immunity*, 10(3):163–171, 2018.
- [53] Natalie Terry and Kara Gross Margolis. Serotonergic Mechanisms Regulating the GI Tract: Experimental Evidence and Therapeutic Relevance. *Handbook of experimental pharmacology*, 239:319–342, 2017.
- [54] Antonio Molinaro, Annika Wahlström, and Hanns Ulrich Marschall. Role of Bile Acids in Metabolic Control. *Trends in Endocrinology and Metabolism*, 29(1):31–41, 2018.
- [55] Subbiah Pugazhenth, Limei Qin, and P. Hemachandra Reddy. Common neurodegenerative pathways in obesity, diabetes, and Alzheimer’s disease. *Biochimica et Biophysica Acta - Molecular Basis of Disease*, 1863(5):1037–1045, 2017.
- [56] Stephen M. Collins, Michael Surette, and Premysl Bercik. The interplay between the intestinal microbiota and the brain. *Nature Reviews Microbiology*, 10(11):735–742, 2012.
- [57] Constantine Tsigos and George P Chrousos. Hypothalamic–pituitary–adrenal axis, neuroendocrine factors and stress. *Journal of Psychosomatic Research*, 53:865–871, 2002.
- [58] Bruno Bonaz, Thomas Bazin, and Sonia Pellissier. The vagus nerve at the interface of the microbiota-gut-brain axis. *Frontiers in Neuroscience*, 12:1–9, 2018.
- [59] John B Furness, Brid P Callaghan, Leni R Rivera, and Hyun-Jung Cho. The enteric nervous system and gastrointestinal innervation: integrated local and central control. *Advances in experimental medicine and biology*, 817:39–71, 2014.
- [60] Behtash Ghazi Nezami and Shanthi Srinivasan. Enteric nervous system in the small intestine: pathophysiology and clinical implications. *Current gastroenterology reports*, 12(5):358–365, 2010.
- [61] Lv Wang, Claus T. Christophersen, Michael J. Soric, Jacobus P. Gerber, Manya T. Angley, and Michael A. Conlon. Low relative abundances of the mucolytic bacterium *Akkermansia muciniphila* and *Bifidobacterium* spp. in feces of children with autism. *Applied and Environmental Microbiology*, 77(18):6718–6721, 2011.
- [62] Laura de Magistris, Valeria Familiari, Antonio Pascotto, Anna Sapone, Alessandro Frolli, Patrizia Iardino, Maria Carteni, Mario De Rosa, Ruggiero Francavilla, Gabriele Riegler, Roberto Militeri, and Carmela Bravaccio. Alterations of the Intestinal Barrier in Patients With Autism Spectrum Disorders and in Their First-degree Relatives. *Journal of Pediatric Gastroenterology and Nutrition*, 51(4), 2010.
- [63] Maria De Angelis, Ruggiero Francavilla, Maria Piccolo, Andrea De Giacomo, and Marco Gobetti. Autism spectrum disorders and intestinal microbiota. *Gut Microbes*, 6(3):207–213, 2015.
- [64] Jennifer Mead and Paul Ashwood. Evidence supporting an altered immune response in ASD. *Immunology Letters*, 163(1):49–55, 2015.

- 
- [65] Enriqueta Garcia-Gutierrez, Arjan Narbad, and Juan Miguel Rodríguez. Autism Spectrum Disorder Associated With Gut Microbiota at Immune, Metabolomic, and Neuroactive Level. *Frontiers in Neuroscience*, 14:1–14, 2020.
- [66] Kimberly A Schreck and Keith Williams. Food preferences and factors influencing food selectivity for children with autism spectrum disorders. *Research in developmental disabilities*, 27(4):353–363, 2006.
- [67] Y. P. Ooi, S. J. Weng, L. Y. Jang, L. Low, J. Seah, S. Teo, R. P. Ang, C. G. Lim, A. Liew, D. S. Fung, and M. Sung. Omega-3 fatty acids in the management of autism spectrum disorders: Findings from an open-label pilot study in Singapore. *European Journal of Clinical Nutrition*, 69(8):969–971, 2015.
- [68] David A Geier, Janet K Kern, Georgia Davis, Paul G King, James B Adams, John L Young, and Mark R Geier. A prospective double-blind, randomized clinical trial of levocarnitine to treat autism spectrum disorders. *Medical science monitor : international medical journal of experimental and clinical research*, 17(6):PI15–23, 2011.
- [69] Enzo Grossi, Sara Melli, Delia Dunca, and Vittorio Terruzzi. Unexpected improvement in core autism spectrum disorder symptoms after long-term treatment with probiotics. *SAGE Open Medical Case Reports*, 4:2050313X16666231, 2016.
- [70] Elisa Santocchi, Letizia Guiducci, Margherita Prosperi, Sara Calderoni, Melania Gaggini, Fabio Apicella, Raffaella Tancredi, Lucia Billeci, Paola Mastromarino, Enzo Grossi, Amalia Gastaldelli, Maria Aurora Morales, and Filippo Muratori. Effects of Probiotic Supplementation on Gastrointestinal, Sensory and Core Symptoms in Autism Spectrum Disorders: A Randomized Controlled Trial. *Frontiers in Psychiatry*, 11:1–12, 2020.
- [71] Ying Han, Qinrui Li, Angel Belle C. Dy, and Randi J. Hagerman. The Gut Microbiota and Autism Spectrum Disorders. *Frontiers in Cellular Neuroscience*, 11:120, 2017.
- [72] Dae Wook Kang, James B. Adams, Devon M. Coleman, Elena L. Pollard, Juan Maldonado, Sharon McDonough-Means, J. Gregory Caporaso, and Rosa Krajmalnik-Brown. Long-term benefit of Microbiota Transfer Therapy on autism symptoms and gut microbiota. *Scientific Reports*, 9(1):1–9, 2019.
- [73] A Elbaz, L Carcaillon, S Kab, and F Moisan. Epidemiology of Parkinson’s disease. *Revue neurologique*, 172(1):14–26, 2016.
- [74] R D Abbott, H Petrovitch, L R White, K H Masaki, C M Tanner, J D Curb, A Grandinetti, P L Blanchette, J S Popper, and G W Ross. Frequency of bowel movements and the future risk of Parkinson’s disease. *Neurology*, 57(3):456–462, 2001.
- [75] R Sakakibara, T Odaka, T Uchiyama, M Asahina, K Yamaguchi, T Yamaguchi, T Yamanishi, and T Hattori. Colonic transit time and rectoanal videomanometry in Parkinson’s disease. *Journal of Neurology, Neurosurgery & Psychiatry*, 74(2):268–272, 2003.

## Bibliography

---

- [76] Timothy R Sampson, Justine W Debelius, Taren Thron, Stefan Janssen, Gauri G Shastri, Zehra Esra Ilhan, Collin Challis, Catherine E Schretter, Sandra Rocha, Viviana Gradinaru, Marie-Francoise Chesselet, Ali Keshavarzian, Kathleen M Shannon, Rosa Krajmalnik-Brown, Pernilla Wittung-Stafshede, Rob Knight, and Sarkis K Mazmanian. Gut Microbiota Regulate Motor Deficits and Neuroinflammation in a Model of Parkinson's Disease. *Cell*, 167(6):1469–1480.e12, 2016.
- [77] Kristina Endres and Karl Herbert Schäfer. Influence of Commensal Microbiota on the Enteric Nervous System and Its Role in Neurodegenerative Diseases. *Journal of Innate Immunity*, 10(3):172–180, 2018.
- [78] Maria G Cersosimo, Gabriela B Raina, Cristina Pecci, Alejandro Pellene, Cristian R Calandra, Cristian Gutierrez, Federico E Micheli, and Eduardo E Benarroch. Gastrointestinal manifestations in Parkinson's disease: prevalence and occurrence before motor symptoms. *Journal of neurology*, 260(5):1332–1338, 2013.
- [79] Ali Keshavarzian, Stefan J Green, Phillip A Engen, Robin M Voigt, Ankur Naqib, Christopher B Forsyth, Ece Mutlu, and Kathleen M Shannon. Colonic bacterial composition in Parkinson's disease. *Movement disorders : official journal of the Movement Disorder Society*, 30(10):1351–1360, 2015.
- [80] Franziska Hopfner, Axel Künstner, Stefanie H Müller, Sven Künzel, Kirsten E Zeuner, Nils G Margraf, Günther Deuschl, John F Baines, and Gregor Kuhlenbäumer. Gut microbiota in Parkinson disease in a northern German cohort. *Brain research*, 1667:41–45, 2017.
- [81] Velma T E Aho, Pedro A B Pereira, Sari Voutilainen, Lars Paulin, Eero Pekkonen, Petri Auvinen, and Filip Scheperjans. Gut microbiota in Parkinson's disease: Temporal stability and relations to disease progression. *EBioMedicine*, 44:691–707, 2019.
- [82] Daniele Pietrucci, Rocco Cerroni, Valeria Unida, Alessio Farcomeni, Mariangela Pierantozzi, Nicola Biagio Mercuri, Silvia Biocca, Alessandro Stefani, and Alessandro Desideri. Dysbiosis of gut microbiota in a selected population of Parkinson's patients. *Parkinsonism related disorders*, 65:124–130, 2019.
- [83] Marcus M Unger, Jörg Spiegel, Klaus-Ulrich Dillmann, David Grundmann, Hannah Philippeit, Jan Bürmann, Klaus Faßbender, Andreas Schwartz, and Karl-Herbert Schäfer. Short chain fatty acids and gut microbiota differ between patients with Parkinson's disease and age-matched controls. *Parkinsonism related disorders*, 32:66–72, 2016.
- [84] Michael Zimmermann, Maria Zimmermann-Kogadeeva, Rebekka Wegmann, and Andrew L Goodman. Mapping human microbiome drug metabolism by gut bacteria and their genes. *Nature*, 570(7762):462–467, 2019.
- [85] Junmei Shang, Shurong Ma, Caixia Zang, Xiuqi Bao, Yan Wang, and Dan Zhang. Gut microbiota mediates the absorption of FLZ, a new drug for Parkinson's disease treatment. *Acta Pharmaceutica Sinica B*, 11(5):1213–1226, 2021.

- [86] Arik Segal, Yair Zlotnik, Keren Moyal-Atias, Ran Abuhasira, and Gal Ifergane. Fecal microbiota transplant as a potential treatment for Parkinson's disease – A case series. *Clinical Neurology and Neurosurgery*, 207:106791, 2021.
- [87] Anouck Becker, Georges Pierre Schmartz, Laura Gröger, Nadja Grammes, Valentina Galata, Hannah Philippeit, Jacqueline Weiland, Nicole Ludwig, Eckart Meese, Sascha Tierling, Jörn Walter, Andreas Schwiertz, Jörg Spiegel, Gudrun Wagenpfeil, Klaus Faßbender, Andreas Keller, and Marcus M Unger. Effects of Resistant Starch on Symptoms, Fecal Markers and Gut Microbiota in Parkinson's Disease – the RESISTA-PD Trial. *Genomics, Proteomics Bioinformatics*, 2021.
- [88] Jing Sun, Haijun Li, Yangjie Jin, Jiaheng Yu, Shiyin Mao, Kuan-Pin Su, Zongxin Ling, and Jiaming Liu. Probiotic *Clostridium butyricum* ameliorated motor deficits in a mouse model of Parkinson's disease via gut microbiota-GLP-1 pathway. *Brain, Behavior, and Immunity*, 91:703–715, 2021.
- [89] Nicholas M. Vogt, Robert L. Kerby, Kimberly A. Dill-McFarland, Sandra J. Harding, Andrew P. Merluzzi, Sterling C. Johnson, Cynthia M. Carlsson, Sanjay Asthana, Henrik Zetterberg, Kaj Blennow, Barbara B. Bendlin, and Federico E. Rey. Gut microbiome alterations in Alzheimer's disease. *Scientific Reports*, 7(1):1–11, 2017.
- [90] Annamaria Cattaneo, Nadia Cattane, Samantha Galluzzi, Stefania Provasi, Nicola Lopez, Cristina Festari, Clarissa Ferrari, Ugo Paolo Guerra, Barbara Paghera, Cristina Muscio, Angelo Bianchetti, Giorgio Dalla Volta, Marinella Turla, Maria Sofia Cotelli, Michele Gennuso, Alessandro Prella, Orazio Zanetti, Giulia Lussignoli, Dario Mirabile, Daniele Bellandi, Simona Gentile, Gloria Belotti, Daniele Villani, Taoufiq Harach, Tristan Bolmont, Alessandro Padovani, Marina Boccardi, and Giovanni B Frisoni. Association of brain amyloidosis with pro-inflammatory gut bacterial taxa and peripheral inflammation markers in cognitively impaired elderly. *Neurobiology of aging*, 49:60–68, 2017.
- [91] T Harach, N Marungruang, N Duthilleul, V Cheatham, K D Mc Coy, G Frisoni, J J Neher, F Fåk, M Jucker, T Lasser, and T Bolmont. Reduction of Abeta amyloid pathology in APPPS1 transgenic mice in the absence of gut microbiota. *Scientific Reports*, 7(1):41802, 2017.
- [92] L Mosconi, J Murray, W H Tsui, Y Li, M Davies, S Williams, E Pirraglia, N Spector, R S Osorio, L Glodzik, P McHugh, and M J de Leon. Mediterranean Diet and Magnetic Resonance Imaging-Assessed Brain Atrophy in Cognitively Normal Individuals at Risk for Alzheimer's Disease. *The journal of prevention of Alzheimer's disease*, 1(1):23–32, 2014.
- [93] Katarzyna Szczechowiak, Breno S Diniz, and Jerzy Leszek. Diet and Alzheimer's dementia - Nutritional approach to modulate inflammation. *Pharmacology, biochemistry, and behavior*, 184:172743, 2019.

## Bibliography

---

- [94] Laura Bonfili, Valentina Cekarini, Olee Gogoi, Sara Berardi, Silvia Scarpona, Mauro Angeletti, Giacomo Rossi, and Anna Maria Eleuteri. Gut microbiota manipulation through probiotics oral administration restores glucose homeostasis in a mouse model of Alzheimer's disease. *Neurobiology of Aging*, 87:35–43, 2020.
- [95] Zahra Rezaei Asl, Gholamreza Sepehri, and Mahmoud Salami. Probiotic treatment improves the impaired spatial cognitive performance and restores synaptic plasticity in an animal model of Alzheimer's disease. *Behavioural Brain Research*, 376:112183, 2019.
- [96] Milestones in light microscopy. *Nature Cell Biology*, 11(10):1165, 2009.
- [97] David Nguyen, Paul J. Marchand, Arielle L. Planchette, Julia Nilsson, Miguel Sison, Jérôme Extermann, Antonio Lopez, Marcin Sylwestrzak, Jessica Sordet-Dessimoz, Anja Schmidt-Christensen, Dan Holmberg, Dimitri Van De Ville, and Theo Lasser. Optical projection tomography for rapid whole mouse brain imaging. *Biomedical Optics Express*, 8(12):5637, 2017.
- [98] David Nguyen, Virginie Uhlmann, Arielle L Planchette, Paul J Marchand, Dimitri Van De Ville, Theo Lasser, and Aleksandra Radenovic. Supervised learning to quantify amyloidosis in whole brains of an Alzheimer's disease mouse model acquired with optical projection tomography. *Biomedical optics express*, 10(6):3041–3060, 2019.
- [99] P. L. Appleton, A. J. Quyn, S. Swift, and I. Näthke. Preparation of wholemount mouse intestine for high-resolution three-dimensional imaging using two-photon microscopy. *Journal of Microscopy*, 234(2):196–204, 2009.
- [100] Raghuveer Parthasarathy. Monitoring microbial communities using light sheet fluorescence microscopy. *Current Opinion in Microbiology*, 43:31–37, 2018.
- [101] Y. A. Liu, Y. Chen, A. S. Chiang, S. J. Peng, P. J. Pasricha, and S. C. Tang. Optical clearing improves the imaging depth and signal-to-noise ratio for digital analysis and three-dimensional projection of the human enteric nervous system. *Neurogastroenterology and Motility*, 23(10):446–457, 2011.
- [102] Annette Fritscher-Ravens, Detlef Schuppan, Mark Ellrichmann, Stefan Schoch, Christoph Röcken, Jochen Brasch, Johannes Bethge, Martina Böttner, Julius Klose, and Peter J Milla. Confocal endomicroscopy shows food-associated changes in the intestinal mucosa of patients with irritable bowel syndrome. *Gastroenterology*, 147(5):1012–20.e4, 2014.
- [103] Jeremiah Bernier-Latmani and Tatiana V. Petrova. High-resolution 3D analysis of mouse small-intestinal stroma. *Nature Protocols*, 11(9):1617–1629, 2016.
- [104] Luigi Maiuri, Alessia Candeo, Ilenia Sana, Eleonora Ferrari, Cosimo D'Andrea, Gianluca Valentini, and Andrea Bassi. Virtual unfolding of light sheet fluorescence microscopy dataset for quantitative analysis of the mouse intestine. *Journal of Biomedical Optics*, 21(05):1, 2016.



- 
- [105] Mark F. Cesta. Normal Structure, Function, and Histology of Mucosa-Associated Lymphoid Tissue. *Toxicologic Pathology*, 34(5):599–608, 2006.
- [106] Urs M. Mörbe, Peter B. Jørgensen, Thomas M. Fenton, Nicole von Burg, Lene B. Riis, Jo Spencer, and William W. Agace. Human gut-associated lymphoid tissues (GALT); diversity, structure, and function. *Mucosal Immunology*, 14(4):793–802, 2021.
- [107] Ki-Jong Rhee, Periannan Sethupathi, Adam Driks, Dennis K. Lanning, and Katherine L. Knight. Role of Commensal Bacteria in Development of Gut-Associated Lymphoid Tissues and Preimmune Antibody Repertoire. *The Journal of Immunology*, 172(2):1118–1124, 2004.
- [108] Hiromasa Hamada, Takachika Hiroi, Yasuhiro Nishiyama, Hidemi Takahashi, Yohei Masunaga, Satoshi Hachimura, Shuichi Kaminogawa, Hiromi Takahashi-Iwanaga, Toshihiko Iwanaga, Hiroshi Kiyono, Hiroshi Yamamoto, and Hiromichi Ishikawa. Identification of Multiple Isolated Lymphoid Follicles on the Antimesenteric Wall of the Mouse Small Intestine. *The Journal of Immunology*, 168(1):57–64, 2002.
- [109] Bridget R. Glaysher and Neil A. Mabbott. Isolated lymphoid follicle maturation induces the development of follicular dendritic cells. *Immunology*, 120(3):336–344, 2007.
- [110] David S. Donaldson, Kathryn J. Else, and Neil A. Mabbott. The Gut-Associated Lymphoid Tissues in the Small Intestine, Not the Large Intestine, Play a Major Role in Oral Prion Disease Pathogenesis. *Journal of Virology*, 89(18):9532–9547, 2015.
- [111] Peter B. Jørgensen, Thomas M. Fenton, Urs M. Mörbe, Lene B. Riis, Henrik L. Jakobsen, Ole H. Nielsen, and William W. Agace. Identification, isolation and analysis of human gut-associated lymphoid tissues. *Nature Protocols*, 16(4):2051–2067, 2021.
- [112] Sebastian Zundler, Anika Klingberg, Daniela Schillinger, Sarah Fischer, Clemens Neufert, Imke Atreya, Matthias Gunzer, and Markus F Neurath. Three-Dimensional Cross-Sectional Light-Sheet Microscopy Imaging of the Inflamed Mouse Gut. *Gastroenterology*, 153(4):898–900, 2017.
- [113] Richard Mayeux and Yaakov Stern. Epidemiology of Alzheimer disease. *Cold Spring Harbor perspectives in medicine*, 2(8):a006239, 2012.
- [114] E S Athan, J Williamson, A Ciappa, V Santana, S N Romas, J H Lee, H Rondon, R A Lantigua, M Medrano, M Torres, S Arawaka, E Rogaeva, Y Q Song, C Sato, T Kawarai, K C Fafel, M A Boss, W K Seltzer, Y Stern, P St George-Hyslop, B Tycko, and R Mayeux. A founder mutation in presenilin 1 causing early-onset Alzheimer disease in unrelated Caribbean Hispanic families. *JAMA*, 286(18):2257–2263, 2001.
- [115] Lars Bertram, Christoph Lange, Kristina Mullin, Michele Parkinson, Monica Hsiao, Meghan F Hogan, Brit M M Schjeide, Basavaraj Hooli, Jason Divito, Iuliana Ionita, Hongyu Jiang, Nan Laird, Thomas Moscarillo, Kari L Ohlsen, Kathryn Elliott, Xin Wang,

## Bibliography

---

- Diane Hu-Lince, Marie Ryder, Amy Murphy, Steven L Wagner, Deborah Blacker, K David Becker, and Rudolph E Tanzi. Genome-wide association analysis reveals putative Alzheimer's disease susceptibility loci in addition to APOE. *American journal of human genetics*, 83(5):623–632, 2008.
- [116] Xin Wang, Xuan Zhou, Gongying Li, Yun Zhang, Yili Wu, and Weihong Song. Modifications and trafficking of APP in the pathogenesis of alzheimer's disease. *Frontiers in Molecular Neuroscience*, 10:1–15, 2017.
- [117] Sushrut Jangi, Roopali Gandhi, Laura M Cox, Ning Li, Felipe von Glehn, Raymond Yan, Bonny Patel, Maria Antonietta Mazzola, Shirong Liu, Bonnie L Glanz, Sandra Cook, Stephanie Tankou, Fiona Stuart, Kirsy Melo, Parham Nejad, Kathleen Smith, Begüm D Topçuolu, James Holden, Pia Kivisäkk, Tanuja Chitnis, Philip L De Jager, Francisco J Quintana, Georg K Gerber, Lynn Bry, and Howard L Weiner. Alterations of the human gut microbiome in multiple sclerosis. *Nature Communications*, 7(1):12015, 2016.
- [118] Kerstin Berer, Lisa Ann Gerdes, Egle Cekanaviciute, Xiaoming Jia, Liang Xiao, Zhongkui Xia, Chuan Liu, Luisa Klotz, Uta Stauffer, Sergio E Baranzini, Tania Kümpfel, Reinhard Hohlfeld, Gurumoorthy Krishnamoorthy, and Hartmut Wekerle. Gut microbiota from multiple sclerosis patients enables spontaneous autoimmune encephalomyelitis in mice. *Proceedings of the National Academy of Sciences*, 114(40):10719–10724, 2017.
- [119] Elaine Y. Hsiao, Sara W. McBride, Sophia Hsien, Gil Sharon, Embriette R. Hyde, Tyler McCue, Julian A. Codelli, Janet Chow, Sarah E. Reisman, Joseph F. Petrosino, Paul H. Patterson, and Sarkis K. Mazmanian. Microbiota modulate behavioral and physiological abnormalities associated with neurodevelopmental disorders. *Cell*, 155(7):1451–1463, 2013.
- [120] Kimberly A. Krautkramer, Jing Fan, and Fredrik Bäckhed. Gut microbial metabolites as multi-kingdom intermediates. *Nature Reviews Microbiology*, 19(2):77–94, 2021.
- [121] Zihao Ou, Lulu Deng, Zhi Lu, Feifan Wu, Wanting Liu, Dongquan Huang, and Yongzheng Peng. Protective effects of Akkermansia muciniphila on cognitive deficits and amyloid pathology in a mouse model of Alzheimer's disease. *Nutrition and Diabetes*, 10(1), 2020.
- [122] Ting Zhang, Qianqian Li, Lei Cheng, Heena Buch, and Faming Zhang. Akkermansia muciniphila is a promising probiotic. *Microbial Biotechnology*, 12(6):1109–1125, 2019.
- [123] Kazuyuki Kasahara, Kimberly A. Krautkramer, Elin Org, Kymberleigh A. Romano, Robert L. Kerby, Eugenio I. Vivas, Margarete Mehrabian, John M. Denu, Fredrik Bäckhed, Aldons J. Lusa, and Federico E. Rey. Interactions between Roseburia intestinalis and diet modulate atherogenesis in a murine model. *Nature Microbiology*, 3(12):1461–1471, 2018.
- [124] Nathan T. Porter, Ana S. Luis, and Eric C. Martens. Bacteroides thetaiotaomicron. *Trends in Microbiology*, 26(11):966–967, 2018.

- [125] Qinghui Mu, Vincent J. Tavella, and Xin M. Luo. Role of *Lactobacillus reuteri* in human health and diseases. *Frontiers in Microbiology*, 9:1–17, 2018.
- [126] Christina L. Ohland, Lisa Kish, Haley Bell, Aducio Thiesen, Naomi Hotte, Evelina Pankiv, and Karen L. Madsen. Effects of *Lactobacillus helveticus* on murine behavior are dependent on diet and genotype and correlate with alterations in the gut microbiome. *Psychoneuroendocrinology*, 38(9):1738–1747, 2013.
- [127] Chih Jung Chang, Chuan Sheng Lin, Chia Chen Lu, Jan Martel, Yun Fei Ko, David M. Ojcius, Shun Fu Tseng, Tsung Ru Wu, Yi Yuan Margaret Chen, John D. Young, and Hsin Chih Lai. *Ganoderma lucidum* reduces obesity in mice by modulating the composition of the gut microbiota. *Nature Communications*, 6, 2015.
- [128] Richard K Le Leu, Ying Hu, Ian L Brown, Richard J Woodman, and Graeme P Young. Synbiotic intervention of *Bifidobacterium lactis* and resistant starch protects against colorectal cancer development in rats. *Carcinogenesis*, 31(2):246–251, 2010.
- [129] Jie Xiao, Tian Wang, Yi Xu, Xiaozhen Gu, Danyang Li, Kang Niu, Tiandong Wang, Jing Zhao, Ruiqing Zhou, and Hui Li Wang. Long-term probiotic intervention mitigates memory dysfunction through a novel H3K27me3-based mechanism in lead-exposed rats. *Translational Psychiatry*, 10(1), 2020.
- [130] Michail Mamantopoulos, Francesca Ronchi, Filip Van Hauwermeiren, Sara Vieira-Silva, Bahtiyar Yilmaz, Liesbet Martens, Yvan Saeys, Stefan K Drexler, Amir S Yazdi, Jeroen Raes, Mohamed Lamkanfi, Kathy D McCoy, and Andy Wullaert. Nlrp6- and ASC-Dependent Inflammasomes Do Not Shape the Commensal Gut Microbiota Composition. *Immunity*, 47(2):339–348.e4, 2017.
- [131] Michail Mamantopoulos, Francesca Ronchi, Kathy D McCoy, and Andy Wullaert. Inflammasomes make the case for littermate-controlled experimental design in studying host-microbiota interactions. *Gut Microbes*, 9(4):374–381, 2018.
- [132] Eran Elinav, Jorge Henao-Mejia, Till Strowig, and Richard Flavell. NLRP6 and Dysbiosis: Avoiding the Luring Attraction of Over-Simplification. *Immunity*, 48(4):603–604, 2018.
- [133] Age K. Smilde, Jeroen J. Jansen, Huub C.J. Hoefsloot, Robert Jan A.N. Lamers, Jan van der Greef, and Marieke E. Timmerman. ANOVA-simultaneous component analysis (ASCA): A new tool for analyzing designed metabolomics data. *Bioinformatics*, 21(13):3043–3048, 2005.
- [134] Peter Bankhead, Maurice B. Loughrey, José A. Fernández, Yvonne Dombrowski, Darragh G. McArt, Philip D. Dunne, Stephen McQuaid, Ronan T. Gray, Liam J. Murray, Helen G. Coleman, Jacqueline A. James, Manuel Salto-Tellez, and Peter W. Hamilton. QuPath: Open source software for digital pathology image analysis. *Scientific Reports*, 7(1):1–7, 2017.

## Bibliography

---

- [135] Roberta Caruso, Masashi Ono, Marie E. Bunker, Gabriel Núñez, and Naohiro Inohara. Dynamic and Asymmetric Changes of the Microbial Communities after Cohousing in Laboratory Mice. *Cell Reports*, 27(11):3401–3412.e3, 2019.
- [136] Susan J. Robertson, Paul Lemire, Heather Maughan, Ashleigh Goethel, Williams Turpin, Larbi Bedrani, David S. Guttman, Kenneth Croitoru, Stephen E. Girardin, and Dana J. Philpott. Comparison of Co-housing and Littermate Methods for Microbiota Standardization in Mouse Models. *Cell Reports*, 27(6):1910–1919.e2, 2019.
- [137] Filipe De Vadder, Petia Kovatcheva-Datchary, Daisy Goncalves, Jennifer Vinera, Carine Zitoun, Adeline Duchampt, Fredrik Bäckhed, and Gilles Mithieux. Microbiota-generated metabolites promote metabolic benefits via gut-brain neural circuits. *Cell*, 156(1-2):84–96, 2014.
- [138] Justin L. Sonnenburg and Fredrik Bäckhed. Diet-microbiota interactions as moderators of human metabolism. *Nature*, 535(7610):56–64, 2016.
- [139] Clair R Martin, Vadim Osadchiy, Amir Kalani, and Emeran A Mayer. The Brain-Gut-Microbiome Axis. *Cellular and molecular gastroenterology and hepatology*, 6(2):133–148, 2018.
- [140] Yijing Chen, Jinying Xu, and Yu Chen. Regulation of neurotransmitters by the gut microbiota and effects on cognition in neurological disorders. *Nutrients*, 13(6):1–21, 2021.
- [141] Jae-Won Kim, Hyo-Sang Ahn, Ja-Hyun Baik, and Bong-June Yoon. Administration of clomipramine to neonatal mice alters stress response behavior and serotonergic gene expressions in adult mice. *Journal of psychopharmacology (Oxford, England)*, 27(2):171–180, feb 2013.
- [142] Fernando Sánchez-Patán, Mourad Chioua, Ignacio Garrido, Carolina Cueva, Abdelouahid Samadi, José Marco-Contelles, M Victoria Moreno-Arribas, Begoña Bartolomé, and Maria Monagas. Synthesis, Analytical Features, and Biological Relevance of 5-(3,4-Dihydroxyphenyl)- $\gamma$ -valerolactone, a Microbial Metabolite Derived from the Catabolism of Dietary Flavan-3-ols. *Journal of Agricultural and Food Chemistry*, 59(13):7083–7091, 2011.
- [143] P. Fang, S. A. Kazmi, K. G. Jameson, and E. Y. Hsiao. The Microbiome as a Modifier of Neurodegenerative Disease Risk. *Cell Host and Microbe*, 28(2):201–222, 2020.
- [144] Amandine Everard, Clara Belzer, Lucie Geurts, Janneke P Ouwerkerk, Céline Druart, Laure B Bindels, Yves Guiot, Muriel Derrien, Giulio G Muccioli, Nathalie M Delzenne, Willem M de Vos, and Patrice D Cani. Cross-talk between *Akkermansia muciniphila* and intestinal epithelium controls diet-induced obesity. *Proceedings of the National Academy of Sciences of the United States of America*, 110(22):9066–9071, 2013.

- [145] Hubert Plovier, Amandine Everard, Céline Druart, Clara Depommier, Matthias Van Hul, Lucie Geurts, Julien Chilloux, Noora Ottman, Thibaut Duparc, Laetitia Lichtenstein, Antonis Myridakis, Nathalie M Delzenne, Judith Klievink, Arnab Bhattacharjee, Kees C H van der Ark, Steven Aalvink, Laurent O Martinez, Marc-Emmanuel Dumas, Dominique Maiter, Audrey Loumaye, Michel P Hermans, Jean-Paul Thissen, Clara Belzer, Willem M de Vos, and Patrice D Cani. A purified membrane protein from *Akkermansia muciniphila* or the pasteurized bacterium improves metabolism in obese and diabetic mice. *Nature medicine*, 23(1):107–113, 2017.
- [146] Robert A. Scott, Hannah G. Williams, Caroline L. Hoad, Ali Alyami, Catherine A. Ortori, Jane I. Grove, Luca Marciani, Gordon W. Moran, Robin C. Spiller, Alex Menys, Guruprasad P. Aithal, and Penny A. Gowland. MR Measures of Small Bowel Wall T2 Are Associated With Increased Permeability. *Journal of Magnetic Resonance Imaging*, 53(5):1422–1431, 2021.
- [147] Rochellys Diaz Heijtz, Shugui Wang, Farhana Anuar, Yu Qian, Britta Björkholm, Annika Samuelsson, Martin L. Hibberd, Hans Forssberg, and Sven Pettersson. Normal gut microbiota modulates brain development and behavior. *Proceedings of the National Academy of Sciences of the United States of America*, 108(7):3047–3052, 2011.
- [148] Shmuel Yannai. *Dictionary of food compounds with CD-ROM : additives, flavors, and ingredients*. Boca Raton, Fla. : Chapman and Hall/CRC, ©2004.
- [149] Yijing Chen, Lihua Fang, Shuo Chen, Haokui Zhou, Yingying Fan, Li Lin, Jing Li, Jinying Xu, Yuewen Chen, Yingfei Ma, and Yu Chen. Gut Microbiome Alterations Precede Cerebral Amyloidosis and Microglial Pathology in a Mouse Model of Alzheimer's Disease. *BioMed Research International*, 2020.
- [150] Carolin Brandscheid, Florian Schuck, Sven Reinhardt, Karl-Herbert Schäfer, Claus U Pietrzik, Marcus Grimm, Tobias Hartmann, Andreas Schwiertz, and Kristina Endres. Altered Gut Microbiome Composition and Tryptic Activity of the 5xFAD Alzheimer's Mouse Model. *Journal of Alzheimer's disease*, 56(2):775–788, 2017.
- [151] Hae-Ji Lee, Kyung-Eon Lee, Jeon-Kyung Kim, and Dong-Hyun Kim. Suppression of gut dysbiosis by *Bifidobacterium longum* alleviates cognitive decline in 5XFAD transgenic and aged mice. *Scientific Reports*, 9(1):11814, 2019.
- [152] Malena Dos Santos Guilherme, Vu Thu Thuy Nguyen, Christoph Reinhardt, and Kristina Endres. Impact of Gut Microbiome Manipulation in 5xFAD Mice on Alzheimer's Disease-Like Pathology. *Microorganisms*, 9(4), 2021.
- [153] Yehudit Shabat, Yoav Lichtenstein, and Yaron Ilan. Short-Term Cohousing of Sick with Healthy or Treated Mice Alleviates the Inflammatory Response and Liver Damage. *Inflammation*, 44(2):518–525, 2021.

## Bibliography

---

- [154] Yuan Zhang, Rongrong Huang, Mengjing Cheng, Lirui Wang, Jie Chao, Junxu Li, Peng Zheng, Peng Xie, Zhijun Zhang, and Honghong Yao. Gut microbiota from NLRP3-deficient mice ameliorates depressive-like behaviors by regulating astrocyte dysfunction via circHIPK2. *Microbiome*, 7(1):1–16, 2019.
- [155] Jane A. Mullaney, Juliette E. Stephens, Brooke E. Geeling, and Emma E. Hamilton-Williams. Early-life exposure to gut microbiota from disease-protected mice does not impact disease outcome in type 1 diabetes susceptible NOD mice. *Immunology and Cell Biology*, 97(1):97–103, 2019.
- [156] Mireia Valles-Colomer, Gwen Falony, Youssef Darzi, Ettje F. Tigchelaar, Jun Wang, Raul Y. Tito, Carmen Schiweck, Alexander Kurilshikov, Marie Joossens, Cisca Wijmenga, Stephan Claes, Lukas Van Oudenhove, Alexandra Zhernakova, Sara Vieira-Silva, and Jeroen Raes. The neuroactive potential of the human gut microbiota in quality of life and depression. *Nature Microbiology*, 4(4):623–632, 2019.
- [157] Takuhiro Uto, De-Xing Hou, Osamu Morinaga, and Yukihiro Shoyama. Molecular Mechanisms Underlying Anti-Inflammatory Actions of 6-(Methylsulfinyl)hexyl Isothiocyanate Derived from Wasabi (*Wasabia japonica*). *Advances in Pharmacological Sciences*, 2012:614046, 2012.
- [158] Takuhiro Uto, Makoto Fujii, and De-Xing Hou. Inhibition of lipopolysaccharide-induced cyclooxygenase-2 transcription by 6-(methylsulfinyl) hexyl isothiocyanate, a chemopreventive compound from *Wasabia japonica* (Miq.) Matsumura, in mouse macrophages. *Biochemical Pharmacology*, 70(12):1772–1784, 2005.
- [159] N Yoshimi, T Futamura, S E Bergen, Y Iwayama, T Ishima, C Sellgren, C J Ekman, J Jakobsson, E Pålsson, K Kakumoto, Y Ohgi, T Yoshikawa, M Landén, and K Hashimoto. Cerebrospinal fluid metabolomics identifies a key role of isocitrate dehydrogenase in bipolar disorder: evidence in support of mitochondrial dysfunction hypothesis. *Molecular Psychiatry*, 21(11):1504–1510, 2016.
- [160] Lucia Abela, Ronen Spiegel, Lisa M. Crowther, Andrea Klein, Katharina Steindl, Sorina Mihaela Papuc, Pascal Joset, Yoav Zehavi, Anita Rauch, Barbara Plecko, and Thomas Luke Simmons. Plasma metabolomics reveals a diagnostic metabolic fingerprint for mitochondrial aconitase (ACO2) deficiency. *PLoS ONE*, 12(5):1–15, 2017.
- [161] Hye Lin Chun, So Yeon Lee, Sung Hoon Lee, Chang Sup Lee, and Hyun Ho Park. Enzymatic reaction mechanism of cis-aconitate decarboxylase based on the crystal structure of IRG1 from *Bacillus subtilis*. *Scientific Reports*, 10(1):1–10, 2020.
- [162] Sunny E. Ohia, Catherine A. Opere, Angela M. LeDay, Manashi Bagchi, Debasis Bagchi, and Sidney J. Stohs. Safety and mechanism of appetite suppression by a novel hydroxycitric acid extract (HCA-SX). *Molecular and Cellular Biochemistry*, 238(1-2):89–103, 2002.

- 
- [163] W Sergio. A natural food, the Malabar Tamarind, may be effective in the treatment of obesity. *Medical Hypotheses*, 27(1):39–40, 1988.
- [164] Paula I Moreira, Cristina Carvalho, Xiongwei Zhu, Mark A Smith, and George Perry. Mitochondrial dysfunction is a trigger of Alzheimer's disease pathophysiology. *Biochimica et Biophysica Acta (BBA) - Molecular Basis of Disease*, 1802(1):2–10, 2010.
- [165] Lu Wang, Lan Guo, Lin Lu, Huili Sun, Muming Shao, Simon J Beck, Lin Li, Janani Ramachandran, Yifeng Du, and Heng Du. Synaptosomal Mitochondrial Dysfunction in 5xFAD Mouse Model of Alzheimer's Disease. *PloS one*, 11(3):e0150441, 2016.
- [166] Javier A. Bravo, Paul Forsythe, Marianne V. Chew, Emily Escaravage, Hélène M. Savignac, Timothy G. Dinan, John Bienenstock, and John F. Cryan. Ingestion of Lactobacillus strain regulates emotional behavior and central GABA receptor expression in a mouse via the vagus nerve. *Proceedings of the National Academy of Sciences of the United States of America*, 108(38):16050–16055, 2011.
- [167] Carli J. Smith, Jacob R. Emge, Katrina Berzins, Lydia Lung, Rebecca Khamishon, Paarth Shah, Colin Reardon, Kim E. Barrett, Mélanie G. Gareau, David M. Rodrigues, Andrew J. Sousa, and Philip M. Sherman. Probiotics normalize the gut-brain-microbiota axis in immunodeficient mice. *American Journal of Physiology - Gastrointestinal and Liver Physiology*, 307(8):G793–G802, 2014.
- [168] Dora Abraham, Janos Feher, Gian Luca Scuderi, Dora Szabo, Arpad Dobolyi, Melinda Cservenak, Janos Juhasz, Balazs Ligeti, Sandor Pongor, Mari Carmen Gomez-Cabrera, Jose Vina, Mitsuru Higuchi, Katsuhiko Suzuki, Istvan Boldogh, and Zsolt Radak. Exercise and probiotics attenuate the development of Alzheimer's disease in transgenic mice: Role of microbiome. *Experimental Gerontology*, 115:122–131, 2019.
- [169] Elmira Akbari, Zatollah Asemi, Reza Daneshvar Kakhaki, Fereshteh Bahmani, Ebrahim Kouchaki, Omid Reza Tamtaji, Gholam Ali Hamidi, and Mahmoud Salami. Effect of Probiotic Supplementation on Cognitive Function and Metabolic Status in Alzheimer's Disease: A Randomized, Double-Blind and Controlled Trial. *Frontiers in aging neuroscience*, 8:256, 2016.
- [170] Friedrich Leblhuber, Michael Egger, Burkhard Schuetz, and Dietmar Fuchs. Commentary: Effect of Probiotic Supplementation on Cognitive Function and Metabolic Status in Alzheimer's Disease: A Randomized, Double-Blind and Controlled Trial. *Frontiers in aging neuroscience*, 10:54, 2018.
- [171] D. Allan Butterfield and Barry Halliwell. Oxidative stress, dysfunctional glucose metabolism and Alzheimer disease. *Nature Reviews Neuroscience*, 20(3):148–160, 2019.
- [172] Sheng Fong, Emelyne Teo, Li Fang Ng, Ce-Belle Chen, Lakshmi Narayanan Lakshmanan, Sau Yee Tsoi, Philip Keith Moore, Takao Inoue, Barry Halliwell, and Jan Gruber. Energy crisis precedes global metabolic failure in a novel Caenorhabditis elegans Alzheimer Disease model. *Scientific Reports*, 6(1):33781, 2016.

## Bibliography

---

- [173] Kai Wang, Mingfang Liao, Nan Zhou, Li Bao, Ke Ma, Zhongyong Zheng, Yujing Wang, Chang Liu, Wenzhao Wang, Jun Wang, Shuang Jiang Liu, and Hongwei Liu. Parabacteroides distasonis Alleviates Obesity and Metabolic Dysfunctions via Production of Succinate and Secondary Bile Acids. *Cell Reports*, 26(1):222–235.e5, 2019.
- [174] Christine A. Olson, Helen E. Vuong, Jessica M. Yano, Qingxing Y. Liang, David J. Nisbaum, and Elaine Y. Hsiao. The Gut Microbiota Mediates the Anti-Seizure Effects of the Ketogenic Diet. *Cell*, 173(7):1728–1741.e13, 2018.
- [175] Catherine Mooser, Mercedes Gomez de Agüero, and Stephanie C. Ganai-Vonarburg. Standardization in host–microbiota interaction studies: challenges, gnotobiology as a tool, and perspective. *Current Opinion in Microbiology*, 44:50–60, 2018.
- [176] Jian Xu, Magnus K. Bjursell, Jason Himrod, Su Deng, Lynn K. Carmichael, Herbert C. Chiang, Lora V. Hooper, and Jeffrey I. Gordon. A genomic view of the human-Bacteroides thetaiotaomicron symbiosis. *Science*, 299(5615):2074–2076, 2003.
- [177] Baokun He, Thomas K. Hoang, Ting Wang, Michael Ferris, Christopher M. Taylor, Xi-angjun Tian, Meng Luo, Dat Q. Tran, Jain Zhou, Nina Tatevian, Fayong Luo, Jose G. Molina, Michael R. Blackburn, Thomas H. Gomez, Stefan Roos, J. Marc Rhoads, and Yuying Liu. Resetting microbiota by Lactobacillus reuteri inhibits T reg deficiency-induced autoimmunity via adenosine A2A receptors. *Journal of Experimental Medicine*, 214(1):107–123, 2017.
- [178] Yasuhiro Uchimura, Madeleine Wyss, Sandrine Brugioux, Julien P Limenitakis, Bärbel Stecher, Kathy D McCoy, and Andrew J Macpherson. Complete Genome Sequences of 12 Species of Stable Defined Moderately Diverse Mouse Microbiota 2. *Genome announcements*, 4(5), 2016.
- [179] Karen J.I. Lee, Grant M. Calder, Christopher R. Hindle, Jacob L. Newman, Simon N. Robinson, Jerome J.H.Y. Avondo, and Enrico S. Coen. Macro optical projection tomography for large scale 3D imaging of plant structures and gene activity. *Journal of Experimental Botany*, 68(3):527–538, 2017.
- [180] Benjamin W. Lindsey and Jan Kaslin. Optical projection tomography as a novel method to visualize and quantitate whole-brain patterns of cell proliferation in the adult zebrafish brain. *Zebrafish*, 14(6):574–577, 2017.
- [181] Vasilis Ntziachristos. Going deeper than microscopy: the optical imaging frontier in biology. *Nature Methods*, 7(8):603–614, 2010.
- [182] Alfonso Fasano, Naomi P Visanji, Louis W C Liu, Antony E Lang, and Ronald F Pfeiffer. Gastrointestinal dysfunction in Parkinson’s disease. *The Lancet Neurology*, 14(6):625–639, 2015.
- [183] Thomas G Beach, Anne-Gaëlle Corbillé, Franck Letournel, Jeffrey H Kordower, Thomas Kremer, David G Munoz, Anthony Intorcchia, Joseph Hentz, Charles H Adler, Lucia I Sue,



- Jessica Walker, Geidy Serrano, and Pascal Derkinderen. Multicenter Assessment of Immunohistochemical Methods for Pathological Alpha-Synuclein in Sigmoid Colon of Autopsied Parkinson's Disease and Control Subjects. *Journal of Parkinson's disease*, 6(4):761–770, 2016.
- [184] S A Schneider, M Boettner, A Alexoudi, D Zorenkov, G Deuschl, and T Wedel. Can we use peripheral tissue biopsies to diagnose Parkinson's disease? A review of the literature. *European journal of neurology*, 23(2):247–261, 2016.
- [185] A.H. Voie, D.H. Burns, and F.A. Spelman. Orthogonal-plane fluorescence optical sectioning: Three-dimensional imaging of macroscopic biological specimens. *Journal of Microscopy*, 14(6):625–639, 1993.
- [186] James Sharpe, Ulf Ahlgren, Paul Perry, Bill Hill, Allyson Ross, Jacob Hecksher-Sørensen, Richard Baldock, and Duncan Davidson. Optical projection tomography as a tool for 3D microscopy and gene expression studies. *Science (New York, N.Y.)*, 296(5567):541–545, 2002.
- [187] A. M. Cormack. Representation of a function by its line integrals, with some radiological applications. *Journal of Applied Physics*, 34(9):2722–2727, 1963.
- [188] G N Hounsfield. Computerized transverse axial scanning (tomography). 1. Description of system. *The British journal of radiology*, 46(552):1016–1022, 1973.
- [189] David W Holdsworth and Michael M Thornton. Micro-CT in small animal and specimen imaging. *Trends in Biotechnology*, 20(8):S34–S39, 2002.
- [190] Avinash C. Kak and M. Slaney. *Principles of Computerized Tomographic Imaging*. Siam, London, 2001.
- [191] A Liu, W Xiao, R Li, L Liu, and L Chen. Comparison of optical projection tomography and light-sheet fluorescence microscopy. *Journal of microscopy*, 275(1):3–10, 2019.
- [192] Robert J Bryson-Richardson and Peter D Currie. Optical Projection Tomography for Spatio-Temporal Analysis in the Zebrafish. In *The Zebrafish: Cellular and Developmental Biology*, volume 76 of *Methods in Cell Biology*, pages 37–50. Academic Press, 2004.
- [193] James McGinty, Harriet B Taylor, Lingling Chen, Laurence Bugeon, Jonathan R Lamb, Margaret J Dallman, and Paul M W French. In vivo fluorescence lifetime optical projection tomography. *Biomed. Opt. Express*, 2(5):1340–1350, 2011.
- [194] Johnathon R Walls, Leigh Coultas, Janet Rossant, and R Mark Henkelman. Three-Dimensional Analysis of Vascular Development in the Mouse Embryo. *PLOS ONE*, 3(8):1–15, 2008.
- [195] Andrea Bassi, Luca Fieramonti, Cosimo D'Andrea, Gianluca Valentini, and Marina Mione. In vivo label-free three-dimensional imaging of zebrafish vasculature with optical projection tomography. *Journal of Biomedical Optics*, 16(10):1–4, 2011.

## Bibliography

---

- [196] Tomas Alanentalo, Amir Asayesh, Harris Morrison, Christina E Lorén, Dan Holmberg, James Sharpe, and Ulf Ahlgren. Tomographic molecular imaging and 3D quantification within adult mouse organs. *Nature Methods*, 4(1):31–33, 2007.
- [197] Marit J Boot, C Henrik Westerberg, Juanjo Sanz-Ezquerro, James Cotterell, Ronen Schweitzer, Miguel Torres, and James Sharpe. In vitro whole-organ imaging: 4D quantification of growing mouse limb buds. *Nature Methods*, 5(7):609–612, 2008.
- [198] Varsha Kumar, Susan Chyou, Jens V Stein, and Theresa T Lu. Optical projection tomography reveals dynamics of HEV growth after immunization with protein plus CFA and features shared with HEVs in acute autoinflammatory lymphadenopathy. *Frontiers in immunology*, 3:282, 2012.
- [199] Karen Lee, Jerome Avondo, Harris Morrison, Lilian Blot, Margaret Stark, James Sharpe, Andrew Bangham, and Enrico Coen. Visualizing plant development and gene expression in three dimensions using optical projection tomography. *The Plant cell*, 18(9):2145–2156, 2006.
- [200] Tomas Alanentalo, Christina E Lorén, Asa Larefalk, James Sharpe, Dan Holmberg, and Ulf Ahlgren. High-resolution three-dimensional imaging of islet-infiltrate interactions based on optical projection tomography assessments of the intact adult mouse pancreas. *Journal of biomedical optics*, 13(5):54070, 2008.
- [201] David Nguyen, Paul J Marchand, Arielle L Planchette, Julia Nilsson, Miguel Sison, Jérôme Extermann, Antonio Lopez, Marcin Sylwestrzak, Jessica Sordet-Dessimoz, Anja Schmidt-Christensen, Dan Holmberg, Dimitri Van De Ville, and Theo Lasser. Optical projection tomography for rapid whole mouse brain imaging. *Biomed. Opt. Express*, 8(12):5637–5650, 2017.
- [202] Alicia Arranz, Di Dong, Shouping Zhu, Markus Rudin, Christos Tsatsanis, Jie Tian, and Jorge Ripoll. Helical optical projection tomography. *Opt. Express*, 21(22):25912–25925, 2013.
- [203] Natalie Andrews, Marie-Christine Ramel, Sunil Kumar, Yuriy Alexandrov, Douglas J Kelly, Sean C Warren, Louise Kerry, Nicola Lockwood, Antonina Frolov, Paul Frankel, Laurence Bugeon, James McGinty, Margaret J Dallman, and Paul M W French. Visualising apoptosis in live zebrafish using fluorescence lifetime imaging with optical projection tomography to map FRET biosensor activity in space and time. *Journal of biophotonics*, 9(4):414–424, 2016.
- [204] Guanping Feng, Junbo Chen, Xuanlong Lu, Dingan Han, and Yaguang Zeng. Laser speckle projection tomography. *Opt. Lett.*, 38(15):2654–2656, 2013.
- [205] Yaguang Zeng, Ke Xiong, Xuanlong Lu, Guanping Feng, Dingan Han, and Jing Wu. Laser Doppler projection tomography. *Opt. Lett.*, 39(4):904–906, 2014.

- 
- [206] Gianmaria Calisesi, Alessia Candeo, Andrea Farina, Cosimo D'Andrea, Vittorio Magni, Gianluca Valentini, Anna Pistocchi, Alex Costa, and Andrea Bassi. Three-dimensional bright-field microscopy with isotropic resolution based on multi-view acquisition and image fusion reconstruction. *Scientific reports*, 10(1):12771, 2020.
- [207] Jürgen Mayer, Alexandre Robert-Moreno, James Sharpe, and Jim Swoger. Attenuation artifacts in light sheet fluorescence microscopy corrected by OPTiSPIM. *Light: Science and Applications*, 7(1):70, 2018.
- [208] Andrea Bassi, Benjamin Schmid, and Jan Huiskens. Optical tomography complements light sheet microscopy for in toto imaging of zebrafish development. *Development (Cambridge, England)*, 142(5):1016–1020, 2015.
- [209] Abbas Cheddad, Christoffer Svensson, James Sharpe, Fredrik Georgsson, and Ulf Ahlgren. Image processing assisted algorithms for optical projection tomography. *IEEE transactions on medical imaging*, 31(1):1–15, 2012.
- [210] Vadim Y Soloviev, Giannis Zacharakis, George Spiliopoulos, Rosy Favicchio, Teresa Correia, Simon R Arridge, and Jorge Ripoll. Tomographic imaging with polarized light. *J. Opt. Soc. Am. A*, 29(6):980–988, 2012.
- [211] Daniele Ancora, Diego Di Battista, Georgia Giasafaki, Stylianos E Psycharakis, Evangelos Liapis, Jorge Ripoll, and Giannis Zacharakis. Optical projection tomography via phase retrieval algorithms. *Methods*, 136:81–89, 2018.
- [212] Anna K Trull, Jelle van der Horst, Willem Jan Palenstijn, Lucas J van Vliet, Tristan van Leeuwen, and Jeroen Kalkman. Point spread function based image reconstruction in optical projection tomography. *Physics in medicine and biology*, 62(19):7784–7797, 2017.
- [213] Anna K Trull, Jelle van der Horst, Lucas J van Vliet, and Jeroen Kalkman. Comparison of image reconstruction techniques for optical projection tomography. *Appl. Opt.*, 57(8):1874–1882, 2018.
- [214] Jelle van der Horst and Jeroen Kalkman. Image resolution and deconvolution in optical tomography. *Opt. Express*, 24(21):24460–24472, 2016.
- [215] Claudio Vinegoni, Daniel Razansky, Jose-Luiz Figueiredo, Matthias Nahrendorf, Vasilis Ntziachristos, and Ralph Weissleder. Normalized Born ratio for fluorescence optical projection tomography. *Optics letters*, 34(3):319–321, 2009.
- [216] Teresa Correia, Nicola Lockwood, Sunil Kumar, Jun Yin, Marie-Christine Ramel, Natalie Andrews, Matilda Katan, Laurence Bugeon, Margaret J Dallman, James McGinty, Paul Frankel, Paul M W French, and Simon Arridge. Accelerated Optical Projection Tomography Applied to In Vivo Imaging of Zebrafish. *PLOS ONE*, 10(8):1–17, 2015.
- [217] Lingling Chen, Yuriy Alexandrov, Sunil Kumar, Natalie Andrews, Margaret J Dallman, Paul M W French, and James McGinty. Mesoscopic in vivo 3-D tracking of sparse cell

## Bibliography

---

- populations using angular multiplexed optical projection tomography. *Biomed. Opt. Express*, 6(4):1253–1261, 2015.
- [218] Laura Quintana and James Sharpe. Preparation of mouse embryos for optical projection tomography imaging. *Cold Spring Harbor protocols*, (6):664–669, 2011.
- [219] Raoul-Amadeus Lorbeer, Marko Heidrich, Christina Lorbeer, Diego Fernando Ramírez Ojeda, Gerd Bicker, Heiko Meyer, and Alexander Heisterkamp. Highly efficient 3D fluorescence microscopy with a scanning laser optical tomograph. *Opt. Express*, 19(6):5419–5430, 2011.
- [220] Thomas H Jamieson. Thick meniscus field correctors. *Appl. Opt.*, 21(15):2799–2803, 1982.
- [221] Thomas Watson, Natalie Andrews, Samuel Davis, Laurence Bugeon, Margaret D Dallman, and James McGinty. OPTiM: Optical projection tomography integrated microscope using open-source hardware and software. *PLOS ONE*, 12(7):1–13, 2017.
- [222] T. Aumeyr, M. G. Billing, L. M. Bobb, B. Bolzon, P. Karataev, T. Lefevre, and S. Mazzoni. Zemax simulations of transition and diffraction radiation. *Journal of Physics: Conference Series*, 517(1):9–15, 2014.
- [223] Bruno Sanguinetti and Christoph Clausen. Method And Device For Steganographic Processing And Compression Of Image Data. *USPTO*, (13), 2021.
- [224] Frank Natterer. *The Mathematics of Computerized Tomography*. Siam, London, 2001.
- [225] Wim van Aarle, Willem Jan Palenstijn, Jeroen Cant, Eline Janssens, Folkert Bleichrodt, Andrei Dabrovolski, Jan De Beenhouwer, K Joost Batenburg, and Jan Sijbers. Fast and flexible X-ray tomography using the ASTRA toolbox. *Opt. Express*, 24(22):25129–25147, 2016.
- [226] Di Dong, Shouping Zhu, Chenghu Qin, V Kumar, J V Stein, S Oehler, C Savakis, Jie Tian, and J Ripoll. Automated recovery of the center of rotation in optical projection tomography in the presence of scattering. *IEEE journal of biomedical and health informatics*, 17(1):198–204, 2013.
- [227] Anish Mittal, Anush Krishna Moorthy, and Alan Conrad Bovik. No-Reference Image Quality Assessment in the Spatial Domain. *IEEE Transactions on Image Processing*, 21(12):4695–4708, 2012.
- [228] David Hörl, Fabio Rojas Rusak, Friedrich Preusser, Paul Tillberg, Nadine Randel, Raghav K Chhetri, Albert Cardona, Philipp J Keller, Hartmann Harz, Heinrich Leonhardt, Mathias Treier, and Stephan Preibisch. BigStitcher: reconstructing high-resolution image datasets of cleared and expanded samples. *Nature Methods*, 16(9):870–874, 2019.

- [229] Johannes Schindelin, Curtis T Rueden, Mark C Hiner, and Kevin W Eliceiri. The ImageJ ecosystem: An open platform for biomedical image analysis. *Molecular reproduction and development*, 82(7-8):518–529, 2015.
- [230] Richard W Cole, Tushare Jinadasa, and Claire M Brown. Measuring and interpreting point spread functions to determine confocal microscope resolution and ensure quality control. *Nature Protocols*, 6(12):1929–1941, 2011.
- [231] C E Shannon. Communication in the Presence of Noise. *Proceedings of the IRE*, 37(1):10–21, 1949.
- [232] Paul C Goodwin. Evaluating optical aberrations using fluorescent microspheres: methods, analysis, and corrective actions. *Methods in cell biology*, 114:369–385, 2013.
- [233] Lingling Chen, James McGinty, Harriet B Taylor, Laurence Bugeon, Jonathan R Lamb, Margaret J Dallman, and Paul M W French. Incorporation of an experimentally determined MTF for spatial frequency filtering and deconvolution during optical projection tomography reconstruction. *Opt. Express*, 20(7):7323–7337, 2012.
- [234] J Calvin Coffey and D Peter O’Leary. The mesentery: structure, function, and role in disease. *The lancet. Gastroenterology and hepatology*, 1(3):238–247, 2016.
- [235] Yasmine Belkaid and Oliver J Harrison. Homeostatic Immunity and the Microbiota - ScienceDirect. *Immunity*, 46(4):562–576, 2017.
- [236] Danping Zheng, Timur Liwinski, and Eran Elinav. Interaction between microbiota and immunity in health and disease. *Cell Research*, 30(6):492–506, 2020.
- [237] Qing Zhao and Charles O. Elson. Adaptive immune education by gut microbiota antigens. *Immunology*, 154(1):28–37, 2018.
- [238] Mercedes Gomez De Agüero, Stephanie C. Ganai-Vonarburg, Tobias Fuhrer, Sandra Rupp, Yasuhiro Uchimura, Hai Li, Anna Steinert, Mathias Heikenwalder, Siegfried Hapfelmeier, Uwe Sauer, Kathy D. McCoy, and Andrew J. Macpherson. The maternal microbiota drives early postnatal innate immune development. *Science*, 351(6279):1296–1302, 2016.
- [239] Giovanna Muscogiuri, Elena Cantone, Sara Cassarano, Dario Tuccinardi, Luigi Barrea, Silvia Savastano, Annamaria Colao, and Education on behalf of the Obesity Programs of nutrition Research and Assessment (OPERA) group. Gut microbiota: a new path to treat obesity. *International Journal of Obesity Supplements*, 9(1):10–19, 2019.
- [240] Manoj Gurung, Zhipeng Li, Hannah You, Richard Rodrigues, Donald B Jump, Andrey Morgun, and Natalia Shulzhenko. EBioMedicine Role of gut microbiota in type 2 diabetes pathophysiology. *EBioMedicine*, 51:102590, 2020.
- [241] Xuan Zhang, Bei di Chen, Li dan Zhao, and Hao Li. The Gut Microbiota: Emerging Evidence in Autoimmune Diseases. *Trends in Molecular Medicine*, 26(9):862–873, 2020.

## Bibliography

---

- [242] Tomasz P. Wypych, Lakshanie C. Wickramasinghe, and Benjamin J. Marsland. The influence of the microbiome on respiratory health. *Nature Immunology*, 20(10):1279–1290, 2019.
- [243] Niki D. Ubags, Aurélien Trompette, Julie Pernot, Britt Nibbering, Nicholas C. Wong, Céline Pattaroni, Alexis Rapin, Laurent P. Nicod, Nicola L. Harris, and Benjamin J. Marsland. Microbiome-induced antigen-presenting cell recruitment coordinates skin and lung allergic inflammation. *Journal of Allergy and Clinical Immunology*, 147(3):1049–1062.e7, 2021.
- [244] Håvard Ove Skjerven, Eva Maria Rehbinder, Riyas Vettukattil, Marissa LeBlanc, Berit Granum, Guttorm Haugen, Gunilla Hedlin, Linn Landrø, Benjamin J. Marsland, Knut Rudi, Kathrine Dønvoid Sjøborg, Cilla Söderhäll, Anne Cathrine Staff, Kai Håkon Carlsen, Anna Asarnoj, Karen Eline Stensby Bains, Oda C.Lødrup Carlsen, Kim M.Advocaat Endre, Peder Annæus Granlund, Johanne Uthus Hermansen, Hrefna Katrín Gudmundsdóttir, Katarina Hilde, Geir Håland, Ina Kreyberg, Inge Christoffer Olsen, Caroline Aleks Olsson Mägi, Live Solveig Nordhagen, Carina Madelen Saunders, Ingebjørg Skrindo, Sandra G. Tedner, Magdalena R. Værnesbranden, Johanna Wiik, Christine Monceyron Jonassen, Björn Nordlund, and Karin C.Lødrup Carlsen. Skin emollient and early complementary feeding to prevent infant atopic dermatitis (PreventADALL): a factorial, multicentre, cluster-randomised trial. *The Lancet*, 395(10228):951–961, 2020.
- [245] Driffa Moussata, Martin Goetz, Annabel Gloeckner, Marcus Kerner, Barry Campbell, Arthur Hoffman, Stephan Biesterfeld, Bernard Flourie, Jean Christophe Saurin, Peter R. Galle, Markus F. Neurath, Alastair J.M. Watson, and Ralf Kiesslich. Confocal laser endomicroscopy is a new imaging modality for recognition of intramucosal bacteria in inflammatory bowel disease in vivo. *Gut*, 60(1):26–33, 2011.
- [246] Timo Rath, Walburga Dieterich, Christiane Kätscher-Murad, Markus F. Neurath, and Yurdagül Zopf. Cross-sectional imaging of intestinal barrier dysfunction by confocal laser endomicroscopy can identify patients with food allergy in vivo with high sensitivity. *Scientific Reports*, 11(1):1–9, 2021.
- [247] Yu Xie, Fei Ding, Wenjuan Di, Yifan Lv, Fan Xia, Yunlu Sheng, Jing Yu, and Guoxian Ding. Impact of a high-fat diet on intestinal stem cells and epithelial barrier function in middle-aged female mice. *Molecular Medicine Reports*, 21(3):1133–1144, 2020.
- [248] Christa Park, Kitty P. Cheung, Natalie Limon, Anne Costanzo, Cindy Barba, Nadia Miranda, Shannon Gargas, Andrew M. F. Johnson, Jerrold M. Olefsky, and Julie M. Jameson. Obesity Modulates Intestinal Intraepithelial T Cell Persistence, CD103 and CCR9 Expression, and Outcome in Dextran Sulfate Sodium–Induced Colitis. *The Journal of Immunology*, 203(12):3427–3435, 2019.
- [249] William C. Joesten, Audrey H. Short, and Michael A. Kennedy. Spatial variations in gut permeability are linked to type 1 diabetes development in non-obese diabetic mice. *BMJ Open Diabetes Research and Care*, 7(1):1–9, 2019.

- [250] G. Eberl and M. Lochner. The development of intestinal lymphoid tissues at the interface of self and microbiota. *Mucosal Immunology*, 2(6):478–485, 2009.
- [251] Allan M. Mowat and William W. Agace. Regional specialization within the intestinal immune system. *Nature Reviews Immunology*, 14(10):667–685, 2014.
- [252] Djahida Bouskra, Christophe Brézillon, Marion Bérard, Catherine Werts, Rosa Varona, Ivo Gomperts Boneca, and Gérard Eberl. Lymphoid tissue genesis induced by commensals through NOD1 regulates intestinal homeostasis. *Nature*, 456(7221):507–510, 2008.
- [253] Thomas M Fenton, Peter B Jørgensen, Kristoffer Niss, Samuel J S Rubin, Urs M Mörbe, Lene B Riis, Clément Da Silva, Adam Plumb, Julien Vandamme, Henrik L Jakobsen, Søren Brunak, Aida Habtezion, Ole H Nielsen, Bengt Johansson-Lindbom, and William W Agace. Immune Profiling of Human Gut-Associated Lymphoid Tissue Identifies a Role for Isolated Lymphoid Follicles in Priming of Region-Specific Immunity. *Immunity*, 52(3):557–570.e6, 2020.
- [254] Bruno Cunha Fialho Cantarelli, Rafael Santiago de Oliveira, Aldo Maurici Araújo Alves, Bruno Jucá Ribeiro, Fernanda Velloni, and Giuseppe D’ippolito. Evaluating inflammatory activity in crohn’s disease by cross-sectional imaging techniques. *Radiologia Brasileira*, 53(1):38–46, 2020.
- [255] Zhonghong Wei, Peiliang Shen, Peng Cheng, Yin Lu, Aiyun Wang, and Zhiguang Sun. Gut Bacteria Selectively Altered by Sennoside A Alleviate Type 2 Diabetes and Obesity Traits. *Oxidative Medicine and Cellular Longevity*, 2020.
- [256] Emily W. Sun, Dayan De Fontgalland, Philippa Rabbitt, Paul Hollington, Luigi Sposato, Steven L. Due, David A. Wattchow, Christopher K. Rayner, Adam M. Deane, Richard L. Young, and Damien J. Keating. Mechanisms controlling glucose-induced GLP-1 secretion in human small intestine. *Diabetes*, 66(8):2144–2149, 2017.
- [257] Xiaoxiao Huang, Ying Shi, Yajing Liu, Hongzhi Xu, Yu Liu, Chuanxing Xiao, Jianlin Ren, and Liming Nie. Noninvasive photoacoustic identification and imaging of gut microbes. *Optics Letters*, 42(15):2938, 2017.
- [258] Cédric Schmidt, Arielle Planchette, David Nguyen, Gabriel Giardina, Yoan Neuen-schwander, Di Franco Mathieu, Alessio Mylonas, Adrien Descloux, Enrico Pomarico, Aleksandra Radenovic, and Extermann Jérôme. High resolution optical projection tomography platform for multispectral imaging of the mouse gut. *Biomedical Optics Express*, 12(6):3619–3629, 2021.
- [259] June L. Round and Sarkis K. Mazmanian. The gut microbiota shapes intestinal immune responses during health and disease. *Nature Reviews Immunology*, 9(5):313–323, 2009.
- [260] Rémy Burcelin. Gut microbiota and immune crosstalk in metabolic disease. *Molecular Metabolism*, 5(9):771–781, 2016.

## Bibliography

---

- [261] Panida Sittipo, Stefani Lobionda, Yun Kyung Lee, and Craig L. Maynard. Intestinal microbiota and the immune system in metabolic diseases. *Journal of Microbiology*, 56(3):154–162, 2018.
- [262] Hsin Jung Wu and Eric Wu. The role of gut microbiota in immune homeostasis and autoimmunity. *Gut Microbes*, 3(1):4–14, 2012.
- [263] Bevan S. Main and Myles R. Minter. Microbial immuno-communication in neurodegenerative diseases. *Frontiers in Neuroscience*, 11:1–8, 2017.
- [264] Tatiana Takiishi, Camila Ideli Morales Fenere, and Niels Olsen Saraiva Câmara. Intestinal barrier and gut microbiota: Shaping our immune responses throughout life. *Tissue Barriers*, 5(4), 2017.
- [265] Kathryn A. Knoop and Rodney D. Newberry. Isolated lymphoid follicles are dynamic reservoirs for the induction of intestinal IgA. *Frontiers in Immunology*, 3:1–7, 2012.
- [266] Tao Dumur, Susan Duncan, Katja Graumann, Sophie Desset, Ricardo S. Randall, Ortrun Mittelsten Scheid, Hank W. Bass, Dimiter Prodanov, Christophe Tatout, and Célia Baroux. Probing the 3D architecture of the plant nucleus with microscopy approaches: challenges and solutions. *Nucleus*, 10(1):181–212, 2019.
- [267] A. Ballabeni, F. I. Apollonio, M. Gaiani, and F. Remondino. Advances in image pre-processing to improve automated 3d reconstruction. *International Archives of the Photogrammetry, Remote Sensing and Spatial Information Sciences - ISPRS Archives*, 40(5W4):315–323, 2015.
- [268] Alexandr A. Kalinin, Ari Allyn-Feuer, Alex Ade, Gordon Victor Fon, Walter Meixner, David Dilworth, Syed S. Husain, Jeffrey R. de Wett, Gerald A. Higgins, Gen Zheng, Amy Creekmore, John W. Wiley, James E. Verdone, Robert W. Veltri, Kenneth J. Pienta, Donald S. Coffey, Brian D. Athey, and Ivo D. Dinov. 3D Shape Modeling for Cell Nuclear Morphological Analysis and Classification. *Scientific Reports*, 8(1):1–14, 2018.
- [269] Ya Yuan Fu, Shih Jung Peng, Hsin Yao Lin, Pankaj J. Pasricha, and Shiue Cheng Tang. 3-D imaging and illustration of mouse intestinal neurovascular complex. *American Journal of Physiology - Gastrointestinal and Liver Physiology*, 304(1):1–11, 2013.
- [270] Tianmeng Li, Hui Hui, Chaoen Hu, He Ma, Xin Yang, and Jie Tian. Multiscale imaging of colitis in mice using confocal laser endomicroscopy, light-sheet fluorescence microscopy, and magnetic resonance imaging. *Journal of Biomedical Optics*, 24(01):1, 2019.
- [271] Valérie Abadie, Sangman M. Kim, Thomas Lejeune, Brad A. Palanski, Jordan D. Ernest, Olivier Tastet, Jordan Voisine, Valentina Discepolo, Eric V. Marietta, Mohamed B.F. Hawash, Cezary Ciszewski, Romain Bouziat, Kaushik Panigrahi, Irina Horwath, Matthew A. Zurenski, Ian Lawrence, Anne Dumaine, Vania Yotova, Jean Christophe



- Grenier, Joseph A. Murray, Chaitan Khosla, Luis B. Barreiro, and Bana Jabri. IL-15, gluten and HLA-DQ8 drive tissue destruction in coeliac disease. *Nature*, 578(7796):600–604, 2020.
- [272] Fergus Shanahan, H P Redmond, J K Collins, Am J Physiol, Gastrointest Liver, Donald B Katz, Miguel A L Nicolelis, and S A Simon. Nutrient Tasting and Signaling Mechanisms in the Gut. *Am J Physiol Gastrointest Liver Physiol*, 278:191–196, 2000.
- [273] Kevin J. Maloy and Fiona Powrie. Intestinal homeostasis and its breakdown in inflammatory bowel disease. *Nature*, 474(7351):298–306, 2011.
- [274] Francesca D’Addio and Paolo Fiorina. Type 1 Diabetes and Dysfunctional Intestinal Homeostasis. *Trends in Endocrinology and Metabolism*, 27(7):493–503, 2016.
- [275] Michelle L. Hermiston, Zheng Xu, and Arthur Weiss. CD45: A critical regulator of signaling thresholds in immune cells. *Annual Review of Immunology*, 21:107–137, 2003.
- [276] Catherine M. Sawai, Sonja Babovic, Samik Upadhaya, David J.H.F. Knapp, Yonit Lavin, Colleen M. Lau, Anton Goloborodko, Jue Feng, Joji Fujisaki, Lei Ding, Leonid A. Mirny, Miriam Merad, Connie J. Eaves, and Boris Reizis. Hematopoietic Stem Cells Are the Major Source of Multilineage Hematopoiesis in Adult Animals. *Immunity*, 45(3):597–609, 2016.
- [277] Lora V. Hooper and Andrew J. MacPherson. Immune adaptations that maintain homeostasis with the intestinal microbiota. *Nature Reviews Immunology*, 10(3):159–169, 2010.
- [278] Nabil Bosco and Mario Noti. The aging gut microbiome and its impact on host immunity. *Genes Immunity*, 22(5):289–303, 2021.
- [279] Yasmine Belkaid and Timothy W. Hand. Role of the microbiota in immunity and inflammation. *Cell*, 157(1):121–141, 2014.
- [280] June L. Round and Sarkis K. Mazmanian. The gut microbiota shapes intestinal immune responses during health and disease. *Nature Reviews Immunology*, 9(8):600–600, 2009.
- [281] William H. Gendron, Emre Fertan, Stephanie Pelletier, Kyle M. Roddick, Timothy P. O’Leary, Younes Anini, and Richard E. Brown. Age related weight loss in female 5xFAD mice from 3 to 12 months of age. *Behavioural Brain Research*, 406:113214, 2021.
- [282] Antonio J. López-Gamero, Cristina Rosell-Valle, Dina Medina-Vera, Juan Antonio Navarro, Antonio Vargas, Patricia Rivera, Carlos Sanjuan, Fernando Rodríguez de Fonseca, and Juan Suárez. A negative energy balance is associated with metabolic dysfunctions in the hypothalamus of a humanized preclinical model of alzheimer’s disease, the 5xfad mouse. *International Journal of Molecular Sciences*, 22(10):1–35, 2021.
- [283] Bjoern O Schroeder and Fredrik Bäckhed. Signals from the gut microbiota to distant organs in physiology and disease. *Nature medicine*, 22(10):1079–1089, 2016.

## Bibliography

---

- [284] Claire L. Boulangé, Ana Luisa Neves, Julien Chilloux, Jeremy K. Nicholson, and Marc-Emmanuel Dumas. Impact of the gut microbiota on inflammation, obesity, and metabolic disease. *Genome Medicine*, 8(1):42, 2016.
- [285] Eun Ran Kim and Poong-Lyul Rhee. How to interpret a functional or motility test - colon transit study. *Journal of neurogastroenterology and motility*, 18(1):94–99, 2012.
- [286] Nicolai M. Stoye, Malena dos Santos Guilherme, and Kristina Endres. Alzheimer’s disease in the gut—Major changes in the gut of 5xFAD model mice with ApoA1 as potential key player. *FASEB Journal*, 34(9):11883–11899, 2020.
- [287] P Davies and A J Maloney. Selective loss of central cholinergic neurons in Alzheimer’s disease. *The Lancet*, 2(8000):1403, 1976.
- [288] John Hardy and David Allsop. Amyloid deposition as the central event in the aetiology of Alzheimer’s disease. *Trends in Pharmacological Sciences*, 12:383–388, 1991.
- [289] Arun K Ghosh and Heather L Osswald. BACE1 ( $\beta$ -secretase) inhibitors for the treatment of Alzheimer’s disease. *Chem. Soc. Rev.*, 43(19):6765–6813, 2014.
- [290] Qin Nie, Xiao Guang Du, and Mei Yu Geng. Small molecule inhibitors of amyloid  $\beta$  peptide aggregation as a potential therapeutic strategy for Alzheimer’s disease. *Acta Pharmacologica Sinica*, 32(5):545–551, 2011.
- [291] Vladimir Volloch and Sophia Rits. Results of Beta Secretase-Inhibitor Clinical Trials Support Amyloid Precursor Protein-Independent Generation of Beta Amyloid in Sporadic Alzheimer’s Disease. *Medical sciences (Basel, Switzerland)*, 6(2), 2018.
- [292] Alice Bittar, Urmi Sengupta, and Rakez Kaye. Prospects for strain-specific immunotherapy in Alzheimer’s disease and tauopathies. *npj Vaccines*, 3(1), 2018.
- [293] Li-Kai Huang, Shu-Ping Chao, and Chaur-Jong Hu. Clinical trials of new drugs for Alzheimer disease. *Journal of Biomedical Science*, 27(1):18, 2020.
- [294] Eamonn M M Quigley, Prianka Gajula, Tom Van De Wiele Belgium, and Hospital Val D’hebron. Recent advances in modulating the microbiome. *F1000 Faculty Rev*, 9:46, 2020.
- [295] Gwen Falony, Marie Joossens, Sara Vieira-Silva, Jun Wang, Youssef Darzi, Karoline Faust, Alexander Kurilshikov, Marc Jan Bonder, Mireia Valles-Colomer, Doris Vandeputte, Raul Y. Tito, Samuel Chaffron, Leen Rymenans, Chloë Verspecht, Lise De Sutter, Gipsi Lima-Mendez, Kevin D’hoë, Karl Jonckheere, Daniel Homola, Roberto Garcia, Ettje F. Tigchelaar, Linda Eeckhaut, Jingyuan Fu, Liesbet Henckaerts, Alexandra Zhernakova, Cisca Wijmenga, and Jeroen Raes. Population-level analysis of gut microbiome variation. *Science*, 352(6285):560–564, 2016.

- [296] Claudia Kolm, Isabella Cervenka, Ulrich J. Aschl, Niklas Baumann, Stefan Jakwerth, Rudolf Krska, Robert L. Mach, Regina Sommer, Maria C. DeRosa, Alexander K.T. Kirschner, Andreas H. Farnleitner, and Georg H. Reischer. DNA aptamers against bacterial cells can be efficiently selected by a SELEX process using state-of-the art qPCR and ultra-deep sequencing. *Scientific Reports*, 10(1):1–16, 2020.
- [297] Guo Qing Liu, Ying Qi Lian, Chao Gao, Xiao Feng Yu, Ming Zhu, Kai Zong, Xue Jiao Chen, and Yi Yan. In vitro selection of DNA aptamers and fluorescence-based recognition for rapid detection *Listeria monocytogenes*. *Journal of Integrative Agriculture*, 13(5):1121–1129, 2014.
- [298] Carolina Tropini, Kristen A. Earle, Kerwyn Casey Huang, and Justin L. Sonnenburg. The Gut Microbiome: Connecting Spatial Organization to Function. *Cell Host and Microbe*, 21(4):433–442, 2017.
- [299] Irfan Akhtar, Fiona A. Stewart, Anna Härle, Andrea Droste, and Mathias Beller. Visualization of endogenous gut bacteria in *Drosophila melanogaster* using fluorescence in situ hybridization. *PLoS ONE*, 16:1–15, 2021.



# Arielle Louise PLANCHETTE

I am a scientist who thrives in inter-disciplinary research contexts, with a strong background in microbiology and molecular science. My values have led me from exploring the impact of the microbiome on health to its importance in finding sustainable solutions for agriculture. The holistic scientific approach I have developed has brought me to combine these perspectives to promote health at the societal and ecological levels simultaneously.

Chemin de Veilloud, 52  
Ecublens 1024  
Vaud, SWITZERLAND  
[planchettea@gmail.com](mailto:planchettea@gmail.com)  
+41/786637893

Holder of a Swiss  
driver's license

## STRENGTHS

Inquisitive  
Collaborative  
Critical thinker  
Receptive to feedback  
Highly organised

## LANGUAGES

English ●●●●  
French ●●●●  
Spanish ●●○○

## SKILLS

### Analytical

**Statistical analysis** (standard and multivariate – PCA, PLS-DA, ASCA)

**Image processing**  
(ImageJ, Ilastik, Qupath)

**GraphPad Prism**

### Transferable

**Scientific communication**

**Scientific writing**

**Lab management**

**Experimental license redaction**

### In vitro/Ex vivo

**Molecular biology**

(CRISPR, (q)PCR, ChIP, transfection, DNA ligation, cell transformation)

**Cell culture**

**Protein quantification**

(WB, ELISA, SIMOA)

**Histology**

**Microscopy**

(fluorescence, 3D Tomography)

**16S rRNA sequencing analysis**

**Mass spectrometry analysis**

### In vivo

**Mouse colony breeding**

**Behavioural testing**

(Morris water maze, new object recognition, y-maze, open field)

**Metabolism testing**

(CLAMS, OGTT, EchoMRI, GI transit)

**Surgery**

(transcardiac perfusion, CSF tapping)

## QUALIFICATIONS

October 2016 – November 2021



**PhD in Biotechnology and Bioengineering**

**École Polytechnique Fédérale de Lausanne (EPFL)**, Lausanne, Switzerland



Supervisors: Prof. Aleksandra Radenovic Laboratory of Nanoscale Biology EPFL

Prof. Andrew Macpherson Laboratory of Gastroenterology and Mucosal Immunology  
University of Bern

**H2020 European Union *Alzheimer's Disease – Gut Connection* project** (<http://adgut.eu/>)

Thesis title: ADgut: Understanding the link between the gut microbiome and Alzheimer's disease

September 2014 – September 2015



**MRes in SYNTHETIC BIOLOGY**

**University College London**, London, UK

Supervisor: Dr. Renos Savva, Rosalind Franklin Laboratory Birkbeck College London

Distinction awarded, Department of Biochemical Engineering UCL

Thesis: Towards the construction of synthetic circuits for repurposing bacteriophage

October 2011 – June 2014



**BSc in Biomedicine**

**University of Lancaster**, Lancaster, UK

Upper Second Class degree awarded

Thesis: Cloning and Analysis of cDNA from Human Tissue

September 2008 – June 2011



**International Baccalaureate**

**International School of Geneva**, La Châtaigneraie campus, Switzerland

36 points awarded out of 45

## PUBLICATIONS

*Published*

**High resolution optical projection tomography platform for multispectral imaging of the mouse gut (2021)**

Schmidt, Cédric and Planchette, Arielle L. (co-authors), Nguyen, David, Giardina, Gabriel, Neuenschwander, Yoan, Mathieu, Di Franco, Mylonas, Alessio, Descloux, Adrien, Pomarico, Enrico, Radenovic, Aleksandra, Jérôme, Extermann  
*Biomedical Optics Express* 12(6):3619-3629

**Supervised learning to quantify amyloidosis in whole brains of an Alzheimer's disease mouse model acquired with optical projection tomography (2019)**

Nguyen, David, Uhlmann, Virginie, Planchette, Arielle L., Marchand, Paul J., Van De Ville, Dimitri, Lasser, Theo, Radenovic, Aleksandra  
*Biomedical Optics Express* 10(6):3041-3060

## PUBLICATIONS

### Published

#### Optical projection tomography for rapid whole mouse brain imaging (2017)

Nguyen, David, Marchand, Paul J., Planchette, Arielle L., Nilsson, Julia, Sison, Miguel, Extermann, Jérôme, Lopez, Antonio, Sylwestrzak, Marcin, Sordet-Dessimoz, Jessica, Schmidt-Christensen, Anja, Holmberg, Dan, Van De Ville, Dimitri, Lasser, Theo  
*Biomedical Optics Express* 8(12):5637-5650

### In preparation

#### Investigation of the theragnostic potential of gut microbiome modulation in a model of Alzheimer's disease

Planchette, Arielle L., Mylonas, Alessio, Ronchi, Francesca, Mueller, Terry, Iacchizzi, Monica, Vitale, Raffaele, Prykhodko, Olena, Burleigh, Stephen, Nguyen, Thao D., Ghaffarzadegan, Tannaz, Cao, Ling, Bovet, Cédric, Freiburghaus, Katrin, Fak-Hallenius, Frida, Macpherson, Andrew, Radenovic, Aleksandra, Gomez de Agüero, Mercedes  
*Scientific Reports (to be determined)*

#### Optical Imaging of the Small Intestine Across Scales

Planchette, Arielle L., Schmidt, Cédric, Mylonas, Alessio, Burri, Olivier, Guiet, Romain, Giardina, Gabriel, Descloux, Adrien, Pomarico, Enrico, Radenovic, Aleksandra, Jérôme, Extermann  
*Nature Biotechnology (to be determined)*

## WORK EXPERIENCE

January 2016 – August 2016



**Research Intern in Systems biology and Genetics Laboratory, École Polytechnique Fédérale de Lausanne (EPFL)**, Lausanne, Switzerland Supervisors: Prof. Bart Deplancke and Dr. Daniil Alpern

Research project: *Experimental Validation of the Variable Chromatin Module concept*  
Validation of VCM-wide effect of InDel within Axin2 variable chromatin module in HEK cells using CRISPR and chromatin immunoprecipitation (ChIP)

## LEADERSHIP

September 2014 – September 2015



**Member of UCLU Taekwondo Club**, University College London, UK  
Silver medalist at British Student Taekwondo Federation National competition

October 2013 – June 2014



**Captain of Fylde College Ladies Pool Team**, Lancaster University, UK  
Lancaster University College League winners 2014

March 2013



**Co-founder of the Nomadic Culture Society**, Lancaster University, UK

January 2013 – December 2013



**Publicity Officer OF Fylde College Junior Common Room Committee**, Lancaster University, UK

## INTERESTS

### • Wellness

Practicing yoga for 5 and pilates for 11 years

To find **balance** using meditative practice and strength training

### • Creativity

Singing, reading, cooking, knitting, drawing, photography

To nurture my **creative streak**

### • Exploring

Travelling, sharing experiences with family and friends

To **broaden horizons** and remain grounded

## REFEREES

### • Thesis directors

Prof. Aleksandra Radenovic, EPFL  
[aleksandra.radenovic@epfl.ch](mailto:aleksandra.radenovic@epfl.ch)

Prof. Andrew Macpherson, University of Bern  
[Andrew.Macpherson@insel.ch](mailto:Andrew.Macpherson@insel.ch)

### • Mentors

Prof. Carlotta Guiducci, EPFL  
[carlotta.guiducci@epfl.ch](mailto:carlotta.guiducci@epfl.ch)

Dr. Raphaël Doënen, EPFL  
[raphael.doenen@epfl.ch](mailto:raphael.doenen@epfl.ch)

### • Collaborators

Dr. Alessio Mylonas, AC Immune  
[alessio.mylonas@epfl.ch](mailto:alessio.mylonas@epfl.ch)

Prof. Mercedes Gomez, Würzburg Institute  
[mercedes.gomez@uni-wuerzburg.de](mailto:mercedes.gomez@uni-wuerzburg.de)